University of New Hampshire
University of New Hampshire Scholars' Repository

Doctoral Dissertations | Student Scholarship

Winter 2000

A non-derivatization approach to HPLC fluorescence detection for some important amino group-containing compounds based on a ligand displacement reaction

Min Yang
University of New Hampshire, Durham

Follow this and additional works at: https://scholars.unh.edu/dissertation

Recommended Citation
Yang, Min, "A non-derivatization approach to HPLC fluorescence detection for some important amino group-containing compounds based on a ligand displacement reaction" (2000). *Doctoral Dissertations*. 2151.
https://scholars.unh.edu/dissertation/2151

This Dissertation is brought to you for free and open access by the Student Scholarship at University of New Hampshire Scholars' Repository. It has been accepted for inclusion in Doctoral Dissertations by an authorized administrator of University of New Hampshire Scholars' Repository. For more information, please contact nicole.hentz@unh.edu.

INFORMATION TO USERS

This manuscript has been reproduced from the microfilm master. UMI films the text directly from the original or copy submitted. Thus, some thesis and dissertation copies are in typewriter face, while others may be from any type of computer printer.

The quality of this reproduction is dependent upon the quality of the copy submitted. Broken or indistinct print, colored or poor quality illustrations and photographs, print bleedthrough, substandard margins, and improper alignment can adversely affect reproduction.

In the unlikely event that the author did not send UMI a complete manuscript and there are missing pages, these will be noted. Also, if unauthorized copyright material had to be removed, a note will indicate the deletion.

Oversize materials (e.g., maps, drawings, charts) are reproduced by sectioning the original, beginning at the upper left-hand corner and continuing from left to right in equal sections with small overlaps.

Photographs included in the original manuscript have been reproduced xerographically in this copy. Higher quality 6" x 9" black and white photographic prints are available for any photographs or illustrations appearing in this copy for an additional charge. Contact UMI directly to order.

Bell & Howell Information and Learning
300 North Zeeb Road, Ann Arbor, MI 48106-1346 USA

UMI®
800-521-0600

Reproduced with permission of the copyright owner. Further reproduction prohibited without permission.

Reproduced with permission of the copyright owner. Further reproduction prohibited without permission.

A NON-DERIVATIZATION APPROACH TO HPLC FLUORESCENCE DETECTION FOR SOME IMPORTANT AMINO GROUP-CONTAINING COMPOUNDS BASED ON A LIGAND DISPLACEMENT REACTION

BY

Min Yang
B.S. University of Science and Technology of China, 1994

DISSERTATION

Submitted to the University of New Hampshire
in Partial Fulfillment of
the Requirements for the Degree of

Doctor of Philosophy

in

Chemistry

December, 2000

Reproduced with permission of the copyright owner. Further reproduction prohibited without permission.

UMI Number: 9991562

UMI®

UMI Microform 9991562
Copyright 2001 by Bell & Howell Information and Learning Company.
All rights reserved. This microform edition is protected against
unauthorized copying under Title 17, United States Code.

Bell & Howell Information and Learning Company
300 North Zeeb Road
P.O. Box 1346
Ann Arbor, MI 48106-1346

Reproduced with permission of the copyright owner. Further reproduction prohibited without permission.

This dissertation has been examined and approved.

Dissertation Director, Sterling A. Tomellini
Professor of Chemistry

Edward H. Wong
Professor of Chemistry

Christopher F. Bauer
Professor of Chemistry

Carmela C. Amato-Wierda
Assistant Professor of Material Science

Jae O. Kang
Associate Professor of Medical Laboratory Science

October 12, 2000
Date

Reproduced with permission of the copyright owner. Further reproduction prohibited without permission.

To my mother, Xiaofeng Wu

Reproduced with permission of the copyright owner. Further reproduction prohibited without permission.

ACKNOWLEDGEMENTS

I thank Dr. Sterling Tomellini for his help and guidance in the past four years. Dr. Tomellini's enthusiasm and standard for scientific work will always be with me throughout my scientific career. I appreciate the throughout help from the members of my committee. Dr. Wong, Dr. Bauer, Dr. Amata-Wierda and Dr. Kang. I thank Cindy, Peggy, Susan and Bob for their efficient administrative assistance during my stay in UNH. I extend my gratitude to Doug and Ron for proofreading my papers and this dissertation. I must say the help from all these people makes the completion of this program possible.

Reproduced with permission of the copyright owner. Further reproduction prohibited without permission.

TABLE OF CONTENTS

Reproduced with permission of the copyright owner. Further reproduction prohibited without permission.

Reproduced with permission of the copyright owner. Further reproduction prohibited without permission.

Reproduced with permission of the copyright owner. Further reproduction prohibited without permission.

5. Separation and Detection of Aminoglycoside Antibiotics Following HPLC with $Cu(L\text{-}Trp)_2$ as the Postcolumn Reagent

Reproduced with permission of the copyright owner. Further reproduction prohibited without permission.

Reproduced with permission of the copyright owner. Further reproduction prohibited without permission.

Abstract

A NON-DERIVATIZATION APPROACH TO HPLC FLUORESCENCE DETECTION FOR SOME IMPORTANT AMINO GROUP-CONTAINING COMPOUNDS BASED ON A LIGAND DISPLACEMENT REACTION

by

Min Yang

University of New Hampshire. December. 2000

Detection of some important amino group-containing compounds such as amino acids, aliphatic biogenic amines and aminoglycosides can present difficulties since these compounds do not possess strong fluorophores or chromophores. A novel indirect fluorescence detection method for these compounds has been developed, taking advantage of the fact they form complexes with Cu^{2+} ions. The reaction between these compounds and a Cu(II)- L-tryptophan complex (Cu(L-Trp)2) in solution results in the displacement

Reproduced with permission of the copyright owner. Further reproduction prohibited without permission.

of L-Trp from the complex and an increase in L-Trp fluorescence, since the fluorescence of L-Trp is quenched in the Cu(II) complex. The increase in L-Trp fluorescence is taken as the measure of the presence of these amino group-containing compounds. This detection scheme has been interfaced to a HPLC system, by adding a buffered $Cu(L\text{-}Trp)_2$ solution to the column effluent via a postcolumn mixing tee.

The detection system was optimized both theoretically and experimentally, taking into consideration that relevant equilibria existing in the solution that may affect the detection. The pH was found to be the most important detection parameter, affecting detection in several ways, including: 1). Cu(II)- L-Trp complexation; 2). Free L-Trp fluorescence efficiency; and 3). Cu(II) - analyte complexation. Chromatographic experiments were performed to determine the pH which provides the optimum S/N level. Other factors, such as the postcolumn reagent flow rate, and the effect of organic solvent modifier, were also studied.

This approach provides several advantages compared to other methods used to detect these analytes. Detection limits are reasonably good, generally on the order of low pmol injected. Linearity ranges to nmol injected. Our experience also indicates that small postcolumn mixing volumes which introduce minimal postcolumn bandbroadening can be used. Simplicity and robustness are among the other advantages of this approach to analyte detection.

Reproduced with permission of the copyright owner. Further reproduction prohibited without permission.

Chapter 1
Introduction

The detection of small amino group-containing compounds has been studied extensively since high performance liquid chromatography was introduced in the early 1970's [1]. These compounds play important roles in human biological activities and pharmaceutical studies. For instance, amino acids are the essential components of proteins and are present in a wide range of samples, such as biological tissues and fluids, foods and industrial products [2]. Improvements in amino acid analysis and protein sequencing methodology are essential for the continued advancement of many areas of biotechnology and genetic engineering [3]. Aliphatic biogenic diamines and polyamines are naturally occurring compounds [4 - 6]. Biogenic polyamines, such as spermidine and spermine, are important for rapid tissue growth with their concentrations related to several parameters of cell proliferation, such as the concentrations of proteins and nucleic acids [7]. Biogenic polyamines are also important in cancer studies as the polyamine patterns of tumor cells are significantly different from those of normal muscle tissues [8]. The aminoglycoside antibiotics, which have been used as pharmaceuticals since the discovery and clinical use of streptomycin in 1944 [9], are another important class of amino group-containing compounds. The aminoglycosides have been widely used to treat serious infections [10].

Traditionally, HPLC analysis of these amino group-containing compounds involves

Reproduced with permission of the copyright owner. Further reproduction prohibited without permission.

either precolumn or postcolumn derivatization, due to their lack of strong chromophores or fluorophores [11]. Figures 1.1, 1.2 and 1.3 give the molecular structures of several natural amino acids, representative biogenic polyamines and aminoglycosides. For the natural amino acids, the carboxyl group and the amino group have weak UV absorptivities at 200 - 210 nm and 185 nm, respectively. Unfortunately, compounds with absorbances below 220 nm, and particularly below 200 nm, are often difficult to detect with a UV-VIS detector in HPLC because of an overwhelmingly large background absorption due to the mobile phase [1]. On the other hand, most of the biogenic polyamines and aminoglycosides do not have any unsaturated functional groups, which are necessary for direct UV-VIS detection. Basically speaking, derivatization means reacting the analyte with a suitable derivatization reagent to produce a strong UV-absorbing or fluorescing product. Commonly used derivatization reagents include ninhydrin [12, 13], o-phthaldehyde [14, 15], and 7-nitrobenzo-2-oxa-1,3 diazole (NBD) - halide [16]. Several derivatization reactions for amino acids and amines are given in Figure 1.4. Derivatization may occur either before (precolumn derivatization) or after (postcolumn derivatization) the chromatographic separation takes place. Precolumn and postcolumn derivatization techniques each have specific disadvantages associated with their use [17]. For precolumn derivatization, the problems include:

1. Sample preparation may be time-consuming and labor-intensive.

2. Byproducts may be formed as a function of the reaction period, which is often long.

Reproduced with permission of the copyright owner. Further reproduction prohibited without permission.

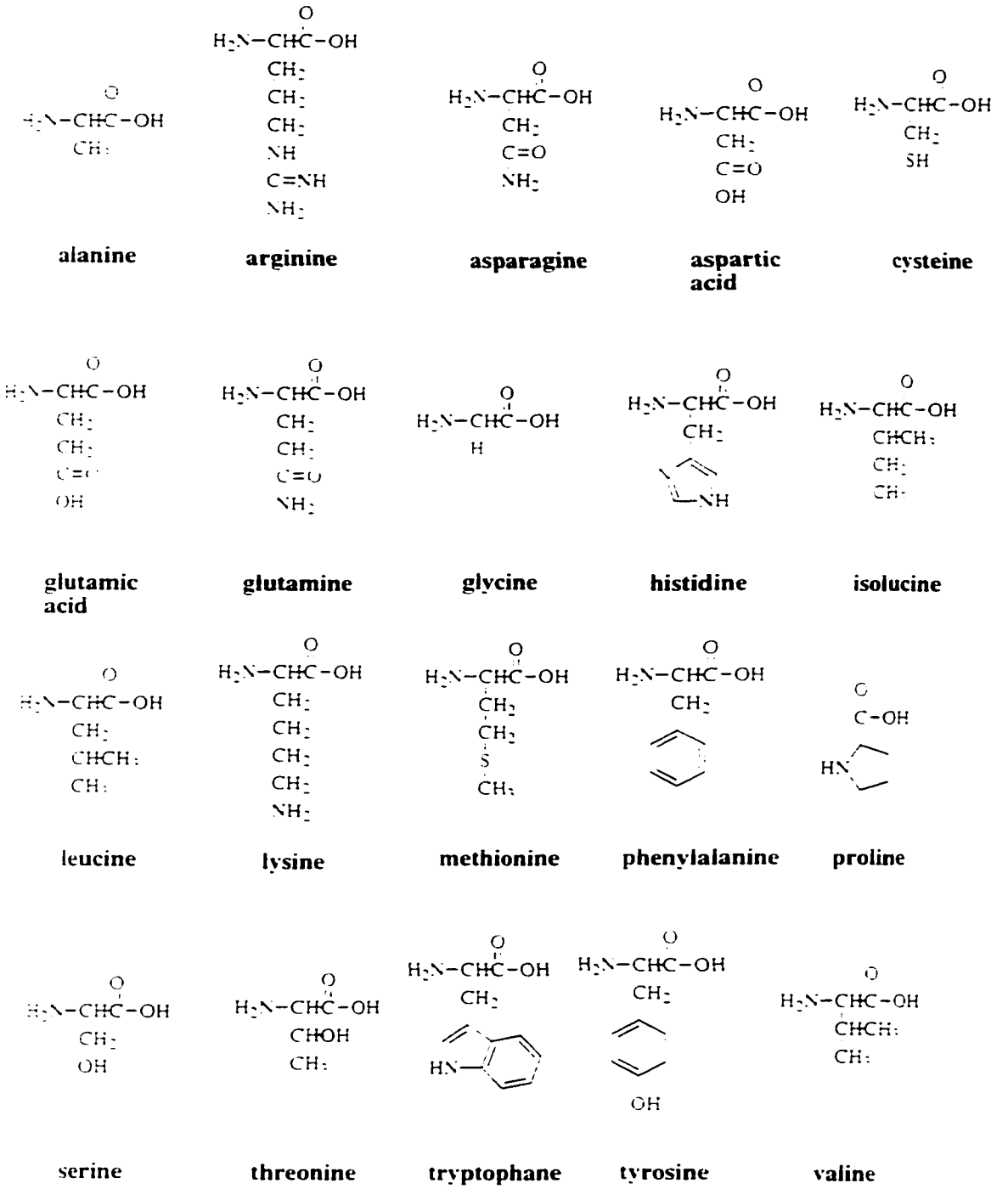

Figure 1.1: Representative molecular structures of several natural amino acids

Reproduced with permission of the copyright owner. Further reproduction prohibited without permission.

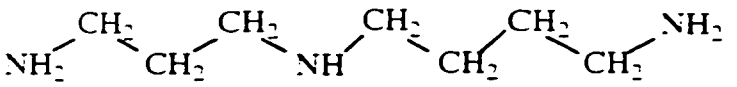

Spermidine

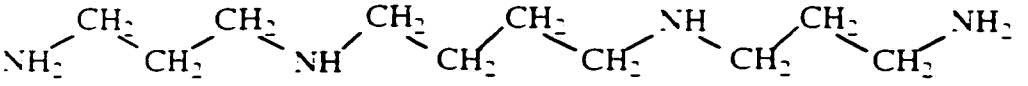

Spermine

Figure 1.2: Molecular structures of selected biogenic polyamines

Reproduced with permission of the copyright owner. Further reproduction prohibited without permission.

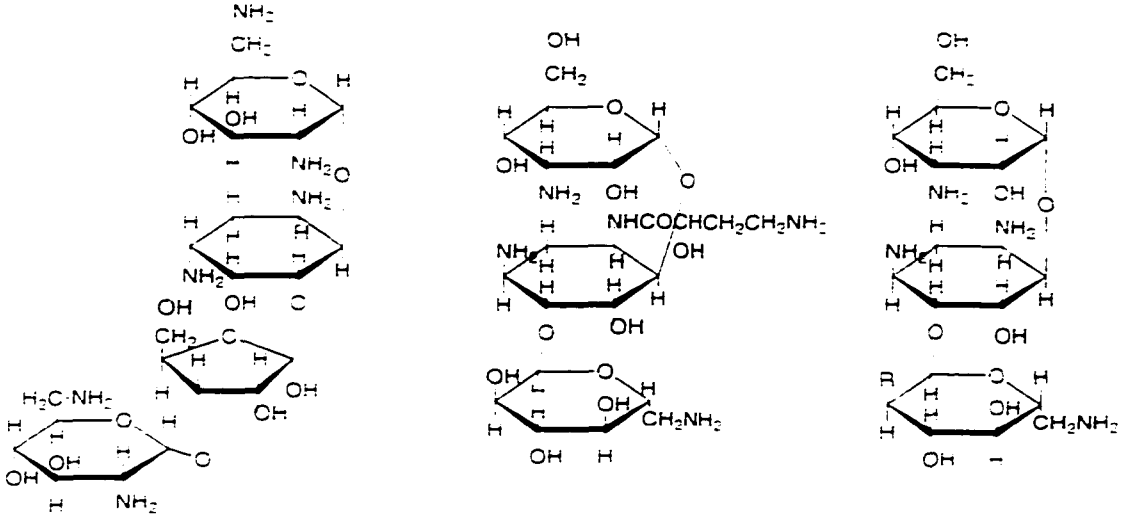

Neomycin **Amikacin** **R=OH Kanamycin A**
R=NH_2 Kanamycin B

Figure 1.3: Molecular structures of selected aminoglycosides

Reproduced with permission of the copyright owner. Further reproduction prohibited without permission.

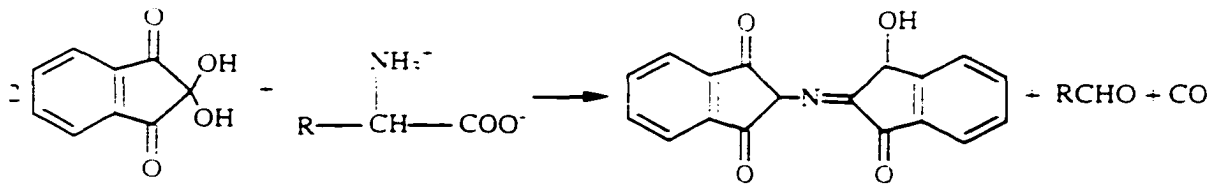

(a)

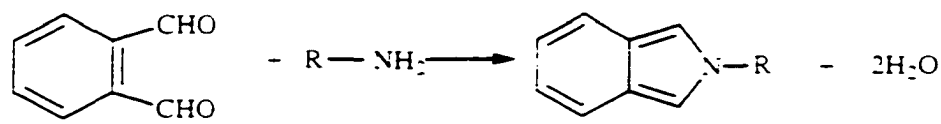

(b)

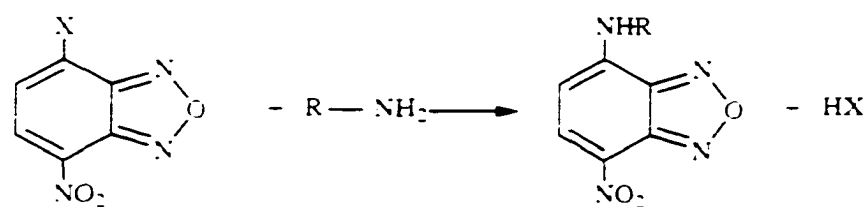

X = Cl or F

(c)

Figure 1.4: (a) The derivatization reaction of ninhydrin with amino acids: (b) and (c) The derivatization reactions of o-phthaldehyde and NBD-halide with amino-containing compounds.

Reproduced with permission of the copyright owner. Further reproduction prohibited without permission.

This results in the presence of additional chromatographic peaks, which may mask the presence of the analytes. Chromatographic peaks due to an excess of the derivatization reagent may also be present.

3. The derivatives may degrade under the specified chromatographic conditions.

4. The various sample compounds become more similar by derivatization, so the chromatographic selectivity may be lower.

For postcolumn derivatization, the disadvantages include:

1. Additional hardware is often required and troubleshooting may be more complex. A block diagram of a typical postcolumn reaction setup is shown in Figure 1.5. A specially designed postcolumn reactor is generally placed between the mixing tee and the detector. The device should have a sufficient volume to enable the reaction to proceed to a fixed endpoint. A conventional postcolumn reaction may take up to 5 minutes to yield a detectable product. For example, if the total flow rate (HPLC) of a system is 2 ml/min, a reaction that requires one minute for completion requires a reactor with a 2 ml volume. Figure 1.6 gives several types of postcolumn reactors. The simplest postcolumn reactor is a length of open tubing containing the volume required for the reaction to reach its endpoint. Construction of knitted open - tubular (KOT) reactors were described [18, 19] and are commercially available from several vendors. As an alternative to open-tubular reactors, columns packed with inert glass beads provided somewhat better mixing ability

Reproduced with permission of the copyright owner. Further reproduction prohibited without permission.

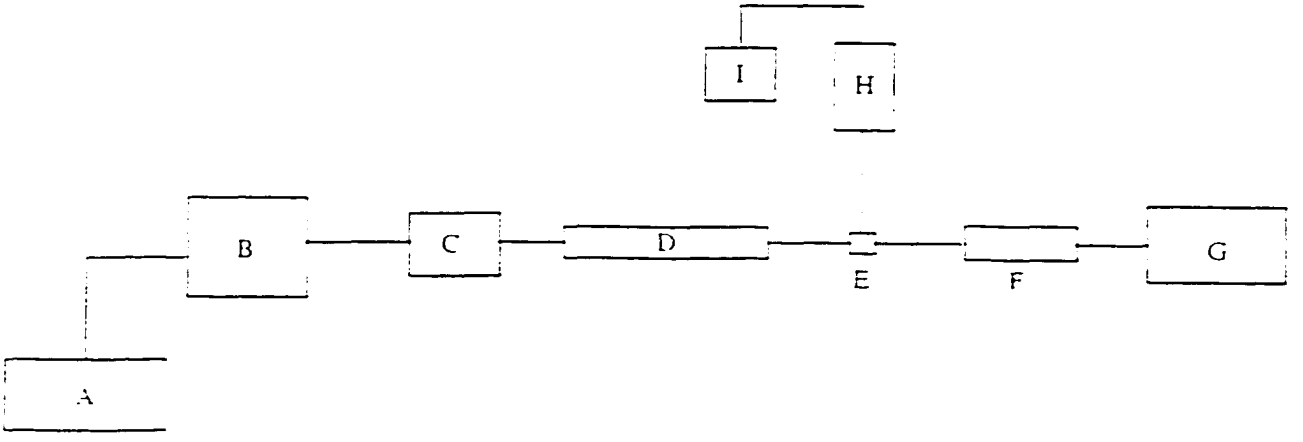

Figure 1.5: Block diagram of a typical postcolumn reaction system. (A) Mobile phase reseervoir. (B) HPLC pump. (C) injector. (D) column. (E) mixing tee. (F) reactor. (G) detector. (H) postcolumn reagent pump. and (I) postcolumn reagent reservoir.

Reproduced with permission of the copyright owner. Further reproduction prohibited without permission.

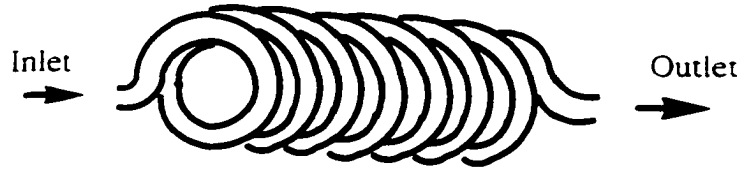

(a)

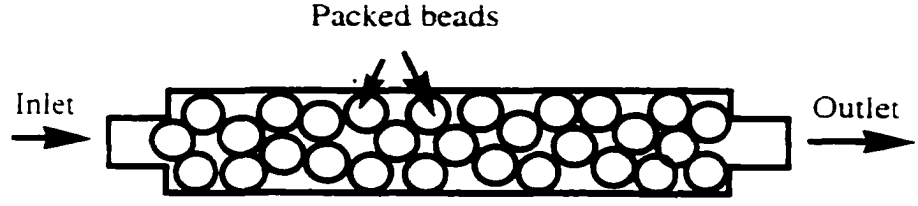

(b)

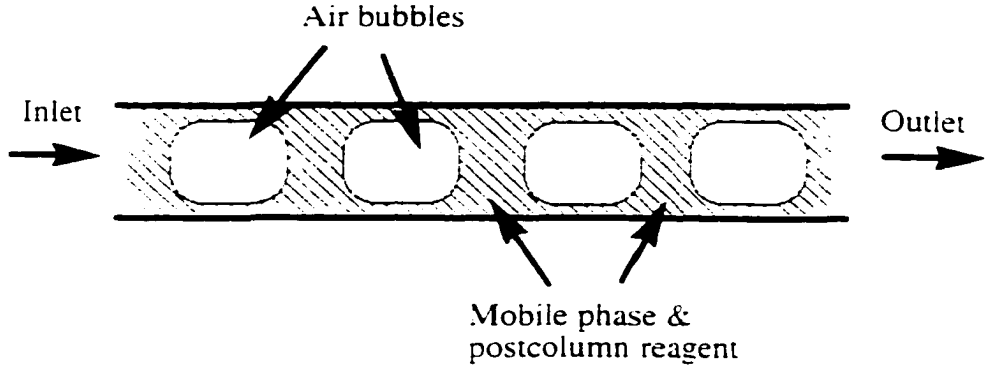

(c)

Figure 1.6: Schematics of postcolumn reactor. (a) Open-tubular reactor; (b) packed-bed reactor; (c) segmented flow reactor.

Reproduced with permission of the copyright owner. Further reproduction prohibited without permission.

compared to KOT reactors [20]. Segmented flow reactors have been successfully used for reaction times of up to 20 minutes [21]. Such systems are based on segmenting the reaction mixture (column effluent plus reagents) with air bubbles. The air bubbles significantly reduce axial dispersion and thus minimize bandbroadening. Unfortunately, such systems require additional specialized hardware to introduce the air segments and remove the bubbles prior to detection. Debubbling is necessary to minimize detector noise. Such hardware is not readily available, and as a consequence, segmented-stream HPLC reactors have not found widespread application. An additional problem is that many postcolumn reagents such as o-phthaldehyde and ninhydrin are air sensitive [22]. Therefore an inert gas supply should be used to assure the reagent stability in the reservoir, which also adds to the complication of the instrumentation.

2. The addition of a postcolumn reactor adds extracolumn bandbroadening which negatively affects the chromatographic separation efficiency by obscuring separation achieved by the HPLC column. The more postcolumn reaction volume added, the more substantial the extracolumn bandbroadening. Figure 1.7 demonstrates several types of bandbroadening processes which may occur during the chromatographic separation. The principles for these bandbroadening apply to the bandbroadening processes taking place in the postcolumn reactor. For the open-tubular reactor, longitudinal diffusion of the analyte molecules along the column dominates the extracolumn bandbroadening. On the other hand, for a packed-bed reactor, eddy diffusion and mass transfer in the packed

Reproduced with permission of the copyright owner. Further reproduction prohibited without permission.

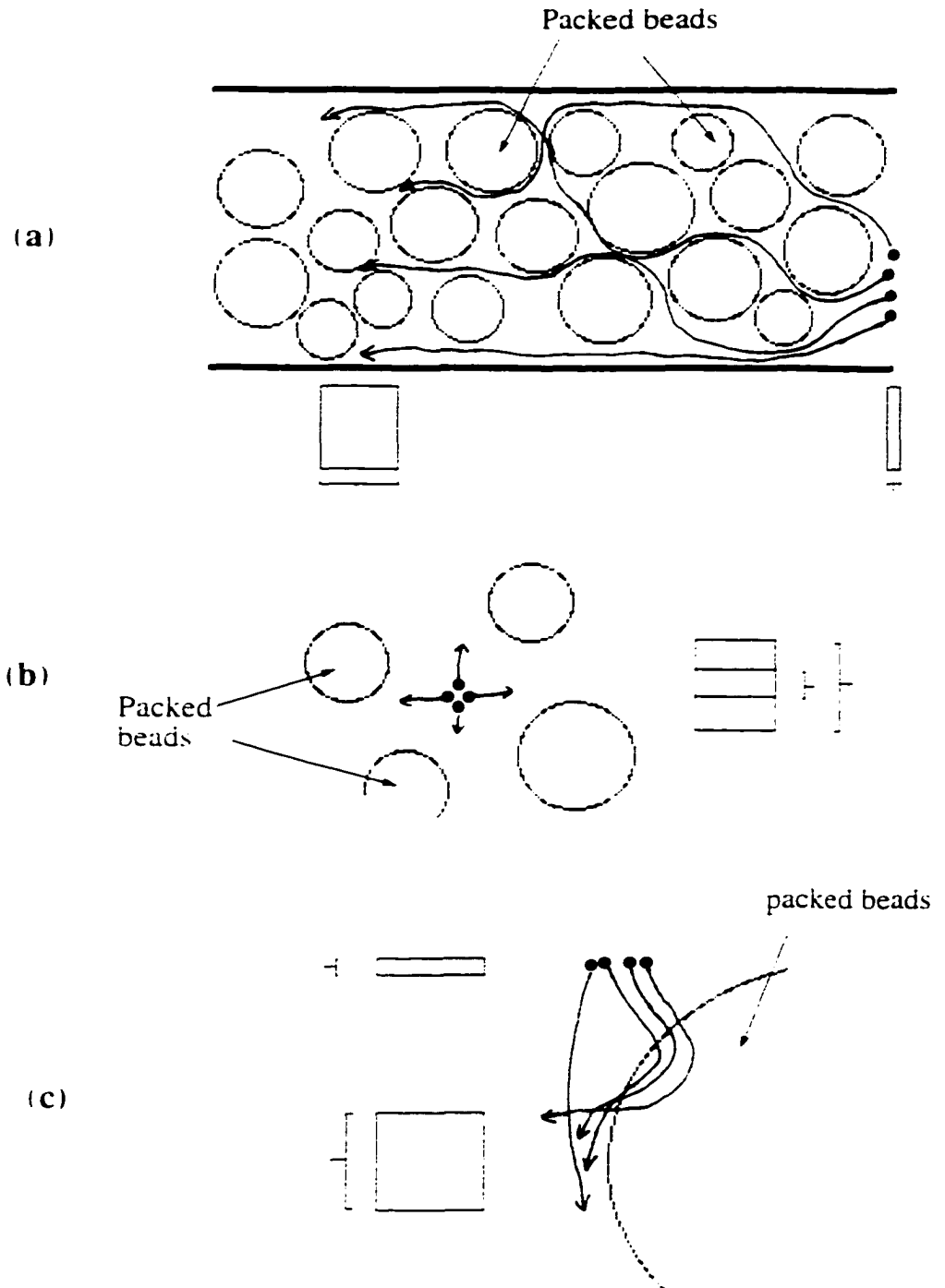

Figure 1.7: Bandbroadening processes: (a) eddy diffusion - analyte molecules take different routes to circumnavigate the beads. (b) diffusion in the mobile phase. (c) mass transfer in stagnant mobile phase in pores. The short bracket indicates initial bandwidth, the broad final bandwidth.

Reproduced with permission of the copyright owner. Further reproduction prohibited without permission.

beads also contribute to the extracolumn bandbroadening.

Since it would be preferable to detect the amino group-containing compounds without needing derivatization, a variety of efforts have been expended to seek nonderivatization methods to detect these compounds following HPLC separation. Chemiluminescence detection, based on a chemiluminescent oxidation-reduction reaction with tris(2,2'-bipyridyl) ruthenium(III), has been achieved for a number of amino group-containing compounds including amino acids [23 - 26], aliphatic amines [27] and aminoglycosides [28]. This promising approach to detection is still under intense investigation, with efforts being made to address several issues, including the complexity of the instrumentation required. Indirect UV-VIS and fluorescence detection of amino acids has been utilized in both HPLC [29, 30] and CZE [31] for detecting amino acids and aliphatic amines. This indirect approach to detection is based on the property that the amines and amino acids exist as ions in solutions of appropriate pH. A UV absorbing or fluorescing ionic species is added to the mobile phase, not only to elute the analytes but also to provide a means for monitoring the presence of the analytes. As the ionized amines elute from the column, the concentration of the counter ions in the mobile phase, which are being monitored, decreases to maintain electroneutrality in the mobile phase. However, one problem with this approach is that it suffers from high detection limits, which limits its application for real biological samples. Matrix interference may also be substantial.

Over the past decade, much interest has been shown in the development of pulsed electrochemical detection for amino group-containing compounds [32 - 34]. In this

Reproduced with permission of the copyright owner. Further reproduction prohibited without permission.

detection mode, current is integrated continuously during a cycle in which the electrode is oxidized and then reduced to the original state. The advantage of pulsed electrochemical detection is that by applying a reducing potential in the second half of a cycle, the oxide layer formed on the surface of the electrode by the oxidizing potential in the first half of the cycle is effectively removed. Thus, poisoning of the electrode surface is avoided and the sensitivity of the electrode is maintained.

Several methods have been reported for amino group-containing compounds based on their ability to bind to transition metal ions. Most of the natural amino acids are bidentate ligands for transition metal ions with both the carboxyl group and the amino group coordinating to the transition metal ion. One of these detection methods takes advantage of the fact that transition metal ions such as Cu^{2+} and Co^{2+} are necessary catalysts for the luminol chemiluminescence reaction [35, 36]. Amino acid complexes of transition metal ions, however, are much less efficient catalysts for the reaction. Detection is based on adding the chemiluminescent reagents to the mobile phase postcolumn. When the separated amino acids elute from the column, they form complexes with the catalytic metal ions, resulting in a loss of the chemiluminescence signal. At least two postcolumn pumps are required to keep the solutions containing the transition metal ions and luminol separated from each other before mixing and entering the detector, due to the short lifetime of chemiluminescence, which increases the instrumental complexity. Relatively high detection limits were obtained at the nmol injected level, due to the high chemiluminescence background and possibly the fact that luminol also complexes

Reproduced with permission of the copyright owner. Further reproduction prohibited without permission.

transition metal ions.

Carmelita and Frei studied a detection method employing a copper-selective electrode as a potentiometric detector [37, 38]. A solution containing Cu^{2+} ion was added to the eluent postcolumn and the loss of Cu^{2+} activity resulting from the formation of the amino acid - Cu(II) complex was taken as an indication of the amino acid concentration of the column effluent. The electrode surface is easily covered with a layer of Cu(II) oxide or Cu(II) hydroxide in either a weakly acidic or an alkaline buffer solution, which makes the electrode reaction kinetically slow. Extra postcolumn mixing volume is required for complete reaction of the amino acids, resulting in additional extracolumn bandbroadening. Recently, another detection method exploited the fact that amino acid - Cu(II) complexes have strong UV-VIS absorption in the region between 230-250 nm [39]. In this approach to detection, Cu^{2+} ion was added to the mobile phase and the amino acids were separated as Cu(II) complexes, which are detectable with a conventional UV-VIS detector.

The interactions between fluorescent agents and transition metal ions have been studied for a long time. Calcein, a fluorescein derivative, has been used for dozens of years as a fluorescence indicator to selectively titrate transition metal ions. At high pH, calcein is nonfluorescent but it forms fluorescent complexes with calcium and other alkaline earths [40]. Although the use of calcein for determination of Ca^{2+} has received the most attention [41], it has also been suggested as a reagent for Cd^{2+} [42], for Al^{3+}, for other alkaline earths, Zn^{2+}, Co^{2+}, Cu^{2+}, and Ni^{2+} [43]. The analyses of Co^{2+}, Cu^{2+}, and Ni^{2+} are based on the observation that they form nonfluorescent complexes at neutral pHs

Reproduced with permission of the copyright owner. Further reproduction prohibited without permission.

where calcein by itself fluoresces strongly. Morin is a widely used spot test reagent for metal ions such as Al^{3+} [44]. Fluorescing weakly by itself but forming highly fluorescent complexes with Al^{3+}, morin has been used as a reagent for the fluorometric analysis of Al^{3+} for many years [45]. Optical sensors for transition metal ions were also developed based on measuring the fluorescence of complexes of transition metal ions with immobilized calcein [46] and morin [47]. In recent years, a variety of fluorescent ion indicators have been developed for selective detection of heavy metal ions including Hg^{2+}, Cu^{2+}, Ni^{2+} and Cd^{2+} by Molecular Probes, Inc. (Eugene, OR, USA) [48]. Either fluorescence or fluorescence quenching can result from the fluorescent agents binding to the metal ions [49]. The decrease or increase in fluorescence intensity can be taken as a measure of the presence of the metal ions.

The research presented here, was aimed at developing an indirect fluorescence detection method for amino group-containing compounds, which have a good binding ability for transition metal ions. Upon the addition of an appropriate amount of metal ions, the fluorescence of a selected fluorescent agent will be effectively quenched due to the complexation between the compound and the metal ions. The degree of fluorescence quenching is related to a number of factors, such as the stoichiometric ratio between concentrations of metal ions and the fluorescent agent, the solution pH, and other experimental conditions. These conditions will be optimized to assure the fluorescence is most efficiently quenched by a minimum amount of metal ions, so that upon addition of the amino group-containing analytes, they will bind to the ions and liberate the

Reproduced with permission of the copyright owner. Further reproduction prohibited without permission.

fluorescent agents. Upon displacement of the fluorescent agent from the complex, the fluorescence will be recovered, with the increase in fluorescence being taken as a measure of the presence of the analytes.

A detection scheme based on this displacement reaction was developed for HPLC. The detection of several amino group-containing classes of compounds was explored. The detection performance was evaluated and compared to other detection methods.

The developed method has the following advantages over traditional derivatization detection methods, chemiluminescence methods, and indirect UV-VIS and fluorescence methods:

1. Compared to conventional postcolumn derivatization reactions, which always require an additional postcolumn volume for the reaction to take place, the proposed indirect fluorescence detection can be accomplished without the need for large postcolumn volumes, which limits the extracolumn bandbroadening.

2. Compared to chemiluminescence detection methods, in which the chemiluminescence reactions always have a very short lifetime, the volume delay between the postcolumn mixer and the flow cell is no longer a problem. A small delay between the mixer and the detection flow cell may cause a significant signal intensity decrease when using a chemiluminescence detection method, because a chemiluminescence signal is triggered by a chemical reaction between the analyte and the postcolumn reagent when they mix, which

Reproduced with permission of the copyright owner. Further reproduction prohibited without permission.

decays quickly. In the method described here, the fluorescence signal is excited by UV emission directly applied to the flow cell, rather than a chemical reaction as in chemiluminescence.

3. Compared to most indirect UV-VIS and fluorescence detection methods, the detection signal is a fluorescence signal out of a relatively "dark" background, rather than a negative signal out of a high background baseline, so the shot noise level, which originates from charged particle movement in a circuit and is proportional to the square root of the total photon counting, should be significantly lower than the detection approaches with a high background [50].

As one of the few naturally fluorescing amino acids, tryptophan (Trp) residues usually dominate the fluorescence of proteins [51]. Both the fluorescence lifetime and quantum yield of Trp residues are strongly influenced by the nature of its chemical environment. This sensitivity is widely exploited through the use of Trp as an intrinsic fluorescence probe for structural and conformational studies of proteins and polypeptides in solution [52]. Fluorescence quenching of Trp by heavy metal ions such as Hg^{2+} and Cu^{2+}, was reported earlier [53 - 56]. These studies, however, were still quite preliminary. Work still needs to be performed to further clarify the relationship between the formation of the complexes and the extent of fluorescence quenching. Although it was reported that fluorescence quenching depends highly on the solution pH [54], no studies have been done to explain this phenomenon in terms of the solution equilibrium chemistry.

Reproduced with permission of the copyright owner. Further reproduction prohibited without permission.

Systematic studies were carried out both theoretically and experimentally to understand the fluorescence characteristics of both free Trp and Trp in the presence of the quencher. Studies were also carried out to optimize the detection conditions for the amino group-containing analytes in the proposed detection scheme.

Reproduced with permission of the copyright owner. Further reproduction prohibited without permission.

Chapter 2

Understanding the Solution Chemistry of a Cu(II)-Tryptophan System and Its Impact on Tryptophan Fluorescence

2.1 Introduction

Tryptophan (Trp) is one of the few naturally fluorescing amino acids. The fluorescence of proteins is usually dominated by that of the tryptophan residues [51]. Both the fluorescence lifetime and quantum efficiency of Trp are affected by the nature of its chemical environment [57]. The emission maximum and quantum yield of Trp residues in proteins can vary greatly. These variations are due to the three-dimensional structure of the proteins [58]. The sensitivity of Trp fluorescence to its local environment has provided a means to study protein conformational transitions, subunit association, substrate binding, all of which can affect the local environment surrounding the indole ring in Trp [59, 60]. In addition to being affected by nearby groups in proteins, Trp fluorescence also appears to be sensitive to externally-added quenchers. Steiner and Chen first discovered that Trp fluorescence is quenched by heavy metal ions, such as Hg^{2+}, Cu^{2+}, Ni^{2+} and Cd^{2+}, with Cu^{2+} and Hg^{2+} having the best quenching efficiencies [53, 61]. Different mechanisms have been proposed to explain this phenomenon of fluorescence quenching. An electron transfer theory has been suggested [53] to attribute the fluorescence quenching to electron transfer from the excited state of the indole ring to the

Reproduced with permission of the copyright owner. Further reproduction prohibited without permission.

transition metal ions, which serve as electron scavenger. In another theory [62], the failure of transition-metal complexes to fluoresce has been attributed to the paramagnetic and heavy-atom effect of the transition metal ion, namely spin-orbital coupling, which populates low-lying, high-multiplicity states that are then deactivated by intersystem crossing. In both theories, it was claimed that fluorescence quenching is in close relation to the formation of transition metal ion - Trp complexes. However, quantitative studies concluded that there is only a 1:1 stoichiometric ratio for the fluorescence quenching between the transition metal ions and Trp [53, 56]. That is to say, each transition metal ion only quenches the fluorescence of one Trp molecule, which was contrary to the well-known observation that heavy metal ions such as Cu^{2+} and Hg^{2+}, tend to coordinate to two amino acid residues [63]. Recent studies indicate there is a more than a 1:1 stoichiometric ratio for the fluorescence quenching by transition metal ions [54, 55], which means each transition metal ion can quench the fluorescence of more than one Trp moiety. No efforts have been made to explain this observation, and no systematic work has been done to clarify the solution chemistry in a transition metal ion - Trp system. It is also unclear that L-Trp fluorescence quenching by transition metal ions such as Cu^{2+} and Ni^{2+} is highly pH - dependent [54, 55], with the quenching most efficient within a narrow pH range.

In this study, both experimental and theoretical studies were conducted to optimize the fluorescence quenching of Trp by Cu^{2+} ion. As a well-studied amino acid, the solution equilibrium data involving Trp are available in the literature [63], which provided a basis

Reproduced with permission of the copyright owner. Further reproduction prohibited without permission.

for performing theoretical calculations to understand the solution chemistry of the Cu(II) - Trp system. The problem was approached by taking into consideration the relevant equilibria in the solution which can affect the interaction between Cu(II) and Trp. This study also paved the way for a systematic optimization of the fluorescence interaction between fluorescent agents and the transition metal ions.

The ratio of $[Cu^{2+}]$ [Trp] is crucial in the detection system proposed in this study. It is understood from the principle on which this detection scheme is based, that the optimum $[Cu^{2+}]$ [Trp] ratio should be one in which the least amount of Cu^{2+} ion results in the most efficient quenching of Trp. This approach allows one to obtain a relatively "dark" background level, and also ensures that the introduction of analytes into the system will lead into the most sensitive fluorescence increase, because every added analyte molecule will compete with the Trp for binding the Cu^{2+} ions in the solution. Cu^{2+} was chosen because previous studies showed it has a better quenching effect on Trp fluorescence than most of the other transition metal ions [53]. On the other hand, a major reason to choose Trp in this study was that as a bidentate ligand with one amino group and one carboxyl group capable of binding to transition metal ions, it provides a comparable affinity for these metal ions as do an important class of analytes - the natural amino acids. Compared to other fluorescent agents which have more than two binding groups for metal ions, this will allow Trp to be more easily displaced from the transition metal - Trp complex by analytes such as natural amino acids.

Reproduced with permission of the copyright owner. Further reproduction prohibited without permission.

2.2 Material and Methods

2.2.1 Materials

L-tryptophan (L-Trp) (manufacturer's stated purity, 99% by TLC) was purchased from Sigma (St. Louis, MO, USA). Reagent-grade copper sulfate and sodium borate ($Na_2B_4O_7 \cdot 10H_2O$) were purchased from Baker (Phillipsburg, NJ, USA). The deionized water used in the preparation of standard solutions was obtained from a Milli-Q water system (Millipore, Bedford, MA, USA). Reagent grade N-(2-Hydroxyethyl) piperazine-N'-(2-ethanesulfonic acid) (HEPES) was obtained from Research Organics (Cleveland, OH, USA). Dilute aqueous solutions of reagent-grade sodium hydroxide (Fisher, Pittsburgh, PA, USA) and hydrochloric acid (Baker, Phillipsburg, NJ, USA) were used to adjust the pH of the solutions. A SIM AMINCO luminescence spectrometer (SIM Instruments Inc., Urbana, IL, USA) was used to obtain the excitation and fluorescence emission spectra. A Perkin-Elmer Model 204 fluorescence spectrophotometer (Norwalk, CT, USA) was used for the rest of the fluorescence studies.

2.2.2 Fluorescence Excitation and Emission Scan of L-Trp

The excitation spectrum of 0.1 mM L-Trp buffered at pH 8.1 with 4 mM sodium borate was measured at an emission wavelength of 350 nm. The emission spectrum of the same solution was measured at an excitation wavelength of 280 nm.The excitation and emission spectra of L-Trp are given in Figure 2.1 and 2.2, respectively.

Reproduced with permission of the copyright owner. Further reproduction prohibited without permission.

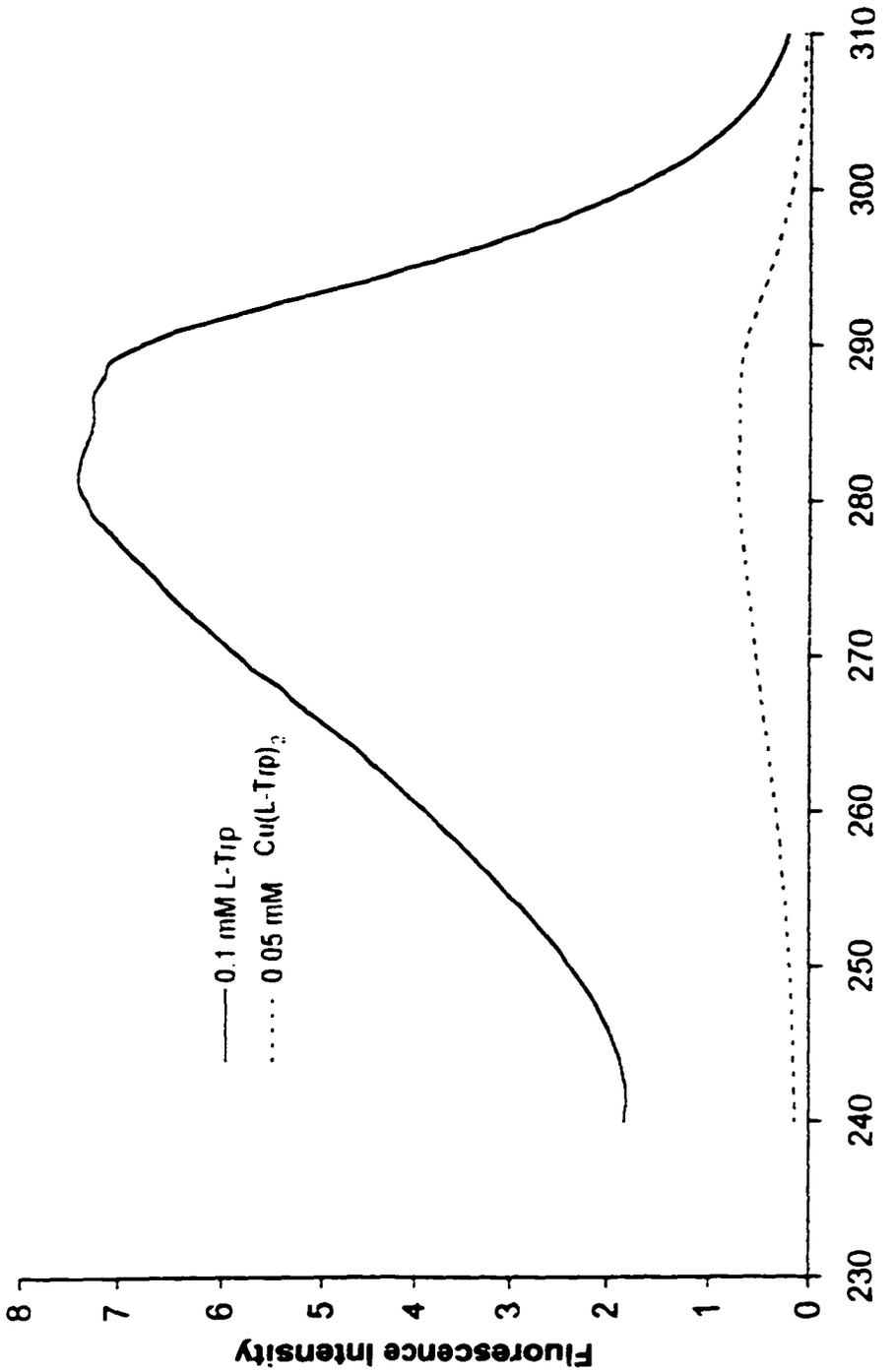

Figure 2.1: Excitation scan of 0.1 mM L-Trp and 0.05 mM $Cu(L\text{-}Trp)_2$ at pH 8.1. The emission wavelength was 350 nm.

Reproduced with permission of the copyright owner. Further reproduction prohibited without permission.

Reproduced with permission of the copyright owner. Further reproduction prohibited without permission.

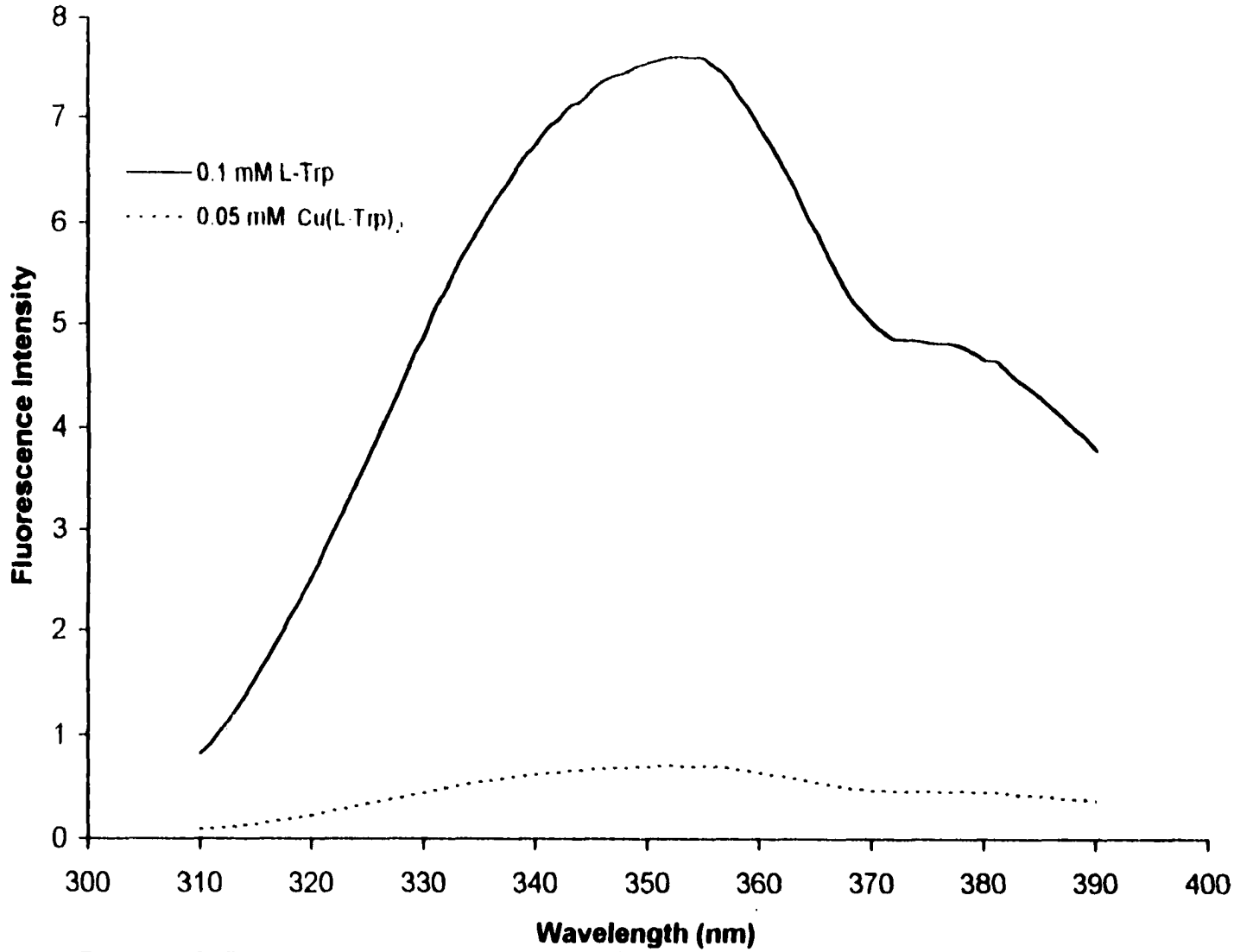

Figure 2.2: Fluorescence spectra of 0.1 mM L-Trp and 0.05 mM $Cu(L\text{-}Trp)_2$ at pH 8.1. The excitation wavelength was 280 nm.

2.2.3 Fluorescence Excitation and Emission Scan of $Cu(L\text{-}Trp)_2$

A solution of 0.05 mM $Cu(L\text{-}Trp)_2$ was prepared by dissolving the appropriate masses of solid L-Trp and $CuSO_4 \cdot 5H_2O$ in sodium borate solution. The excitation spectrum of 0.05 mM $Cu(L\text{-}Trp)_2$ buffered at pH 8.1 with 4 mM sodium borate ($Na_2B_4O_7$) was measured at an emission wavelength of 350 nm. The emission spectrum of the same solution was measured at an excitation wavelength of 280 nm. The excitation and emission spectra of $Cu(L\text{-}Trp)_2$ are given in Figure 2.1 and 2.2, respectively.

2.2.4 Fluorescence of 0.1 mM L-Trp as a Function of pH

A solution of 0.1 mM L-Trp was prepared by dissolving the appropriate mass of solid L-Trp in deionized water. The pH of the solution was adjusted in the pH range of 1.8-11.0. Fluorescence data of solutions at different pHs were measured. The excitation and emission wavelengths were set at 280 nm and 350 nm, respectively. The fluorescence profile of 0.1mM L-Trp as a function of pH is given in Figure 2.3.

2.2.5 Fluorescence of 0.05 mM $Cu(L\text{-}Trp)_2$ as a Function of pH

A solution of 0.05 mM $Cu(L\text{-}Trp)_2$ was prepared by dissolving the appropriate masses of solid L-Trp and $CuSO_4 \cdot 5H_2O$ in deionized water. The pH of the solution was adjusted in the pH range of 1.8 - 11.0. Fluorescence data of solutions at different pHs were measured. The excitation and emission wavelengths were set at 280 nm and 350 nm.

Reproduced with permission of the copyright owner. Further reproduction prohibited without permission.

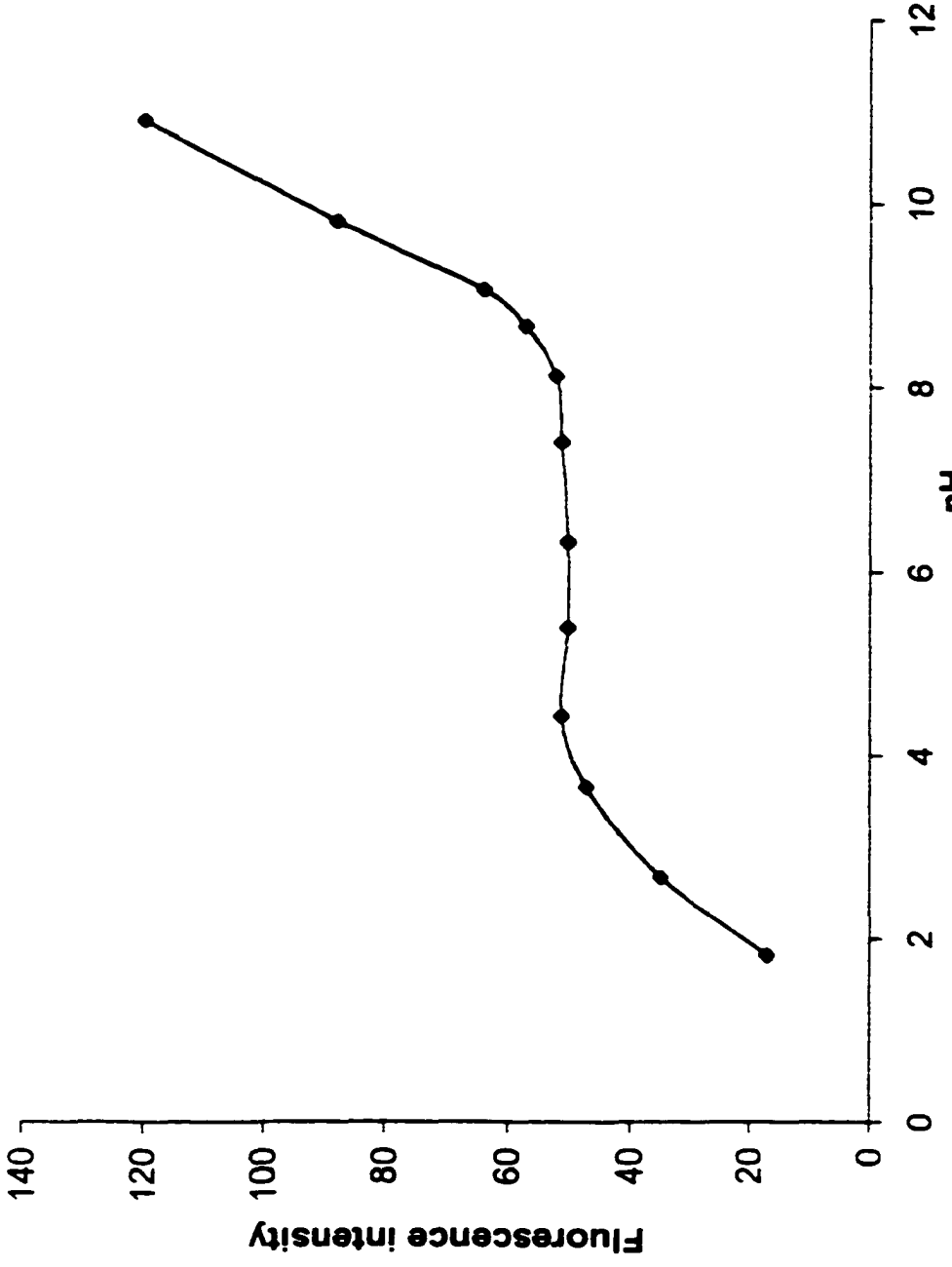

Figure 2.3: Fluorescence as a function of pH of L-Trp. The exicitation and emission wavelengths were 280 nm and 350 nm, respectively.

Reproduced with permission of the copyright owner. Further reproduction prohibited without permission.

respectively. The fluorescence profile of 0.05 mM Cu(L-Trp)$_2$ as a function of pH is given in Figure 2.4.

2.2.6 Fluorescence of 0.05 mM Cu(L-Trp)$_2$ with the Presence of 1 mM EDTA as a Function of pH

A solution of 0.05 mM Cu(L-Trp)$_2$ containing 1mM EDTA was prepared by dissolving the appropriate masses of solid L-Trp, $CuSO_4 \cdot 5H_2O$ and EDTA in deionized water. The pH of the solution was adjusted in the pH range of 1.8-11.0. Fluorescence data of solutions at different pHs were measured. The excitation and emission wavelengths were set at 280 nm and 350 nm, respectively. Figure 2.5 gives the fluorescence profile of a 0.05 mM Cu(L-Trp)$_2$ solution containing 1mM EDTA.

2.2.7 "Fluorescence Titration" of 0.1 mM L-Trp by Cu(II) with Sodium Borate as the Buffer

Solutions with different concentrations of $CuSO_4$ were added to a L-Trp solution buffered with 4 mM sodium borate ($Na_2B_4O_7$) at pH 8.1, appropriate amounts of deionized water were added to the solution to make the concentration of L-Trp 0.1 mM for all of the solutions. Fluorescence data of the solutions were measured. The excitation and emission wavelengths were set at 280 nm and 350 nm, respectively. Because the fluorescence of the L-Trp solution changes with the addition of Cu(II), this resulted in the "fluorescence titration" of 0.1 mM L-Trp with Cu^{2+} ion. The relationship between the

Reproduced with permission of the copyright owner. Further reproduction prohibited without permission.

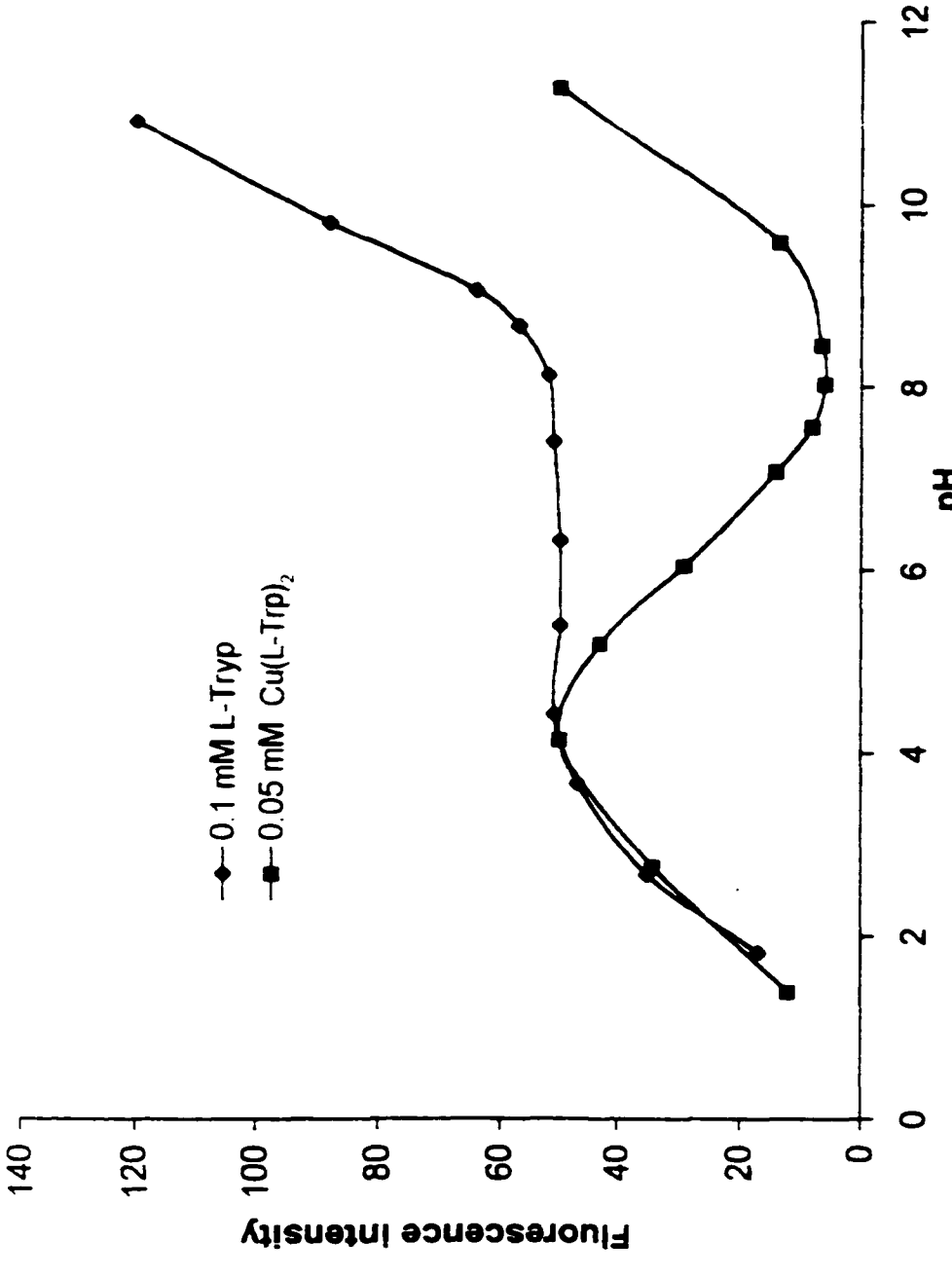

Figure 2.4: Fluorescence as a function of pH of L-Trp and Cu(L-Trp)$_2$. The exicitation and emission wavelengths were set at 280 nm and 350 nm, respectively.

Reproduced with permission of the copyright owner. Further reproduction prohibited without permission.

Reproduced with permission of the copyright owner. Further reproduction prohibited without permission.

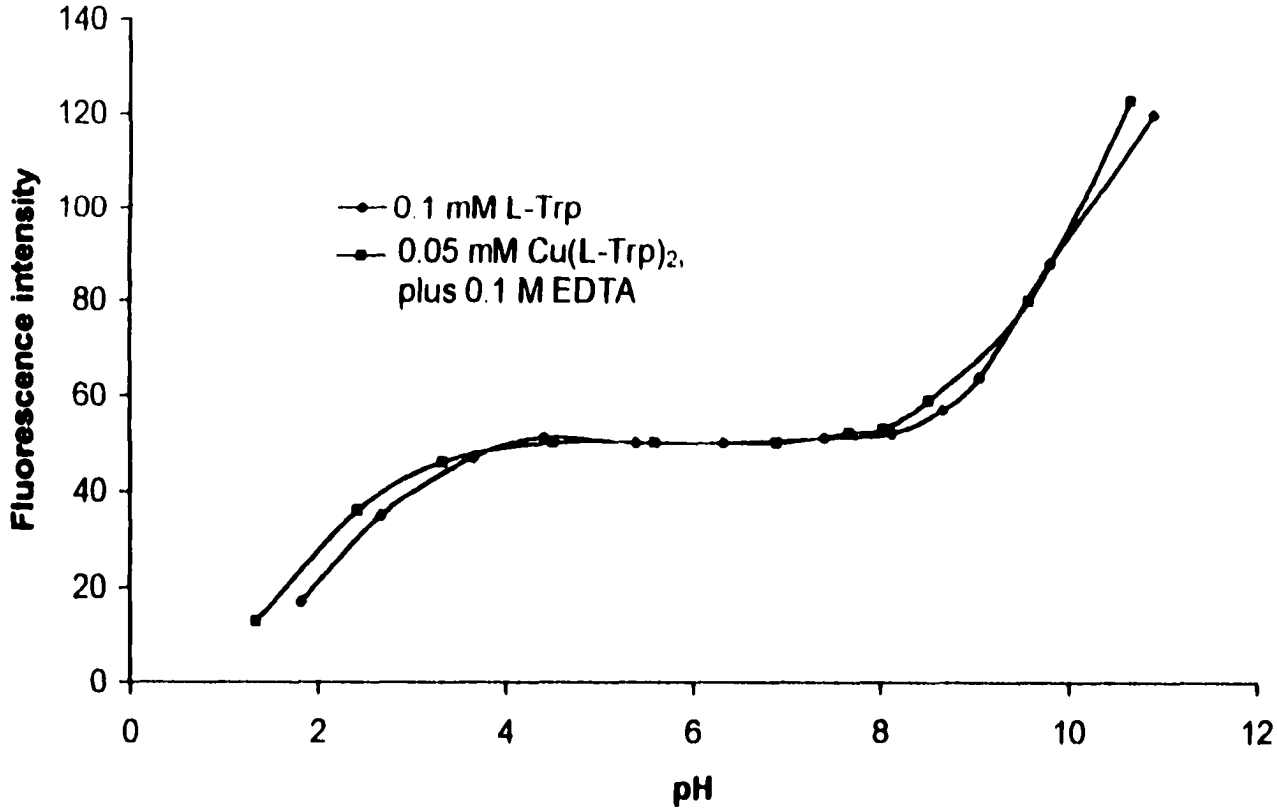

Figure 2.5: Comparison of fluorescence profiles of 0.1 mM L-Trp and 0.05 mM $Cu(L\text{-}Trp)_2$ with the presence of 0.1 mM EDTA. The exicitation and emission wavelengths were 280 nm and 350 nm, respectively.

concentration of Cu^{2+} ion and the solution fluorescence is presented in Figure 2.6. with sodium borate ($Na_2B_4O_7$) as the pH buffer.

2.2.8 "Fluorescence Titration" of 0.1 mM L-Trp by Cu(II) with HEPES as the Buffer

Solutions with different concentrations of $CuSO_4$ were added to a L-Trp solution buffered with HEPES. Appropriate amounts of deionized water were added to the solution to maintain the concentration of L-Trp at 0.1 mM for all of the solutions. The fluorescence data of the solutions with different concentrations of HEPES at pH 8.1 and 7.0 were measured with the excitation and emission wavelengths set to 280 nm and 350 nm. respectively. The "fluorescence titration" data are presented in Figure 2.7.

2.3 Results and Discussions

The molecular structure of Trp is given in Figure 1.1. Based on the fluorescence excitation and emission data for L-Trp as presented in Figures 2.1 and 2.2. the optimum excitation and emission wavelengths are 280 nm and 350 nm. respectively. Fluorescence data obtained for $Cu(L\text{-}Trp)_2$ presented in Figures 2.1 and 2.2 indicate there are no emission and excitation wavelength shifts due to complexation with Cu^{2+}. which means the observed fluorescence intensity decrease for $Cu(L\text{-}Trp)_2$ is due to fluorescence quenching. rather than fluorescence wavelength shifts. Based on these results. fluorescence excitation and emission wavelengths were set at 280 nm and 350 nm for all

Reproduced with permission of the copyright owner. Further reproduction prohibited without permission.

Reproduced with permission of the copyright owner. Further reproduction prohibited without permission.

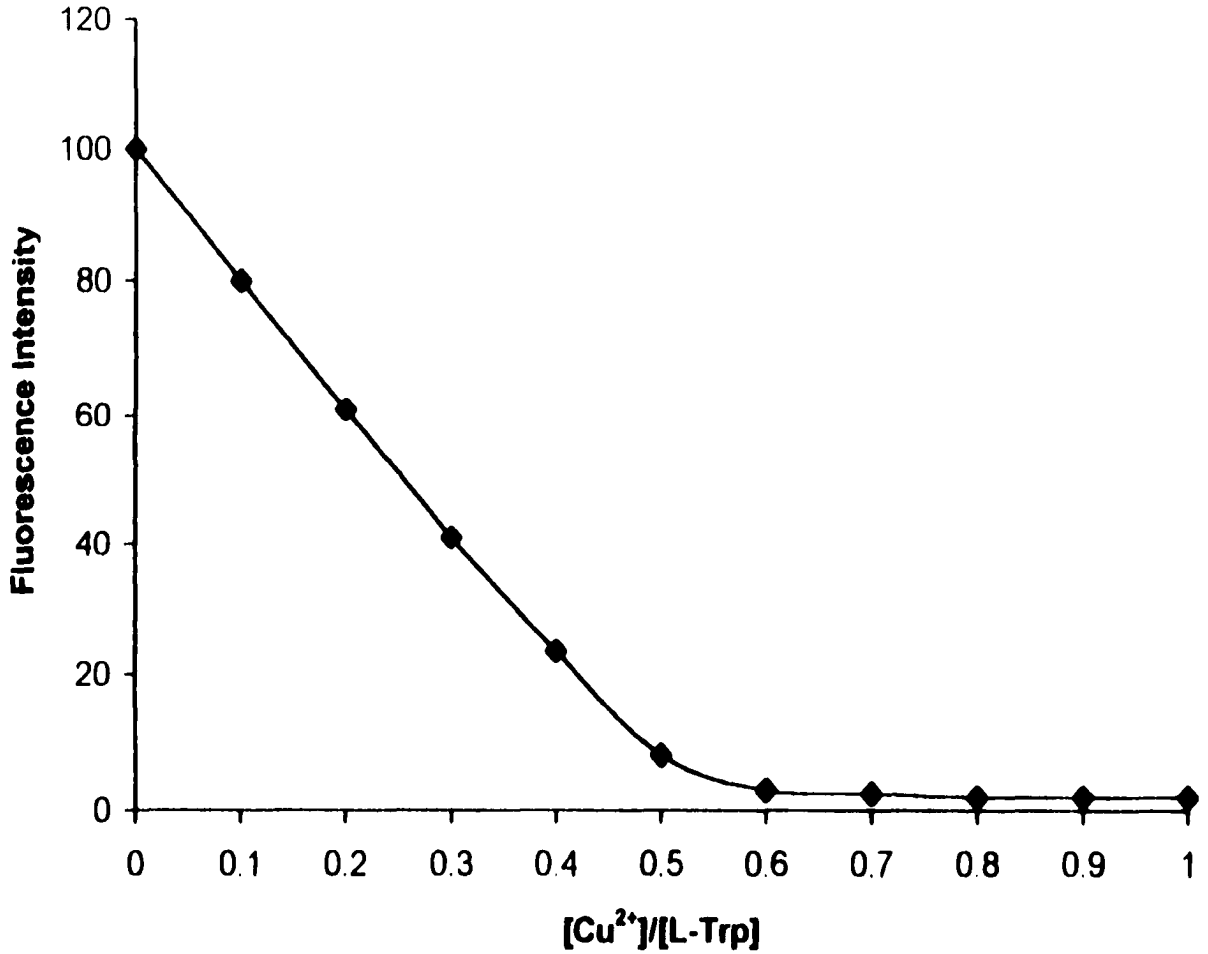

Figure 2.6: Fluorescence quenching of 0.05 mM L-Trp in relation to the concentration of Cu^{2+} . The solutions are buffered with 4mM sodium borate at pH 8.1. The excitation and emission wavelengths were 280 nm and 350 nm, respectively.

Reproduced with permission of the copyright owner. Further reproduction prohibited without permission.

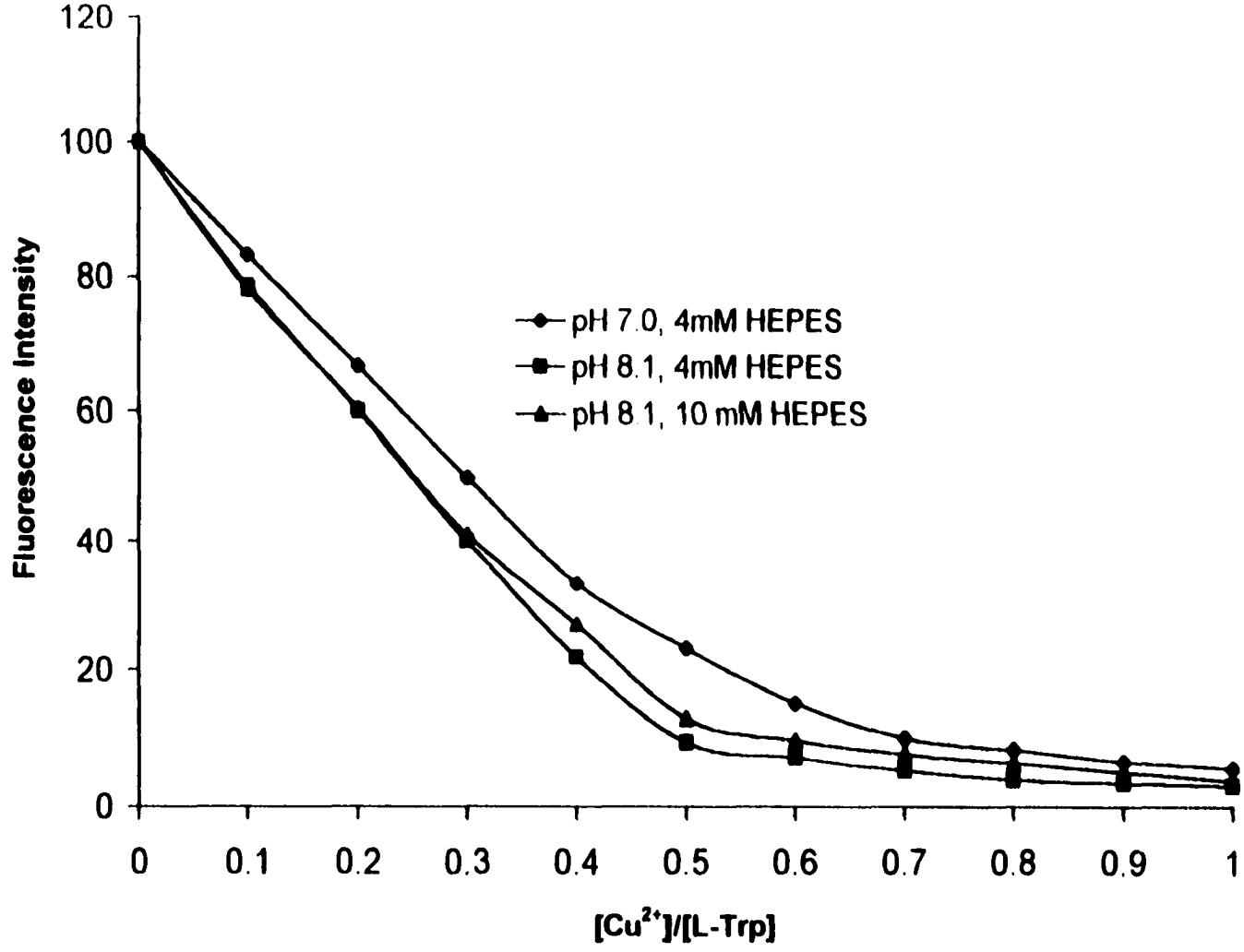

Figure 2.7: "Fluorescence titration" of L-Trp by Cu(II) with HEPES as the buffer. The exicitation and emission wavelengths were at 280 nm and 350 nm, respectively.

studies involving L-Trp.

2.3.1 pH Dependence of the Fluorescence of Free L-Trp

As shown in Figure 2.3, the fluorescence of free L-Trp is highly pH dependent. There are three distinct regions in the L-Trp fluorescence profile as a function of pH. The fluorescence increases from pH 1 to pH 4.2; the fluorescence remains unchanged from pH 4.2 to pH 8.0; and the fluorescence increases significantly from pH 8.0 to pH 11.1.

This pH dependent pattern is in agreement with the observations made earlier [64 - 66]. White [64] noticed the fluorescence of Trp decreases steadily when the solution pH is below 4.0, and the pH of half-quenching (compared to the fluorescence of Trp above pH 4.0) corresponds approximately to the acidic dissociation constant of the carboxyl group in Trp. Fleming etc. found that at pH 11.0 Trp has a significantly longer fluorescence life-time than at pH 7.0 [65 -67]. The fluorescence life-time is generally proportional to the fluorescence quantum efficiency [57]. Weber [68] correlated the Trp fluorescence life-times with the molar ratio between zwitterionic and deprotonated Trp in a narrow pH range from pH 8 - 10 and noticed there is a direct relationship between the fluorescence life-time with the different forms of Trp in the solution. However, a correlation between the fluorescence changes observed and the existence of different forms of Trp in the solution in the whole pH range was not provided.

In fact, as given in Figure 2.3, pH 2.4 and 9.4, around which pHs the L-Trp fluorescence significantly increases as solution pH increases, are the acidic dissociation

Reproduced with permission of the copyright owner. Further reproduction prohibited without permission.

constants of the carboxyl and amino groups in L-Trp. respectively. Keeping in mind there are three forms of L-Trp. protonated L-Trp. zwitterionic L-Trp and deprotonated L-Trp in the solution. a model is proposed to illustrate how the proton equilibria affect the solution. with an attempt made to correlate different forms of L-Trp to different fluorescence efficiencies. The solution fluorescence is expressed as:

$$FlUO = K\,(a * \partial_{H_2A^-} - b * \partial_{HA} - c * \partial_{A^-}) \qquad \text{(Eq. 2.1)}$$

in which a. b. c represent relative fluorescence efficiencies for protonated L-Trp. zwitterionic L-Trp and deprotonated L-Trp. respectively: K is an arbitrary constant. HA represents L-Trp: $\partial_{H_2A^-}$. ∂_{HA}. and ∂_{A^-} are the fractions of the three forms. H_2A^-. HA and A^-. respectively. which can be expressed as:

$$\partial_{H_2A^-} = [H^-]^2 / (K_{a1} * K_{a2} - K_{a1} * [H^-] - [H^-]^2) \qquad \text{(Eq. 2.2)}$$

$$\partial_{HA} = K_{a1} * [H^-] / (K_{a1} * K_{a2} - K_{a1} * [H^-] - [H^-]^2) \qquad \text{(Eq. 2.3)}$$

$$\partial_{A^-} = K_{a1} * K_{a2} / (K_{a1} * K_{a2} - K_{a1} * [H^-] - [H^-]^2) \qquad \text{(Eq. 2.4)}$$

Fitting the data with the use of MS EXCEL indicated that when a = 0. b = 1 and c = 2.3. the pH dependence pattern from the calculations based on the model is consistent with the experimental data from pH=1 to pH = 11.2. as shown in Figure 2.8. The pH dependent pattern based on the calculations is in good agreement with the experimental

Reproduced with permission of the copyright owner. Further reproduction prohibited without permission.

Reproduced with permission of the copyright owner. Further reproduction prohibited without permission.

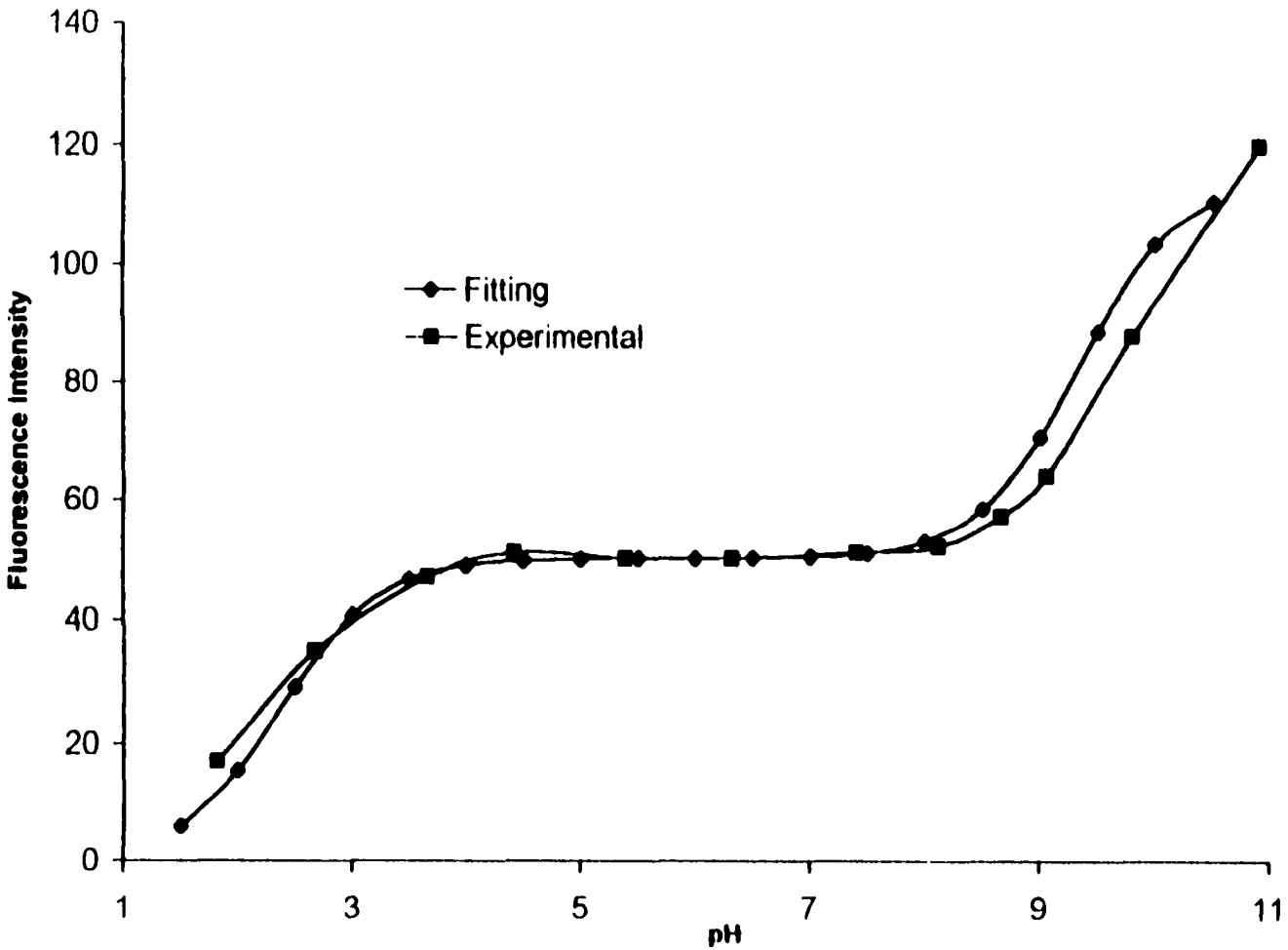

Figure2.8: Comparision of experimental fluorescence data for L-Trp and fitting data. For the experimental data obtained, the exicitation and emission wavelengths were 280 nm and 350 nm, respectively.

data. Thus. the model explains the experimental pH dependent pattern of fluorescence for free L-Trp. taking into consideration the two L-Trp protonation equilibria existing in the solution. Data indicate protonated L-Trp is a nonfluorescent form of L-Trp. and the deprotonated form of L-Trp has a fluorescence quantum efficiency which equals 2.3 times that of the zwitterionic form of L-Trp. Measurements were made earlier at different pHs for Trp fluorescence lifetime [68]. yielding a lifetime of 8.2 nano seconds at pH 11 with Trp existing mostly as deprotonated Trp. and a 3.2 nano seconds at pH 7 with Trp existing mostly as zwitterionic Trp. The fluorescence life time is proportional to the fluorescence quantum efficiency [57]. Thus. the ratio of fluorescence quantum efficiencies. 8.2 3.2. equals to 2.5. which is in good agreement with the ratio obtained in this study. which is 2.3.

2.3.2 pH Dependence of L-Trp Fluorescence Quenching by Cu(II)

The quenching of L-Trp fluorescence by Cu^{2+} ion is highly pH dependent. Figure 2.4 gives the comparison of fluorescence profiles of 0.05 mM $Cu(L\text{-}Trp)_2$ and 0.1mM L-Trp as a function of pH. Based on the data presented in Figure 2.4. L-Trp fluorescence is not quenched by Cu^{2+} ion as the pH is below 4. Fluorescence quenching increases as the pH increases from 4 to 8.1 with the highest level of L-Trp fluorescence quenching by Cu(II) was achieved in a limited pH range around 8.1. As the pH increases beyond 8.1. the fluorescence of the $Cu(L\text{-}Trp)_2$ solution increases. This pH dependence pattern is in good agreement with the data obtained earlier [54].

Reproduced with permission of the copyright owner. Further reproduction prohibited without permission.

The fluorescent agent - quencher system here is a complicated equilibrium system in which various secondary protonation and complexation equilibria exist besides the Cu(II) - L-Trp complexation equilibria. The relevant equilibria which can affect Cu(II) - L-Trp complexation are listed in Figure 2.9. Equilibrium constants are taken from Ref. [63] and [69]. The major secondary equilibria existing in the solution are L-Trp multiple protonation equilibria and multiple Cu(II)-hydroxide complexation equilibria. As can be seen from the list of equilibria, as the pH decreases, the protonation of L-Trp increases. As the pH increases, Cu(II)- hydroxide complexation increases. These two types of equilibria compete with Cu(II)- L-Trp complexation for Cu^{2+} ion and L-Trp, and play a negative role on the complexation between Cu^{2+} ion and L-Trp.

To clarify the pH dependence of the Cu(II) - L-Trp complexation on a quantitative base, the conditional stability constant of $Cu(L\text{-}Trp)_2$ can be written by taking into consideration the secondary equilibria as:

$$K'_{Cu(L\text{-}Trp)_2} = \partial_{A^-} * \partial_{Cu^{2+}} * K_{Cu(L\text{-}Trp)_2} \qquad \text{(Eq. 2.5)}$$

where ∂_{A^-} is the fraction of the deprotonated form of uncomplexed L-Trp and $\partial_{Cu^{2+}}$ represents the fraction of uncomplexed Cu^{2+}. $K'_{Cu(L\text{-}Trp)_2}$ and $K_{Cu(L\text{-}Trp)_2}$ are conditional stability constant and stability constant, respectively. ∂_{A^-} and $\partial_{Cu^{2+}}$ can be expressed as:

$$\partial_{A^-} = K_{a1} * K_{a2} / (K_{a1} * K_{a2} + K_{a1} * [H^+] + [H^+]^2) \qquad \text{(Eq. 2.6)}$$

Reproduced with permission of the copyright owner. Further reproduction prohibited without permission.

Cu(II) - L-Trp complexation:

$$Cu^{2+} + X^{-} \rightleftharpoons CuX^{+} \qquad K_{f1} = 10^{8.29}$$

$$Cu^{2+} + 2X^{-} \rightleftharpoons CuX_2 \qquad K_{f2} = 10^{15.48}$$

HX = L-Trp

L-Trp protonation:

$$X^{-} + H^{+} \rightleftharpoons HX \qquad Ka_2 = 10^{-9.39}$$

$$HX + H^{+} \rightleftharpoons H_2X^{+} \qquad Ka_1 = 10^{-2.38}$$

HX = L-Trp

Cu(II) - hydroxide complexation:

$$Cu^{2+} + OH^{-} \rightleftharpoons CuOH^{+} \qquad \beta_1 = 10^{6.3}$$

$$Cu^{2+} + 2OH^{-} \rightleftharpoons Cu(OH)_2 \qquad \beta_2 = 10^{12.8}$$

$$Cu^{2+} + 3OH^{-} \rightleftharpoons Cu(OH)_3^{-} \qquad \beta_3 = 10^{14.5}$$

$$Cu^{2+} + 4OH^{-} \rightleftharpoons Cu(OH)_4^{2-} \qquad \beta_4 = 10^{16.4}$$

$$2Cu^{2+} + 2OH^{-} \rightleftharpoons Cu_2(OH)_2^{2+} \qquad K = 10^{17.7}$$

Figure 2.9: Relevant equilibria related to Cu(II) - L-Trp complexation in a $Cu(L\text{-}Trp)_2$ aqueous solution

Reproduced with permission of the copyright owner. Further reproduction prohibited without permission.

$$\partial_{Cu^{2+}} = 1/(1 + \beta_1 * [OH^-] + \beta_2 * [OH^-]^2 + \beta_3 * [OH^-]^3 + \beta_4 * [OH^-]^4) \qquad \text{(Eq. 2.7)}$$

where K_{a1} and K_{a2} are acid dissociation constants for L-Trp; β_1, β_2, β_3 and β_4 are cumulative stability constants for Cu(II)-hydroxide complexation.

The conditional stability constants, a measure of the affinity between Cu^{2+} and L-Trp in the solution, were calculated from a spreadsheet with MS EXCEL at different pHs. Conditional stability constants are plotted as a function of pH in Figure 2.10. Comparing Figure 2.4 and Figure 2.10, the pH dependent pattern of the fluorescence quenching matches well with that of the conditional stability constants calculated. A pH of 8.1, at which point the fluorescence of L-Trp is most efficiently quenched, is the pH where there is the highest affinity between Cu^{2+} ion and L-Trp, which ideally explains the relationship between the Cu(II)-L-Trp complexation and fluorescence quenching. For the first time, it is demonstrated here that both the Trp protonation and Cu(II)-hydroxide complexation affect the Trp fluorescence quenching by Cu^{2+} ion. Based on the experimental data and the results of the calculations, the optimal pH for the proposed detection scheme is expected approximately 8.1, to ensure both a relatively "dark" background, and that the analyte molecules most efficiently displace L-Trp molecules from Cu(L-Trp)$_2$.

Reproduced with permission of the copyright owner. Further reproduction prohibited without permission.

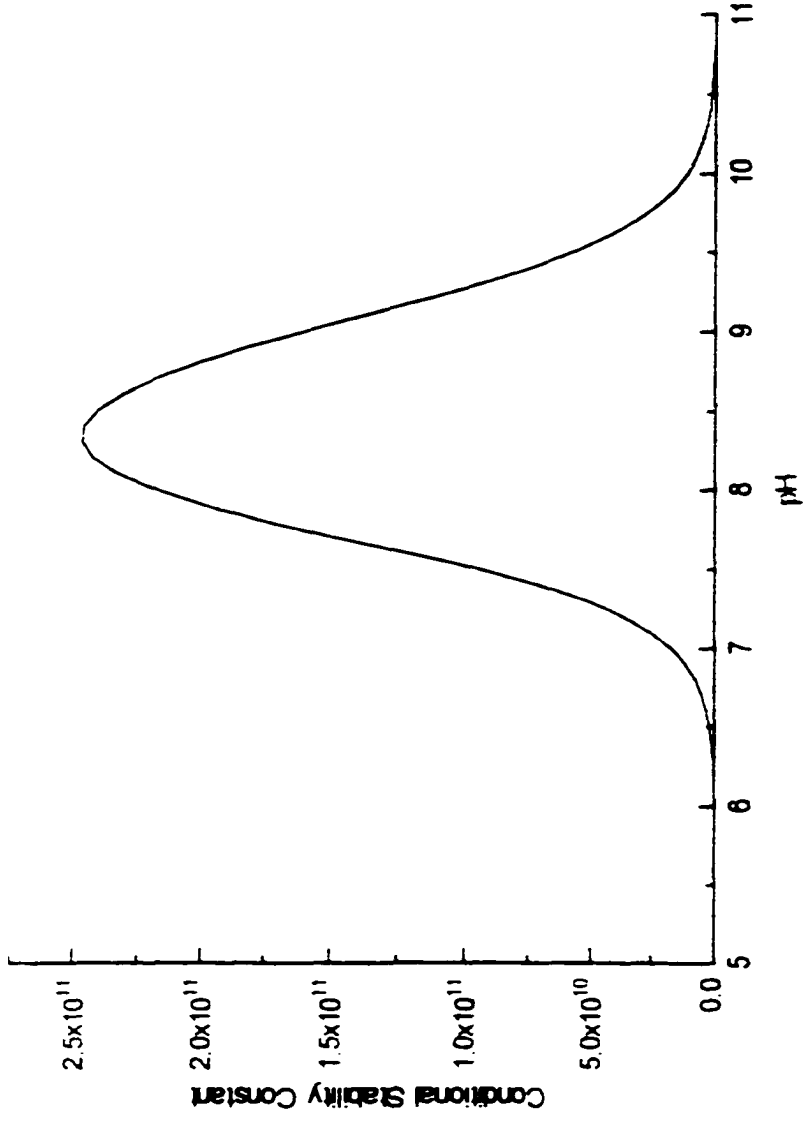

Figure2.10. Calculated conditional stability constant of $Cu(L\text{-}Trp)_2$ as a function of pH

Reproduced with permission of the copyright owner. Further reproduction prohibited without permission.

2.3.4 Further Clarification of the Relationship Between Complex Formation and Fluorescence Quenching

To further clarify the stoichiometric relationship between the formation of $Cu(L\text{-}Trp)_2$ and fluorescence quenching, the fluorescence titration data for L-Trp by Cu^{2+} ion is presented in Figure 2.6, with 4 mM sodium borate ($Na_2B_4O_7$) solution as the employed buffer. The data in Figure 2.6 clearly shows a 1:2 (1 Cu^{2+} : 2 L-Trp) stoichiometric factor of L-Trp quenched by Cu^{2+} ion at the optimized pH of approximately 8.1, which is in accordance with the formation of a $Cu(L\text{-}Trp)_2$ complex.

There is a discrepancy between the results obtained in this study and the claim made by Chen etc [56], that there is only a 1:1 stoichiometric ratio for L-Trp fluorescence quenching by Cu^{2+} ion. This discrepancy is attributed to their use of HEPES buffer which was in large excess compared to the concentration of Trp in that study. This might result in competition from HEPES for binding to Cu(II) [76]. Therefore sodium borate was used to adjust the solution pH in the following studies. Also they studied the quenching effect at pH 7.0, which is not an optimum pH for fluorescence quenching based on data presented in. As we predicted, as shown in Figure 2.7, there is a less than 1:2 pattern for the Cu^{2+}: L-Trp quenching at both a higher concentration of HEPES buffer, or a pH of 7.0.

To determine if there is any additional dynamic quenching effect with the presence of Cu^{2+} ions and other ligands, an excessive amount of EDTA was added to a 0.05 mM $Cu(L\text{-}Trp)_2$ solution. Considering the much higher concentration of EDTA and its strong

Reproduced with permission of the copyright owner. Further reproduction prohibited without permission.

chelating ability ($pK_{f(CuEDTA)}$ = 18.8), it can be reasonably assumed that all of the Cu^{2+} ions are bound to EDTA with the L-Trp being displaced from the complex. Comparing the fluorescence profiles presented in Figure 2.5, almost the same patterns are observed for the free L-Trp fluorescence and for Cu(L-Trp)$_2$ with excessive EDTA. It is concluded therefore, there is no dynamic fluorescence quenching from both the Cu(II) complexes and a large amount of ligand containing amino groups and carboxyl groups. In contrast to the static fluorescence quenching, which is due to the complexation from the fluorescence agents and the metal ions, dynamic fluorescence quenching is due to the molecular collisions between the fluorescence agents and the quencher [57]. The detection scheme proposed earlier is based on the occurrence of static fluorescence quenching between transition metal ions and the fluorescence agents. Although it was claimed Trp fluorescence is sensitive to dynamic quenching from various species [53], the data presented here indicate interference from the collisional fluorescence quenching is not a concern here for this study.

2.4 Conclusion

The fluorescence of solutions of free L-Trp, and Cu(II) - L-Trp were studied systematically. The pH dependence pattern of free L-Trp in aqueous solution can be explained using a model in which deprotonated, zwitterionic and protonated L-Trp have different fluorescence efficiencies. It was observed that the protonated L-Trp is nonfluorescent, while zwitterionic L-Trp has a fluorescence efficiency 2.3 times less than

Reproduced with permission of the copyright owner. Further reproduction prohibited without permission.

that of the deprotonated L-Trp.

The fluorescence quenching of L-Trp by Cu^{2+} ion is highly pH dependent. The fluorescence of L-Trp is most efficiently quenched in the pH range from 7.0 - 9.0. The conditional stability constant of $Cu(L\text{-}Trp)_2$ was calculated at various pHs, taking into consideration both the L-Trp protonation equilibria and Cu(II)-hydroxide complexation equilibria. It was found that the pH region where the L-Trp fluorescence is most efficiently quenched, matches the pH region where the largest value of conditional stability constant is reached. L-Trp protonation equilibria and Cu(II) - hydroxide equilibria affect L-Trp fluorescence quenching by interfering with the complexation between Cu(II) and L-Trp. Thus, it is concluded that fluorescence quenching of L-Trp by Cu^{2+} ion ideally corresponds to the formation of the complex, $Cu(L\text{-}Trp)_2$, which is consistent with the data obtained by the titration of L-Trp by Cu^{2+} ion at the optimum pH of 8.1.

The detection pH for the proposed detection scheme for amino group-containing compounds is predicted to be approximately 8.1 based on the data presented, so that a good "dark" background level will be obtained, while at the same time, ensuring that added analyte molecules will compete favorably with L-Trp for binding to the Cu^{2+} ion. Care must be taken in choosing the buffer for this detection method. Use of amino group-containing buffers, such as HEPES, may interfere with detection by disturbing Cu(II) - L-Trp complexation.

Reproduced with permission of the copyright owner. Further reproduction prohibited without permission.

Chapter 3
HPLC Separation and Detection of Biogenic Polyamines and Diamines with $Cu(L\text{-}Trp)_2$ as the Postcolumn Reagent

3.1 Introduction

The aliphatic biogenic polyamines and diamines are naturally occurring compounds that are found in a wide variety of yeasts [4, 71], plants [5, 72] and animals [6, 73, 74]. Two biogenic polyamines, spermidine and spermine, are closely related to rapid tissue growth. The concentrations of spermidine and spermine were shown to be related to several parameters of cell proliferation, such as the concentrations of proteins and nucleic acids in developing embryos [7]. Enhanced synthesis and accumulation of aliphatic polyamines in rapidly growing tissues occur prior to the synthesis of DNA [75]. The precise biological role of polyamines in this process is still under investigation. It has been suggested, however, that these two polyamines, by virtue of their charged nature under physiological conditions and their conformational flexibility, might serve to stabilize macromolecules such as nucleic acids by anion neutralization [76 - 78]. These aliphatic polyamines are also important in cancer research. It has been shown that polyamine patterns in tumor cells are significantly different from those of normal muscle tissues. For instance, the molar ratio of spermidine to spermine in Ehrlich ascites carcinoma was found to be strikingly lower than the typical ratio for rapidly growing animal tissues [79]. Both

Reproduced with permission of the copyright owner. Further reproduction prohibited without permission.

the spermidine concentration as well as the molar ratio of spermidine to spermine are found to be elevated in RD 3 sarcoma compared with normal muscle tissues [8]. Attempts have also been made to use polyamines for the detection of malignancy [80]. Diamines are important in the synthesis and degradation pathways for amino acids in biological systems [81, 82]. Furthermore, elevated concentrations of certain diamines in blood can be indicative of specific carcinomas and, in organ transplant recipients, evidence of physiological rejection of transplanted tissues [7, 83]. Diamines are also widely recognized as indicators of spoilage in foods, especially in seafood and other meats [84].

Detection of aliphatic amines following HPLC separation has been widely studied [85 - 90]. Most natural aliphatic biogenic polyamines do not possess naturally occurring chromophoric or fluorophoric moieties, which is why they are usually derivatized either prior to [85 - 87] or after [88 - 90] chromatographic separation to facilitate photometric detection. Detection methods which require derivatization have several disadvantages, including the need for additional sample processing, variability of reaction completeness, decomposition of the derivatization products, and toxicity of some derivatizing agents. For these reasons, direct detection without derivatization is preferred whenever possible.

A variety of ways have been developed to detect the aliphatic amines without derivatization. Chemiluminescence detection of aliphatic amines following chromatographic separation, based on a chemiluminescent oxidation - reduction reaction mechanism, has been achieved using the reaction of tris(2,2' - pyridyl)ruthenium(II) with the analytes [27]. Indirect detection of various biogenic aliphatic polyamines has also

Reproduced with permission of the copyright owner. Further reproduction prohibited without permission.

been achieved in ion exchange chromatography [91] and capillary electrophoresis [92] without the need of derivatization. By exploiting the property that the amines exist as ions at appropriate pHs, UV absorbing ionic species were added to the mobile phase, not only to elute the analytes but also to monitor their presence. As the ionized amines elute from the column, the concentration of the counter ions in the mobile phase, which are being monitored, decreases to maintain the electroneutrality of the mobile phase. However, one problem with this approach is that it suffers from high detection limits due to the high background noise, which limits its application for real biological samples. Recently, integrated pulsed amperometric detection (IPAD), a newly developed variant of the pulsed amperometric detection method, has been used to detect underivatized biogenic monoamines and diamines following HPLC separation [32, 33, 93]. In this mode of detection, current is integrated continuously during a cycle where the electrode is oxidized and then reduced to the original state. The advantage of IPAD is that, by canceling the charge from oxide formation and reduction, the effect on the baseline is greatly minimized.

The detection approach presented here is based on monitoring the fluorescence of the amino acid, L-Tryptophan (L-Trp). As demonstrated in Chapter 2, the fluorescence of L-Trp, is quenched in the presence of Cu^{2+} ion. Quenching is due to the formation of a L-Trp copper complex. L-Trp is freed from the complex with the addition of aliphatic polyamines and diamines, which have a greater copper(II) affinity than L-Trp, resulting in the recovery of L-Trp fluorescence, as shown by:

Reproduced with permission of the copyright owner. Further reproduction prohibited without permission.

$$Cu(L\text{-}Trp)_2 + nA = Cu(A)_n + 2\ L\text{-}Trp^* \qquad \text{(Eq. 3.1)}$$

where A is the polyamine or diamine molecule and n is the number of the polyamine or diamine molecules coordinating to Cu(II), and L-Trp* represents the fluorescently active L-Trp. Thus, the presence of these analytes can be inferred by monitoring the fluorescence of L-Trp as described by the following equations:

$$[A] = 2\ n \times [L\text{-}Trp^*] \qquad \text{(Eq. 3.2)}$$

$$[A] = K \times 2\ n \times FLUO \qquad \text{(Eq. 3.3)}$$

where [A] and [L-Trp] are the concentrations of the analytes and L-Trp, respectively, K is an arbitrary constant and FLUO is the fluorescence intensity of L-Trp.

In this study implementation of a postcolumn HPLC detection scheme will be investigated for monitoring spermidine and spermine, as well as 1,2-diamines and 1,3-diamines, using $Cu(L\text{-}Trp)_2$ as the postcolumn reagent. A discussion of the reaction conditions and the detection mechanism will be presented in detail.

3.2 Materials and Methods

3.2.1 Materials

The biogenic polyamines, spermine [manufacturer's stated purity, 99.2% by thin-layer chromatography (TLC)] and spermidine (manufacturer's stated purity, 99.2% by TLC)

Reproduced with permission of the copyright owner. Further reproduction prohibited without permission.

were purchased from Sigma (St. Louis, MO, USA). The 1,2-diamines, ethylenediamine, N-methylethylenediamine and the 1,3-diamine, 1,3-aminopropane (all with manufacturer stated purity, 99.0% by GC) were also purchased from Sigma. Reagent grade copper sulfate, sodium acetate and sodium borate ($Na_2B_4O_7 \cdot 10H_2O$) were purchased from Baker (Phillipsburg, NJ, USA). The deionized water used in the preparation of the standard solutions and eluents was obtained from a Milli-Q™ water system (Millipore, Bedford, MA, USA). All mobile phases were filtered through a 0.45 µm nylon filter (Whatman, Hillsboro, OR, USA) prior to use. Dilute aqueous solutions of reagent grade sodium hydroxide (Fisher, Pittsburgh, PA, USA) and hydrochloric acid (Baker, Phillipsburg, NJ, USA) were used to adjust the pH of the mobile phase and postcolumn reagent.

The chromatographic separations were performed using a Nicolet LC9560 HPLC system (Madison, WI, USA) equipped with a Rheodyne Model 7125 injector (Cotati, CA, USA) fitted with a 10-µl injection loop. Separation of the polyamines was achieved with the use of a Hamilton PRP-X200 column (250 mm x 4.6 mm I.D.) (Reno, NV, USA), containing a polymer-based strong cation exchanger. A Hitachi 655A-11 LC pump (Tokyo, Japan) delivered the postcolumn reagent via a mixing tee. A Varian flow control damper (P/N 03-905320-00) (Palo Alto, CA, USA) was placed between the postcolumn reagent pump and mixing tee to improve flow stability. A Kratos Spectroflow 980 fluorescence detector (Ramsey, NJ, USA) fitted with a 10 µl detection flow cell was used for chromatographic detection. The excitation wavelength of the detector was set at 280

Reproduced with permission of the copyright owner. Further reproduction prohibited without permission.

nm and a 350 nm longpass glass filter was utilized for emission.

3.2.2 Titration of Cu(L-Trp)$_2$ with Polyamines and Diamines

Experiments were performed to study the stoichiometric ratio between Cu(L-Trp)$_2$ and polyamines or diamines in a detection reaction. A solution of Cu(L-Trp)$_2$ was prepared by dissolving the appropriate masses of solid L-Trp and $CuSO_4 \cdot 5H_2O$ in sodium borate solution. Solutions containing different concentrations of the aliphatic polyamines and diamines were added to standard Cu(L-Trp)$_2$ solutions containing 4 mM sodium borate ($Na_2B_4O_7$) adjusted at pH 8.1. Appropriate amounts of deionized water were added to the solution to make the concentration of Cu(L-Trp)$_2$ 0.05 mM for all of the solutions. This resulted in the "titration" of Cu(L-Trp)$_2$ with these compounds. The fluorescence intensities of the solutions versus the concentration of spermine and ethylenediamine are plotted in Figure 3.1 and Figure 3.2.

3.2.3 Chromatographic Separation and Detection

A schematic diagram for the chromatographic separation and detection instrumentation is given in Figure 3.3. Separation of 1,2-diamines, 1,3-diamines, spermine and spermidine was achieved by adjusting the concentration of potassium chloride in the mobile phase. The pH of the mobile phase was buffered with a 1.5 mM sodium acetate solution at pH 5.2. The mobile phase flow rate was set at 0.8 ml/min.

The postcolumn reagent, a 0.05 mM Cu(L-Trp)$_2$ aqueous solution buffered with a 4

Reproduced with permission of the copyright owner. Further reproduction prohibited without permission.

Reproduced with permission of the copyright owner. Further reproduction prohibited without permission.

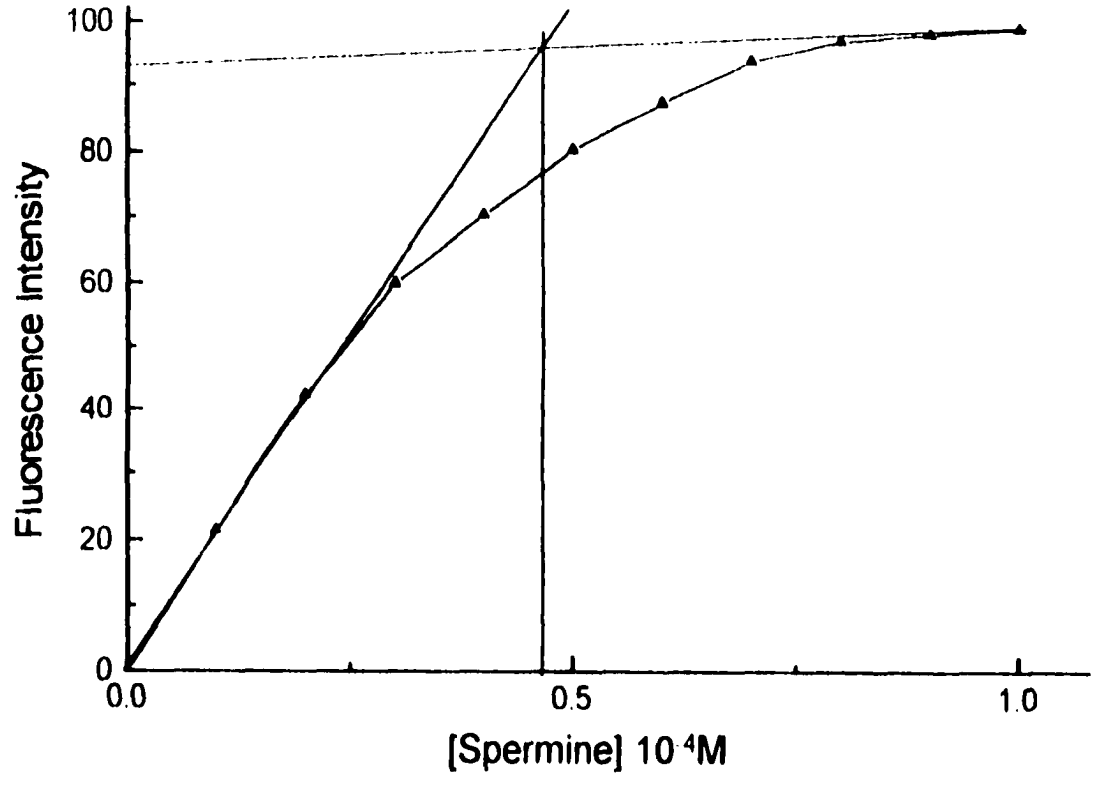

Figure 3.1: Stoichiometric study of the reaction of $Cu(L\text{-}Trp)_2$ with spermine. The concentration of $Cu(L\text{-}Trp)_2$ is 0.05 mM, adjusted to pH 8.1, in 4 mM sodium borate ($Na_2B_4O_7$) solution.

Reproduced with permission of the copyright owner. Further reproduction prohibited without permission.

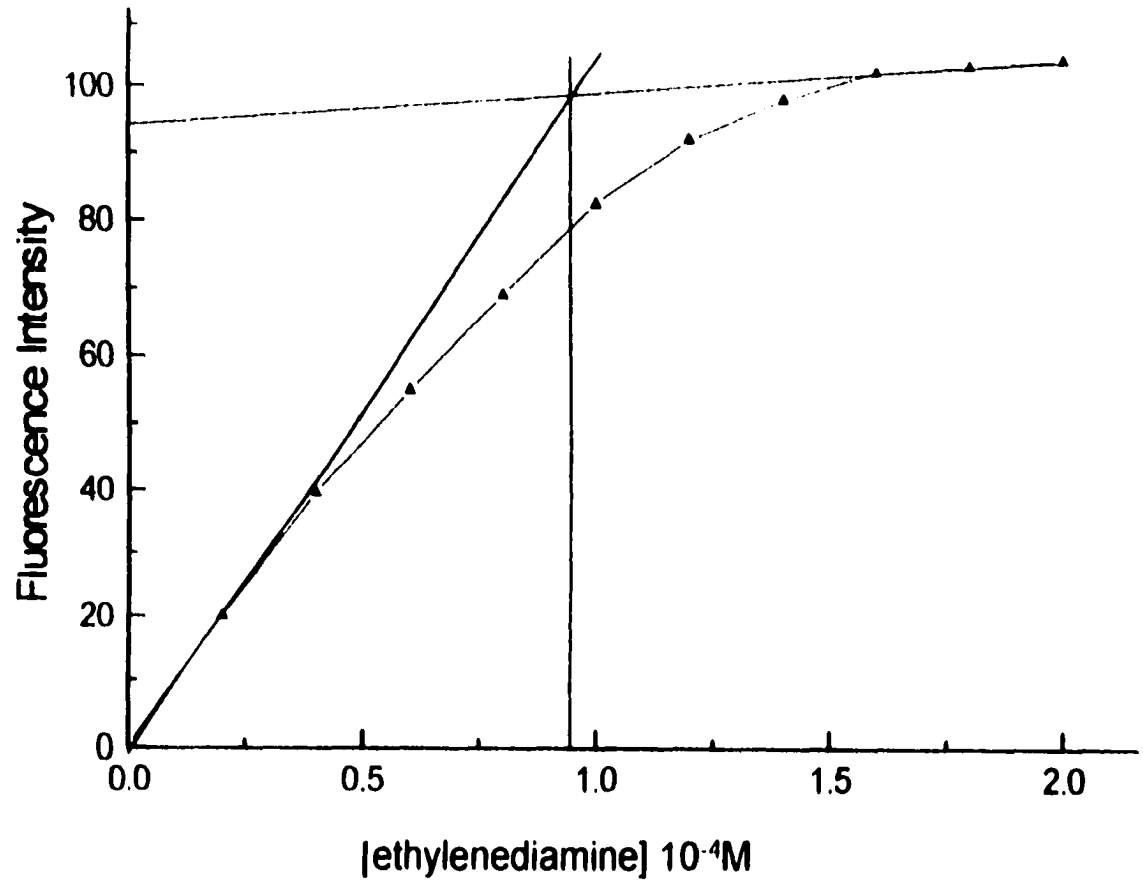

Figure 3.2: Stoichiometric study of the reaction of $Cu(L\text{-}Trp)_2$ with ethylenediamine. The concentration of $Cu(L\text{-}Trp)_2$ is 0.05 mM, adjusted to pH 8.1, in 4mM sodium borate ($Na_2B_4O_7$) solution.

Reproduced with permission of the copyright owner. Further reproduction prohibited without permission.

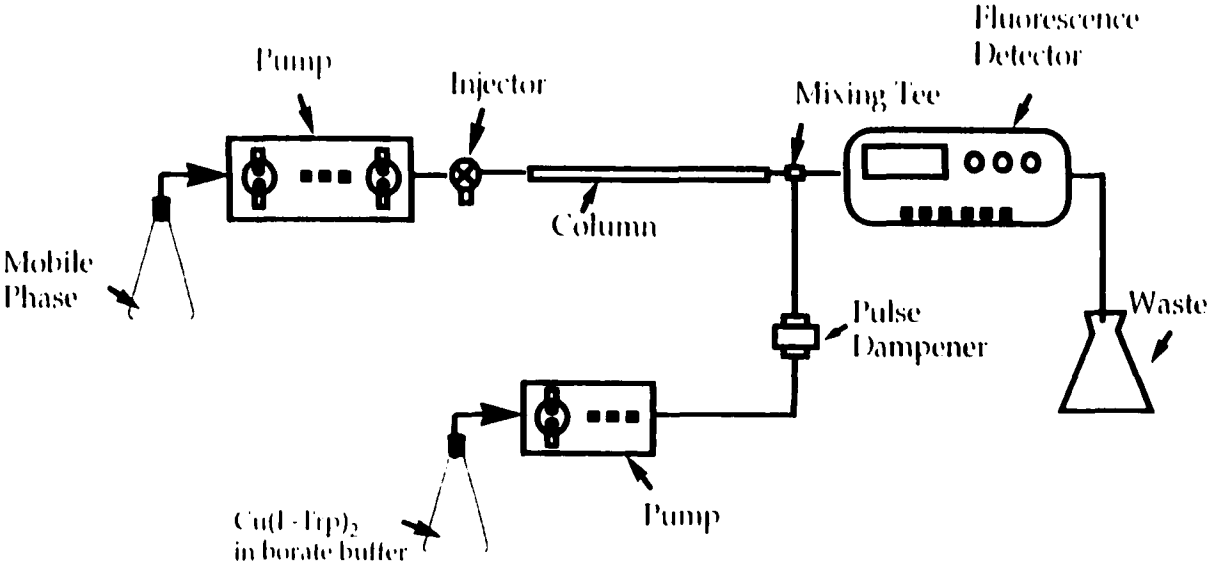

Figure 3.3: Instrumental setup for chromatographic separation/detection

mM sodium borate ($Na_2B_4O_7$), was mixed with the column eluent via a mixing tee before the fluorescence detector. The pH of the postcolumn reagent was adjusted in the range of 7.4 - 9.4 The effect of pH on detection was evaluated in this pH range.

3.3 Results and Discussions

3.3.1 Stoichiometric Study of the Detection Reaction

As shown in Figures 3.1 and 3.2, it can be seen that the fluorescence intensities of the solutions increase as the amounts of added polyamines and diamines increase. Both of these plots show that the recovered fluorescence signal plateaus when a stoichiometric amount of amine is added to the detection reagent. A stoichiometric ratio of 1 : 1 for [Cu(L-Trp)$_2$] : [spermine] is determined from the titration data, within the experimental error. This corresponds to the reaction:

$$Cu(L\text{-}Trp)_2 + \text{spermine} \rightleftharpoons Cu(\text{spermine}) + 2\ Trp \qquad \text{(Eq. 3.4)}$$

However, the stoichiometric ratio for [Cu(L-Trp)$_2$] : [ethylenediamine] is 1 : 2 based on the data obtained, suggesting the reaction:

$$Cu(L\text{-}Trp)_2 + 2\ \text{ethylenediamine} \rightleftharpoons Cu(\text{ethylenediamine})_2 + 2\ Trp \qquad \text{(Eq. 3.5)}$$

The 1 : 2 stoichiometric ratio is also indicated for both N- methylethylenediamine and

Reproduced with permission of the copyright owner. Further reproduction prohibited without permission.

1,3-aminopropane. The discrepancy between the two stoichiometric ratios can be explained by the fact that the polyamines have more amino groups than the diamines, resulting in a larger complexing capacity. These stoichiometric ratios are in good agreement with the equilibrium data obtained for the diamines and polyamines [94], indicating diamines tend to form 2 : 1 complexes with Cu^{2+}, while polyamines only form 1:1 complexes with Cu^{2+}. Thus, the polyamine molecules tested produce two fluorescent L-Trp molecules, while the 1,2-diamine or 1,3-diamine molecules tested displace only one fluorescent L-Trp molecule.

3.3.2 Chromatographic Separation

Underivatized biogenic polyamines are often separated in a cation exchange chromatographic mode [32, 91, 93], instead of using reversed phase chromatography, possibly due to their strong hydrophilicity. A Hamilton SCX200 column was utilized in this work for the separation of aliphatic biogenic polyamines and diamines. The retention of the amines on the column is based upon the cationic nature of these compounds within an appropriate pH range for the protonation of the amino groups. The pH of the mobile phase was set at 5.2, to assure the protonation of these compounds. This pH was established based upon the equilibrium data given in [94], which indicate the polyamines and diamines generally have a first acidic association constant in the range from 9.5 - 10.5. As one of the strongest commonly used monovalent cations, K^+ was chosen to elute the analyte compounds. Care should be taken in choosing the cation to be used to elute the

Reproduced with permission of the copyright owner. Further reproduction prohibited without permission.

analytes from the column, as some of the divalent ions, such as Cu^{2+}, Co^{2+} and Zn^{2+} may interfere with this detection approach by binding to L-Trp and the amines. Other divalent ions, such as Ca^{2+}, and Ba^{2+}, may form hydroxides and precipitate at the detection pH used in this study. KCl was used to adjust the strength of the mobile phase. Plots of the capacity factors of spermine and spermidine versus the KCl concentration of the mobile phase are given in Figure 3.4. Based on these data, a mobile phase containing 0.8M KCl was chosen to elute the mixture of spermine and spermidine isocratically.

3.3.3 Chromatographic Detection Optimization

A Cu(L-Trp)$_2$-based fluorescence detection scheme for detecting spermidine, spermine, 1,2-diamines and 1,3-diamines was implemented following the chromatographic separation. A solution containing 0.05 mM Cu(L-Trp)$_2$ in 4 mM sodium borate was mixed with the column eluent postcolumn. The concentration of sodium borate, the postcolumn reaction buffer was set larger than that of the acetic acid, the mobile phase buffer, to assure a larger buffering capacity for the former.

The pH of the solution in the detector flow cell is a very important experimental parameter which needs to be controlled for several reasons. The fluorescence of Cu(L-Trp)$_2$ is pH dependent since the extent of Cu(II) and L-Trp complexation is a function of pH, and the degree of fluorescence quenching is directly related to the extent of complexation. The complexing affinities of the polyamines to Cu(II) are also dependent on the solution pH, with only the deprotonated forms of the polyamines coordinating

Reproduced with permission of the copyright owner. Further reproduction prohibited without permission.

Reproduced with permission of the copyright owner. Further reproduction prohibited without permission.

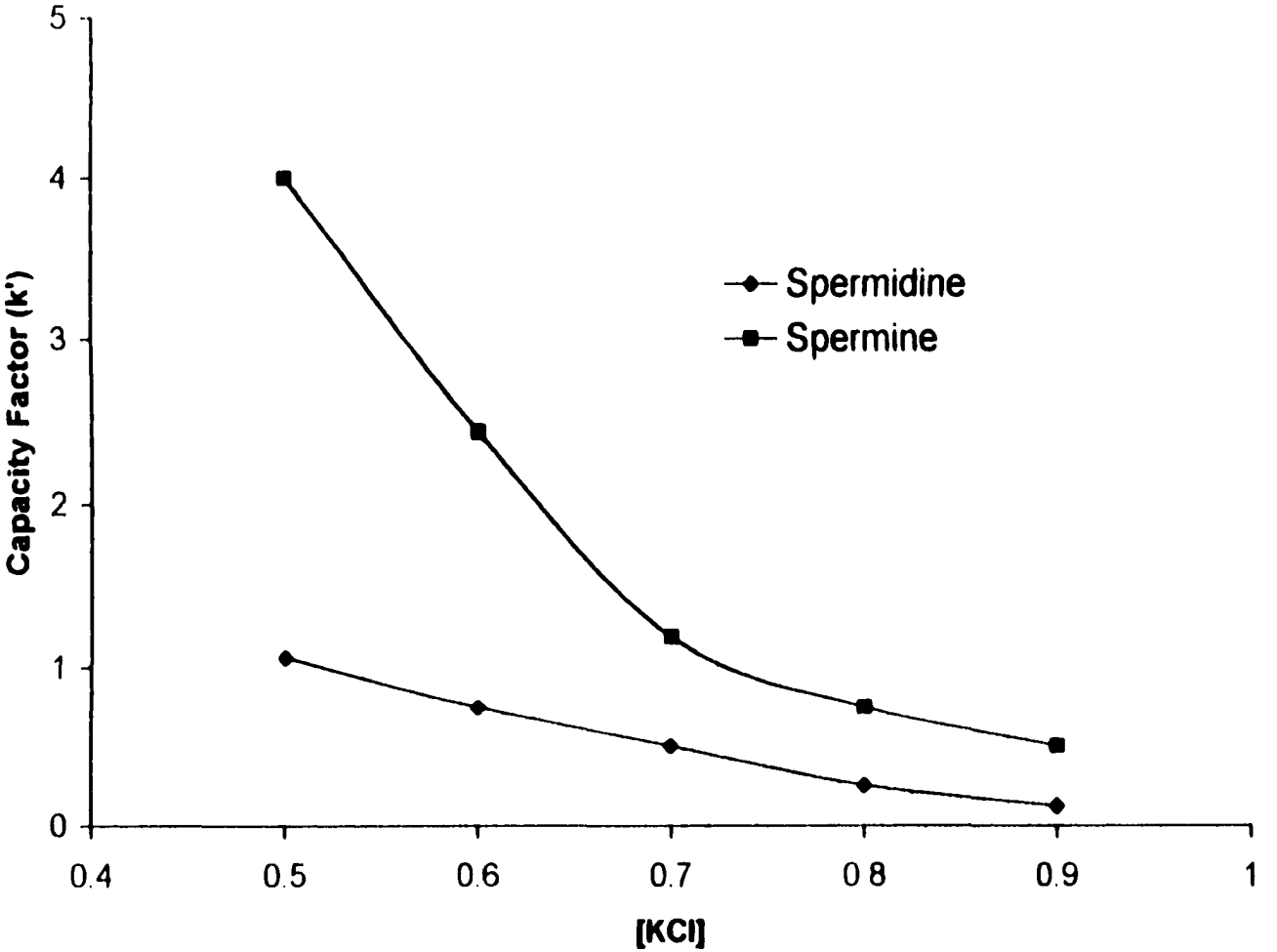

Figure 3.4: Capacity factors (k) for spermine and spermidine plotted versus the concentration of KCl in the mobile phase

efficiently to Cu(II). Based on these considerations, the pH needs to be adjusted so that the background fluorescence of the solution is relatively low, thus providing a "dark" background, while at the same time resulting in high complexing affinities for the analytes. It should be noted that the optimum pH for fluorescence quenching is not necessarily the pH which results in the optimum complexing affinities of the polyamines. Also the optimum detection pH for one particular polyamine might not be the optimum detection pH for other polyamines. So compromises may need to be made between those factors to assure effective complexation between Cu^{2+} and L-Trp, while at the same time provide good complexation affinities of analytes for Cu^{2+} ion.

For an optimized chromatographic separation of these compounds, the pH of the solution in the detector cell was adjusted by changing the pH of the postcolumn reagent. To experimentally determine the optimal detection pH for spermine and spermidine, mixtures of the two were injected into the HPLC, separated, and the fluorescence signal intensities obtained plotted as a function of the pH of the detected solutions (Figure 3.5). The figure shows that the fluorescence signals of the two polyamines change significantly in the pH range from 7.4 to 9.2. For spermidine, the signal increases steadily over this pH range; for spermine, the fluorescence signal increases to a maximum value at pH 8.6, and then slowly decreases. These pH dependent patterns can be explained with the following considerations. There are three factors affecting the signal intensities of these two aliphatic polyamines: 1.) The dissociation of $Cu(L\text{-}Trp)_2$ increases both above pH 8.1 and below pH 8.1; 2.) The fluorescence of free L-Trp steadily increases above pH 8.0.

Reproduced with permission of the copyright owner. Further reproduction prohibited without permission.

Reproduced with permission of the copyright owner. Further reproduction prohibited without permission.

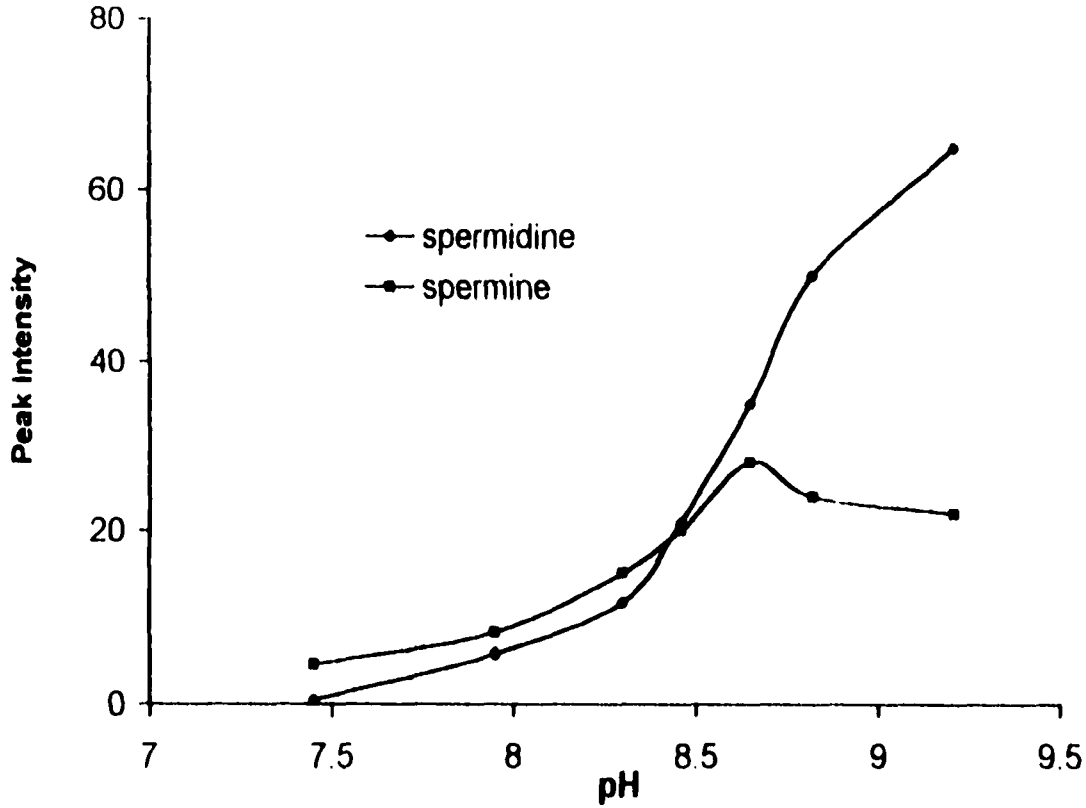

Figure 3.5 Chromatographic peak intensities as a function of detection pH. The mobile phase was 0.8M KCl, buffered at pH 5.2 with 1.5 mM NaAc. The postcolumn reagent was 0.05 mM $Cu(L\text{-}Trp)_2$ in a 4 mM sodium borate ($Na_2B_4O_7$) buffer. The mobile phase and postcolumn reagent flow rates were 0.8 and 2.0 ml/min respectively. The amounts of sample injected were 320 pmol for spermidine and 160 pmol for spermine

due to the fact that the deprotonated form of L-Trp has a higher fluorescence efficiency than zwitterionic L-Trp, as determined in Chapter 2; and 3.) The affinities of the polyamines for Cu^{2+} ion vary as the changes, since complexation is affected by both the degree of polyamine protonation and Cu(II)- hydroxide complexation. To determine how the pH affects Cu(II)-polyamine complexation, the conditional stability constants, K_f', of the two complexes, Cu(spermine) and Cu(spermidine), were calculated using the following formula at different pHs:

$$K_f' = \partial_A \times \partial_{Cu^{2+}} \times K_f \qquad \text{(Eq 3.7)}$$

in which K_f' and K_f are the conditional stability constant and the stability constant of the complex, respectively; ∂_A is the fraction of unprotonated polyamines, which are expressed as for spermine and spermidine, respectively:

$$\partial_A = K_{a1} * K_{a2} * K_{a3} * K_{a4} / (K_{a1} * K_{a2} * K_{a3} * K_{a4} - K_{a1} * K_{a2} * K_{a3} * [H^+] - K_{a1} * K_{a2} * [H^+]^2 - K_{a1} * [H^+]^3 - [H^+]^4) \qquad \text{(Eq. 3.8)}$$

$$\partial_A = K_{a1} * K_{a2} * K_{a3} (K_{a1} * K_{a2} * K_{a3} - K_{a1} * K_{a2} * [H^+] - K_{a1} * [H^+]^2 - [H^+]^3) \qquad \text{(Eq. 3.9)}$$

and $\partial_{Cu^{2+}}$ is the fraction of free Cu^{2+} with the consideration of Cu(II) - hydroxide complexation, which is expressed as:

Reproduced with permission of the copyright owner. Further reproduction prohibited without permission.

$$\partial_{Cu^{2+}} = 1/(1 + \beta_1 * [OH^-] + \beta_2 * [OH^-]^2 + \beta_3 * [OH^-]^3 + \beta_4 * [OH^-]^4) \qquad \text{(Eq. 3.10)}$$

The published pK_a's of the two polyamines were obtained from [95]. The published K_f values of Cu(spermine) and Cu(spermidine) were obtained from references [96] and [97], respectively. From the K_f' versus pH plots presented in Figure 3.6, it can be seen that of the two complexes, Cu(spermine) has a maximum K_f' at pH 9.7, and Cu(spermidine) has a maximum K_f' at pH 9.9. Clearly, the complexing abilities of both polyamines tend to increase in the pH range 7.4 to 9.2. Of the factors affecting signal strength cited above, the first one tends to lead to a decrease in fluorescence signal intensity when the detection solution pH is away from 8.1, while the last two factors indicate increasing pH enhances the signal intensity. The pH dependence patterns of the signals in Figure 3.5 are the combined results of those three factors. Based on the data obtained, it can be concluded for spermine, the first factor dominates at pHs higher than 8.6, thus, resulting in a decrease in signal intensity; while for spermidine, the combined effect of factors 2 and 3 dominates in the pH range from 7.4 to 9.2. The detection pH was set at 8.6 based on these considerations.

Increased baseline variability was observed when the postcolumn flow rate was set lower than 2.0 ml/min due to pump pulsation at the lower flow rates. The postcolumn flow rate was set to 2.0 ml/min, to maintain a stable chromatographic baseline, while at the same time, minimizing the dilution of the eluted analytes by the postcolumn reagent.

Reproduced with permission of the copyright owner. Further reproduction prohibited without permission.

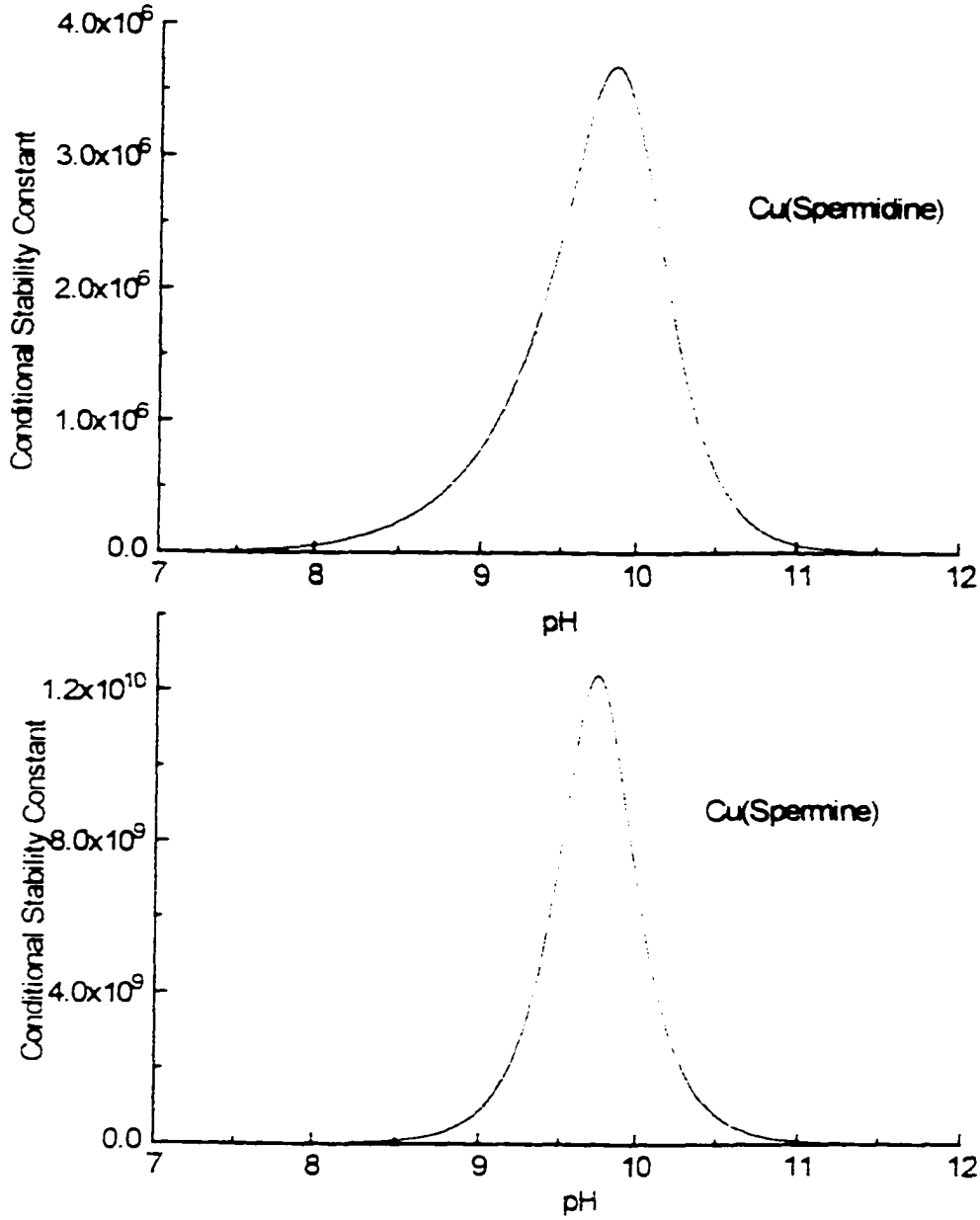

Figure 3.6: Calculated conditional stability constants (Kf') of Cu(spermine) and Cu(spermidine) as a function of pH

Reproduced with permission of the copyright owner. Further reproduction prohibited without permission.

3.3.4 Performance Evaluation for Detection of Aliphatic Biogenic Polyamines

A representative chromatogram of spermine and spermidine obtained at the optimized detection conditions is presented in Figure 3.7. Representative chromatograms of the diamines are presented in Figure 3.8. The fitted parameters for the working curves obtained for spermine and spermidine, including the detection limits (S/N = 3) and associated precision expressed as the relative standard deviation (RSD) are given in Table 3.1. The detection limits of the two biogenic polyamines, spermine and spermidine are 5 pmol and 10 pmol injected, respectively. The linearity is good to the nmol range.

The developed detection method was found to be free from problems associated with derivatization approaches while offering experimental and instrumental simplicity. Detection limits for the biogenic polyamines obtained using the developed method, compare favorably with some of the reported derivatization methods [88, 98]. The developed detection method is also comparable to the well-developed electrochemical methods, which generally have detection limits ranging from 5 - 20 pmol [32, 93, 99, 100].

3.4 Conclusions

A sensitive and simple way of detecting the biogenic aliphatic polyamines and diamines following chromatographic separation has been developed based on a postcolumn, non-derivatization reaction. The basis for this detection scheme is the fluorescence of L-Trp, which is quenched in copper(II)-L-Trp complexes. The fluorescence of L-Trp recovers with the addition of analytes that have a greater Cu^{2+} ion

Reproduced with permission of the copyright owner. Further reproduction prohibited without permission.

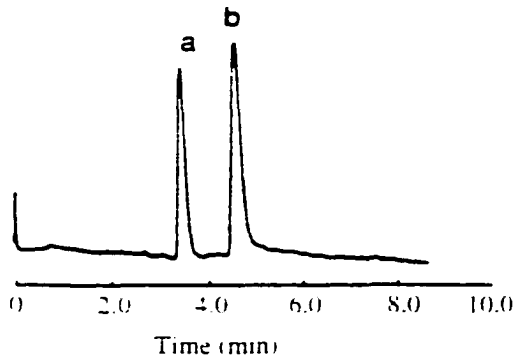

Figure 3.7: Representative chromatogram of spermine and spermidine. Separation was achieved using a Hamilton PRP-X200 SCX column at ambient temperature. The mobile phase was 0.8M KCl adjusted to a pH of 5.2 with 1.5 mM acetate buffer. The postcolumn reagent was 0.05M Cu(L-Trp)$_2$ buffered at pH 8.6 with 4 mM sodium borate ($Na_2B_4O_7$). The eluent and postcolumn reagent flow rates were 0.8ml/min and 2.0ml/min respectively. Peak a: spermidine, 240pmol; peak b: spermine, 320pmol.

Reproduced with permission of the copyright owner. Further reproduction prohibited without permission.

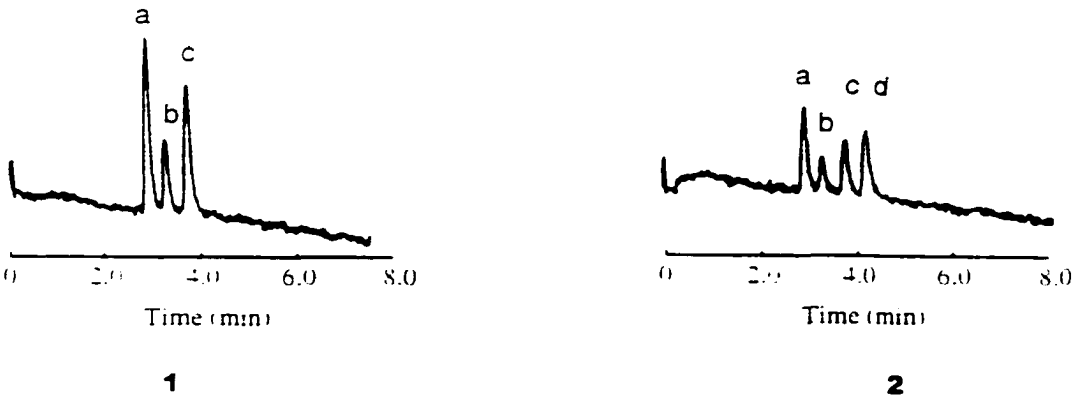

Figure 3.8: Representative chromatograms of diamines: (1) Chromatograms of 2,3-diaminopropionic acid (a), 1,3-diaminopropane(b) and N-methyleneethylenediamine(c), each of 1 nmol. (2) Chromatograms of (a), 1,3-diaminopropane(b) and N-methyleneethylenediamine(c), each of 0.5 nmol, and N,N'-dimethyleneethylenediamine(d), 0.85 nmol. The mobile phase was 0.4M KCl adjusted at pH 5.2 with 1.5 mM acetate buffer. Separation was conducted using a Hamilton PRP-X200 SCX column at ambient temperature. The postcolumn reagent was 0.05 mM Cu(L-Trp)$_2$ buffered at 8.6 with 4 mM sodium borate. The eluent and postcolumn reagent flow rates were 0.8ml/min and 2.0ml/min, respectively.

Reproduced with permission of the copyright owner. Further reproduction prohibited without permission.

Polyamine	linear range(pmol)	regression equation[a]	r[2]	DL[c](pmol)	RSD[d] (%)
spermine	5 - 1.000	H = 0.608 + 0.193 x C	0.9991	5	4.6
spermidine	10 - 1.000	H = 0.745 + 0.074 x C	0.9964	10	3.5

[a] H, peak height; C, analyte moles(in pmols). [b] Correlation coefficient. [c] Detection limit. [d] Relative standard deviation (N = 5 for 320 pmol spermine and 640 pmol spermidine injected, respectively).

Table 3.1: Characteristic parameters of the calibration graphs and analytical figures of merit for the determination of polyamines.

Reproduced with permission of the copyright owner. Further reproduction prohibited without permission.

affinity, such as the aliphatic polyamines and diamines. Thus, the presence of these compounds in the HPLC eluent can be inferred by monitoring the fluorescence of L-Trp. Solution pH has a strong effect on this detection system. Three factors concerning the effect of pH on the Cu^{2+} - L-Trp complexation, the L-Trp fluorescence efficiency, and the Cu^{2+} - analyte complexation were discussed. The detection pH was optimized at 8.6 for the two biogenic polyamines, spermidine and spermine. The detection limits following HPLC separation are 5 and 10 pmol injected for spermine and spermidine, respectively, with linear response regions up to nmol. The performance of the optimized detection method was compared to reported detection methods for the biogenic polyamines. The developed detection method also has the advantages of simplicity and good sensitivity.

Reproduced with permission of the copyright owner. Further reproduction prohibited without permission.

Chapter 4

Detection of Natural Amino Acids Following HPLC Separation with $Cu(L\text{-}Trp)_2$ as the Postcolumn Reagent

4.1 Introduction

Natural amino acids are the essential components of proteins and are found in a wide range of samples, such as biological tissues and fluids, foods and industrial products [2]. Detection of amino acids following chromatographic separation is of great interest due to the biological significance of these compounds [2, 101]. Due to the lack of a strong chromophore or fluorophore, detection of these compounds is far from straightforward with conventional UV-VIS or fluorescence detection. Traditional detection methods involve chemically derivatizing the natural amino acids either prior to or after separation. Dansyl chloride [102, 103], o-phthaldehyde [104] and phenylthiohydantoin [105] are among the most commonly used precolumn derivatization reagents for the analysis of amino acids. Typical issues which can be encountered when using a detection method requiring derivatization include: the sample preparation can be time-consuming and labor intensive; the derivatization process may add impurities to the sample; the derivatives formed may be unstable; and more than one derivative may be produced for some amino acids resulting in the presence of additional, unwanted peaks in the chromatograms.

Considerable efforts have been expended in the development of schemes for detecting the amino acids without derivatization. Detection of underivatized amino acids, based on

Reproduced with permission of the copyright owner. Further reproduction prohibited without permission.

a chemiluminescent oxidation-reduction reaction mechanism, has been achieved with the use of tris(2,2'-bipyridyl)ruthenium(III) [23 - 26]. This is added either postcolumn or generated in situ. Studies are being carried out which are aimed at overcoming several problems encountered with this approach to detection, including reducing the complexity of instrumentation required. It has also been reported that different amino acids show significantly different responses using this detection method, with proline being the most responsive having a chemiluminescence reaction efficiency 250 times greater than the amino acid with the lowest response, serine [24]. These disadvantages might limit further use of this scheme for real biological samples. Indirect UV-VIS and fluorescence detection of amino acids have been utilized in both HPLC [29, 30] and CZE [31], by exploiting the property that the amino acids exist as ionic forms at appropriate pHs. Either ionic UV-VIS absorbing species or fluorescing species are added to the mobile phase, not only to elute the analytes but also to indicate the presence of the analytes. As an ionized amino acid elutes from the column, the concentration of the counter ions in the mobile phase, which are being monitored, decreases to maintain electroneutrality in the mobile phase. Thus, negative peaks indicate the presence of the analytes. Due to the inherently high background, this scheme often suffers from baseline drift and fluctuation, resulting in relatively high detection limits. The high background results in baseline drift when using gradient elution, which is often necessary for complex mixture of analytes which have a wide range of affinities to the stationary phase. A number of electrochemical methods have also been developed and commercialized for detecting amino acids. Reasonably low

Reproduced with permission of the copyright owner. Further reproduction prohibited without permission.

detection limits (~ 20 pmol) have been achieved [34]. Electrochemical methods are also more selective than other methods. A commonly encountered problem when using electrochemical methods for detection is the poisoning of the noble metal electrodes [32, 33].

The literature contains several examples of amino acid detection schemes which exploit the complexation abilities of these compounds. An indirect chemiluminescence detection method has been reported, which takes advantage of the fact that transition metal ions, such as Cu^{2+} and Co^{2+}, catalyze the luminol chemiluminescence reaction [35, 36]. Binding of the metal ions to the amino acids however, make these ions much less efficient catalysts for this reaction. Detection is based on adding the chemiluminescent reagents to the mobile phase via postcolumn mixers. When the separated amino acids elute from column, they form complexes with the catalytic metal ions, resulting in a loss of the chemiluminescence signal being detected. At least two postcolumn pumps are required due to the short-lifetime of the chemiluminescent signals, which increases the instrumental complexity and introduces additional extracolumn bandbroadening. Relatively high detection limits were obtained at the nmol injected level due to the high chemiluminescence background. Another indirect electrochemical detection scheme, used a copper-selective electrode as a potentiometric detector [37, 38]. A solution containing Cu^{2+} ion was added to the eluent postcolumn. Complexation between Cu^{2+} and amino acids results in the loss of Cu^{2+} activity, which is a measure of amino acid concentration in the column effluent. A problem for this method was that Cu(II) oxide and hydroxide

Reproduced with permission of the copyright owner. Further reproduction prohibited without permission.

easily deposit on the electrode surface resulting in the deactivation of the electrode. The fact that amino acid - Cu(II) complexes have a strong UV-VIS absorption around 240 nm. was also used to detect amino acids [39]. Cu^{2+} ion was added to the mobile phase. Amino acids were separated as the Cu(II) - amino acid complexes. which can be detected with a conventional HPLC UV-VIS detector.

The research presented here was directed at developing a new fluorescence detection scheme for amino acids. It has been shown that the fluorescence of L-Tryptophan (L-Trp). an aromatic amino acid. is quenched in the presence of Cu(II) ion [53. 54]. In Chapter 2. calculations were used to demonstrate that fluorescence quenching is due to the formation of a $Cu(L\text{-}Trp)_2$ complex. In the presence of other amino acids. which have a significant affinity for Cu(II). some fraction of the L-Trp is expected to be released from the complex. L-Trp fluorescence is thus recovered. as shown by:

$$Cu(L\text{-}Trp)_2 + nA \rightleftharpoons Cu(A)_n + 2\ L\text{-}Trp^* \qquad \text{(Eq. 4.1)}$$

where A is the analyte molecule: L-Trp* is the fluorescently active form of L-Trp and n is the number of the analyte molecules coordinated to Cu(II).

This approach to HPLC detection may provide several advantages over other indirect UV-VIS. fluorescence and chemiluminescence detection methods. A relatively "dark" background assures baseline stability and a low noise level: the reaction requires minimal added postcolumn mixing: and. in contrast to detection schemes based on a

Reproduced with permission of the copyright owner. Further reproduction prohibited without permission.

chemiluminescence reaction, which have a very short lifetime, no effort is needed to further minimize the volume between the mixing tee and detection cell. Another advantage of this approach is that it should be immune to interference from any compound which does not complex with Cu(II) ion.

4.2 Materials and Methods

4.2.1 Materials

The following L-amino acids were purchased from Sigma Chemical Co. (St. Louis, MO, USA): lysine (Lys), alanine (Ala), glycine (Gly), valine (Val), proline (Pro), isoleucine (Ile), leucine (Leu), methionine (Met), threonine (Thr), serine (Ser), histidine (His), arginine (Arg), phenylalanine (Phen), glutamic acid (Glu), aspartic acid (Asp), cystine (Cys), cysteine (CysH), homocystine (Hcys), homocysteine (HcysH) and tyrosine (Tyr). Reagent grade copper sulfate, sodium acetate and sodium borate ($Na_2B_4O_7 \cdot 10H_2O$) were purchased from J.T. Baker Chemical Co. (Phillipsburg, NJ, USA). All chemicals were used as received without further purification.

The deionized water used in the preparation of standard solutions and eluents was obtained from a Milli-Q water system (Millipore, Bedford, MA, USA). All mobile phases were filtered through a 0.45 μm nylon filter (Whatman, Hillsboro, OR, USA) prior to use. Dilute aqueous solutions of reagent grade sodium hydroxide (Fisher, Pittsburgh, PA, USA) and hydrochloric acid (Baker, Phillipsburg, NJ, USA) were used to adjust the pH of the mobile phases and postcolumn reagents.

Reproduced with permission of the copyright owner. Further reproduction prohibited without permission.

The instrumentations for chromatographic separation and detection are similar to the instrumentations used in Chapter 3, except that separation of the amino acids was achieved with the use of a Dionex (Sunnyvale, CA, USA) SAX AMINOPAC-PA 10 analytical column.

4.2.2 Chromatographic Separation/Detection

The schematic of the instrumental setup is presented in Figure 3.3. The concentration of acetate ion in the mobile phase was adjusted for the baseline separation of the amino acids. The pH of the mobile phase was adjusted to 11.6. The mobile phase flow rate was set at 0.3 ml/min. Mobile phases were purged with helium. The postcolumn reagent, a 0.05 mM $Cu(L\text{-}Trp)_2$ solution buffered with 3 mM sodium borate ($Na_2B_4O_7$), was introduced into the mixing tee, where it mixed with the column eluent. The postcolumn reagent pH was adjusted with either a 2M NaOH solution or a concentrated hydrochloric acid solution.

4.3 Results and Discussions

4.3.1 Chromatographic Conditions for Separation of Amino Acids

The pH of all mobile phases was adjusted above 11.0 to assure appropriate ionization of the amino acids for separation using the anion exchange column, since most amino acids have a first acidic association constant in the pH range of 9.2 - 10.0 [63]. A polymer based anion exchange column was chosen to avoid the degradation of a silica based

Reproduced with permission of the copyright owner. Further reproduction prohibited without permission.

stationary phase at these high pHs. The amino acids: Lys. Ala. Gly. Val. Pro. Ile. Leu. Met. Thr. Ser. His and Arg are weakly retained on the Dionex SAX AMINOPAC-PA10 stationary phase and were separated with an 8 mM NaAc mobile phase. The amino acids: Phen. Glu. Asp. Cys and Tyr. are strongly retained on this particular stationary phase and were baseline separated with a mobile phase containing 0.25M NaAc. The three sulphur-containing amino acids (Met. Cys and Hcys) were baseline separated with a mobile phase containing 0.4M NaAc. For experiments with the twelve weakly retained amino acids. the mobile phase was constantly purged with helium to prevent carbon dioxide absorption from the atmosphere. which affects chromatographic reproducibility significantly. The postcolumn reagent. a 0.05 mM Cu(L-Trp)$_2$ solution buffered with 3 mM sodium borate ($Na_2B_4O_7$). was introduced to the mixing tee. where it mixed with the column eluent at a flow rate of 0.3 ml/min. The use of a flow control dampener was found to significantly improve the postcolumn flow stability.

4.3.2 Effect of pH on the Detection

The pH of the solution affects detection of the analytes in several ways. The extent of L-Trp complexation with Cu^{2+} ion is a function of pH. which thereby affects the degree of fluorescence quenching. The affinities of the amino acids (which are the analytes in this case) for Cu^{2+} are also dependent on solution pH. with the deprotonated forms of the amino acids having a much stronger affinity for the Cu^{2+} ion. Therefore. the pH of the analyte solution entering the detector flow cell needs to be controlled so that the

Reproduced with permission of the copyright owner. Further reproduction prohibited without permission.

background fluorescence of the solution is relatively low, providing a "dark" background, while at the same time allowing high affinities of the analytes for Cu^{2+} ion.

To better understand the nature of this detection scheme, several types of equilibria must be considered in an aqueous solution of $Cu(L\text{-}Trp)_2$, including:

1. Cu(II) ion, L-Trp complexation equilibria:

$$Cu^{2+} + nX^{-} \rightleftharpoons [Cu(X)_n]^{2-n} \qquad (X = L\text{-}Trp,\ n = 1, 2) \qquad \text{(Eq. 4.2)}$$

2. L-Trp protonation equilibria:

$$X^{-} + nH^{+} \rightleftharpoons H_nX^{n-1} \qquad (X = L\text{-}Trp,\ n = 1, 2) \qquad \text{(Eq. 4.3)}$$

3. Cu(II) ion, hydroxide complexation equilibria:

$$Cu^{2+} + nOH^{-} \rightleftharpoons [Cu(OH)_n]^{2-n} \qquad (n = 1, 2, 3, 4) \qquad \text{(Eq. 4.4)}$$

$$2Cu^{2+} + 2OH^{-} \rightleftharpoons Cu_2(OH)_2^{2+} \qquad \text{(Eq. 4.5)}$$

Fluorescence quenching of L-Trp results from the formation of Cu^{2+} - L-Trp complexes. However, the protonation equilibria, and the Cu^{2+} - OH^{-} complexation equilibria compete with Cu^{2+} - L-Trp complexation for both Cu^{2+} and L-Trp. As the pH of the solution decreases, L-Trp protonation increases, while as the pH of the solution increases, Cu^{2+} - OH^{-} complexation increases. Calculations in the earlier part of this study indicated that at a pH of 8.1, the complexation of Cu^{2+} - L-Trp is optimum, resulting in optimum fluorescence quenching.

Reproduced with permission of the copyright owner. Further reproduction prohibited without permission.

Though the above discussion suggests that pH 8.1 is the optimum pH to monitor fluorescence quenching of L-Trp by the Cu(II) ion, it might not be the ideal pH for analyte detection for several reasons. For example, the complexation abilities of the amino acids to be detected are also affected by the pH of the solution. Complicating the situation further, the fluorescence efficiency of L-Trp is also dependent on pH. For these reasons, three factors which are dependent on the pH of the solution must be considered: 1.) The dissociation of $Cu(L\text{-}Trp)_2$ increases both above pH 8.1 and below pH 8.1; 2.) The fluorescence of free L-Trp steadily increases above pH 8.0, as demonstrated in Figure 2.3. This pH dependence can be explained by the fact that the deprotonated form of L-Trp has a higher fluorescence efficiency than zwitterionic L-Trp. 3). The affinities of the amino acids for Cu(II) ion vary with pH, since complexation is affected by both the degrees of amino acid protonation and Cu(II) - hydroxide complexation.

To determine how changes in the pH of the solution affect Cu(II) - amino acid complexation, the conditional stability constants, K_f', of the Cu(II) - amino acid complexes, represented as $Cu(A)_2$, were calculated using the following formula at several pHs:

$$K_f' = K_f \times \partial_{A^-}{}^2 \times \partial_{Cu^{2+}} \qquad \text{(Eq. 4.6)}$$

in which ∂_{A^-} is the fraction of unprotonated amino acid, and $\partial_{Cu^{2+}}$ is the fraction of free Cu^{2+}, taking into consideration the Cu(II) - hydroxide complexation, which are expressed

Reproduced with permission of the copyright owner. Further reproduction prohibited without permission.

as:

$$\partial_{A^-} = K_{a1} * K_{a2} / (K_{a1} * K_{a2} - K_{a1} * [H^+] + [H^+]^2) \qquad \text{(Eq. 4.7)}$$

$$\partial_{Cu^{2+}} = 1 / (1 + \beta_1 * [OH^-] + \beta_2 * [OH^-]^2 + \beta_3 * [OH^-]^3 + \beta_4 * [OH^-]^4) \qquad \text{(Eq. 4.8)}$$

where K_f' and K_f are the conditional stability constant and the stability constant of the complexes, respectively. The pK_a's of the amino acids and K_f values of the Cu(II) - amino acid complexes were obtained from the literature [63]. Representative plots of the calculated conditional stability constant K_f' versus pH for $Cu(Gly)_2$, $Cu(Phen)_2$, $Cu(Lys)_2$, $Cu(Asp)_2$, $Cu(Glu)_2$, $Cu(Pro)_2$, $Cu(Ala)_2$, $Cu(Tyr)_2$, $Cu(Val)_2$, $Cu(Leu)_2$, $Cu(Met)_2$, $Cu(Thr)_2$, $Cu(His)_2$ and $Cu(CysH)_2$ are presented in Figures 4.1 through 4.14. These plots show that the conditional stability constants for the amino acids have maximum affinities for Cu^{2+} ranging in pH from 7.8 for CysH to 9.0 for Pro.

Of the three pH dependent factors given above which affect analyte detection, the first one tends to lead to a decrease in fluorescence signal intensity when the pH of the detection solution is either greater or less than 8.1; since the signal intensity is inferred from the fluorescence of free L-Trp, the second factor indicates that an increase in pH results in an increase in the signal intensity; and the third factor indicates that most of the amino acids have a maximum complexing ability at pHs other than 8.1.

To determine how the combination of these three factors affects the intensities measured for the chromatographic peaks, experiments were conducted in which the pH of

Reproduced with permission of the copyright owner. Further reproduction prohibited without permission.

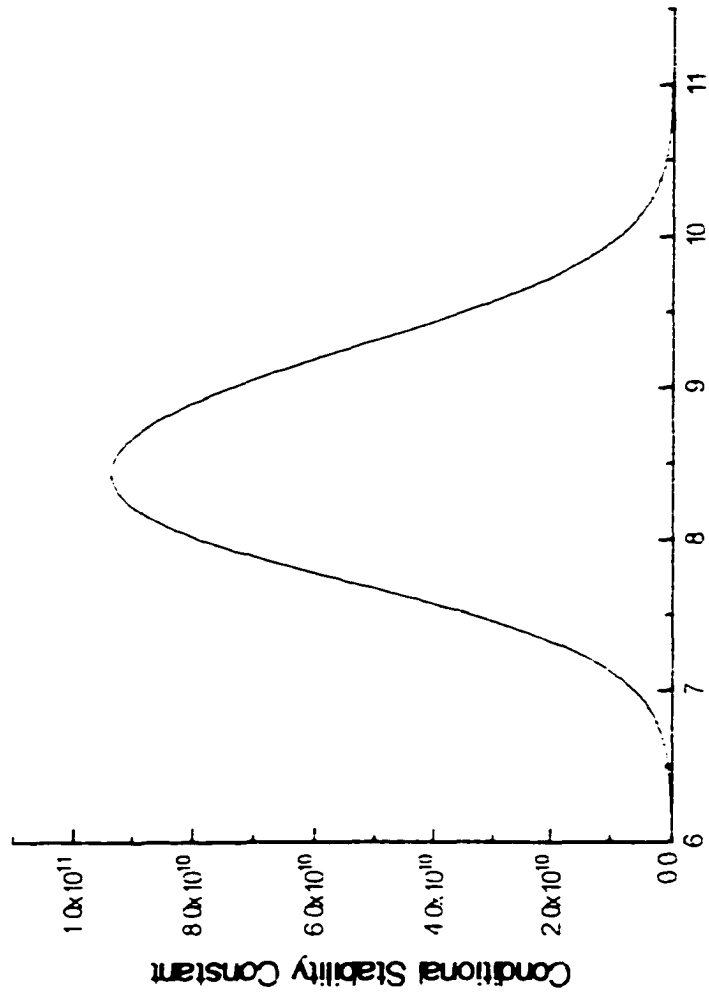

Figure 4.1: Calculated conditional stability constant of $Cu(Gly)_2$ as a function of pH

Reproduced with permission of the copyright owner. Further reproduction prohibited without permission.

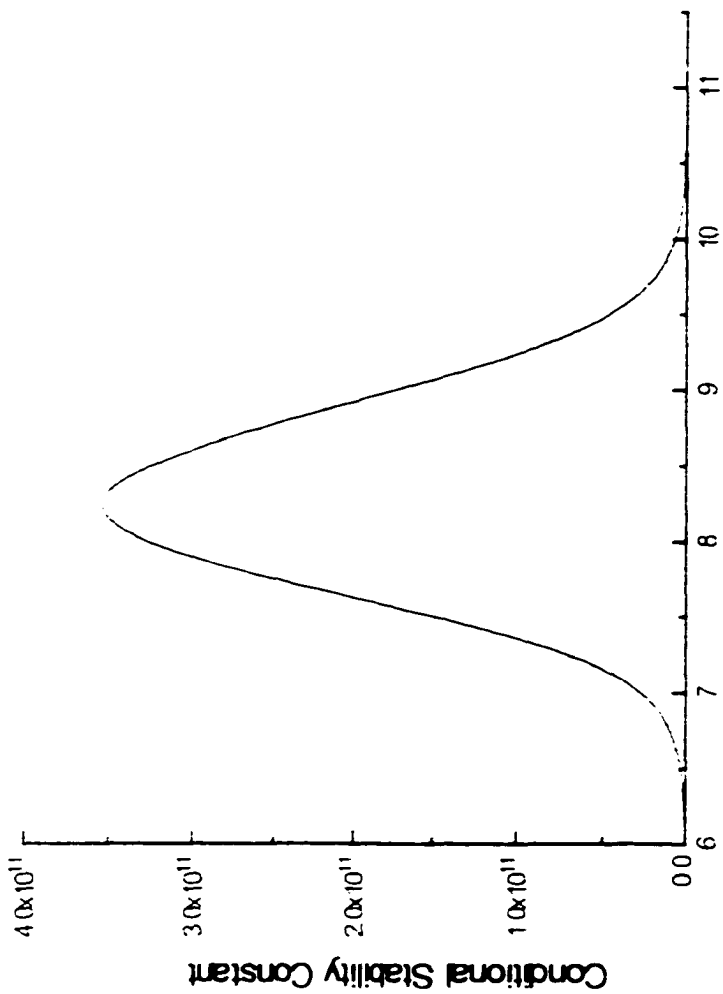

Figure 4.2: Calculated conditional stability constant of $Cu(Phen)_2$ as a function of pH

Reproduced with permission of the copyright owner. Further reproduction prohibited without permission.

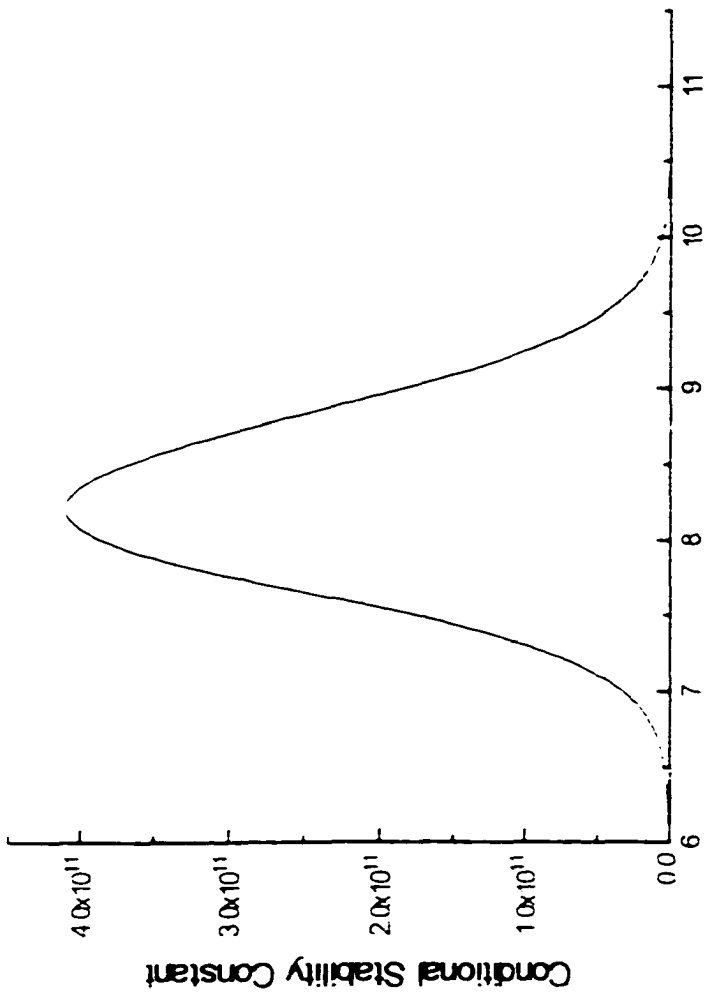

Figure 4.3: Calculated conditional stability constant of $Cu(Lys)_2$ as a function of pH

Reproduced with permission of the copyright owner. Further reproduction prohibited without permission.

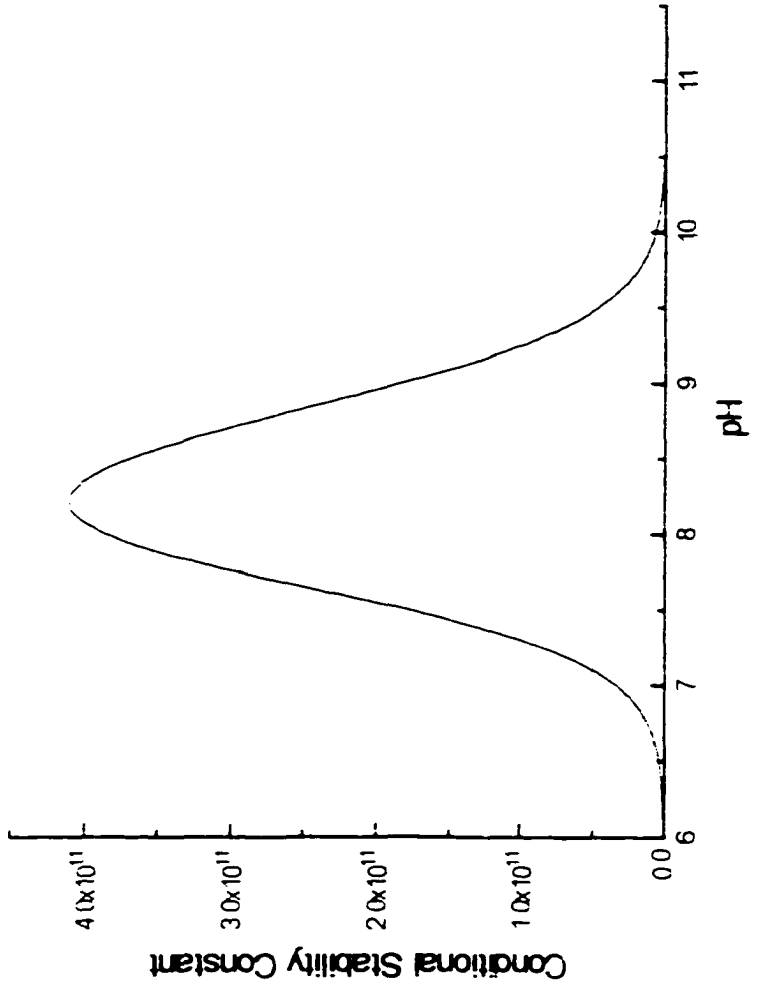

Figure 4.4: Calculated conditional stability constant of $Cu(Met)_2$ as a function of pH

Reproduced with permission of the copyright owner. Further reproduction prohibited without permission.

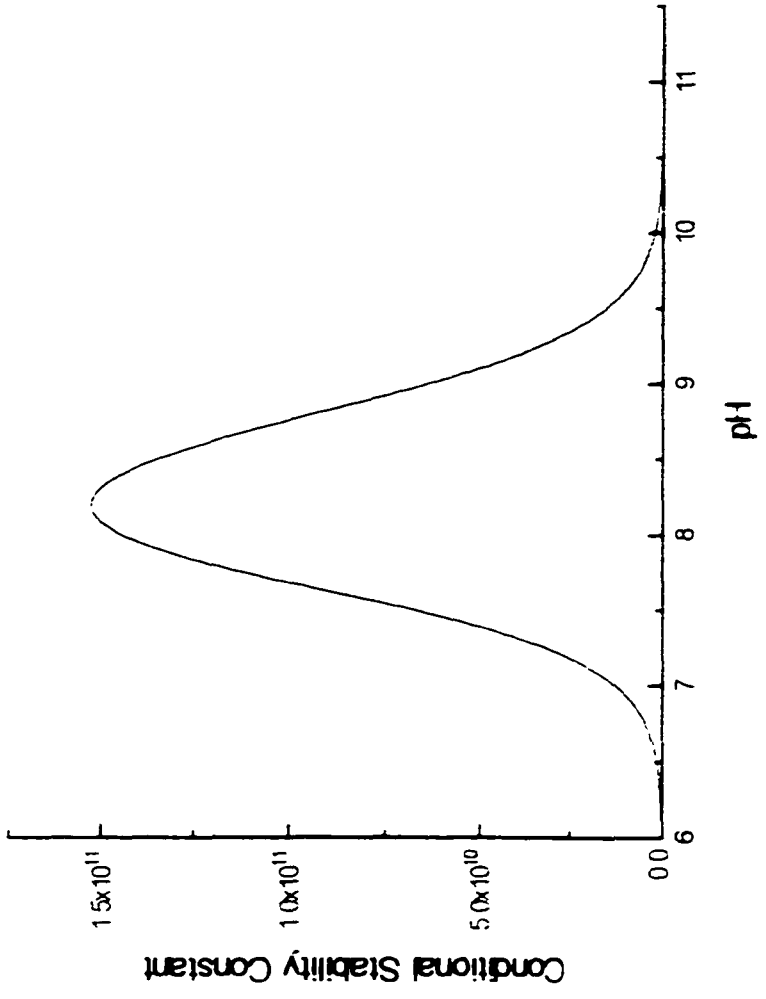

Figure 4.5: Calculated conditional stability constant of $Cu(Glu)_2$ as a function of pH

Reproduced with permission of the copyright owner. Further reproduction prohibited without permission.

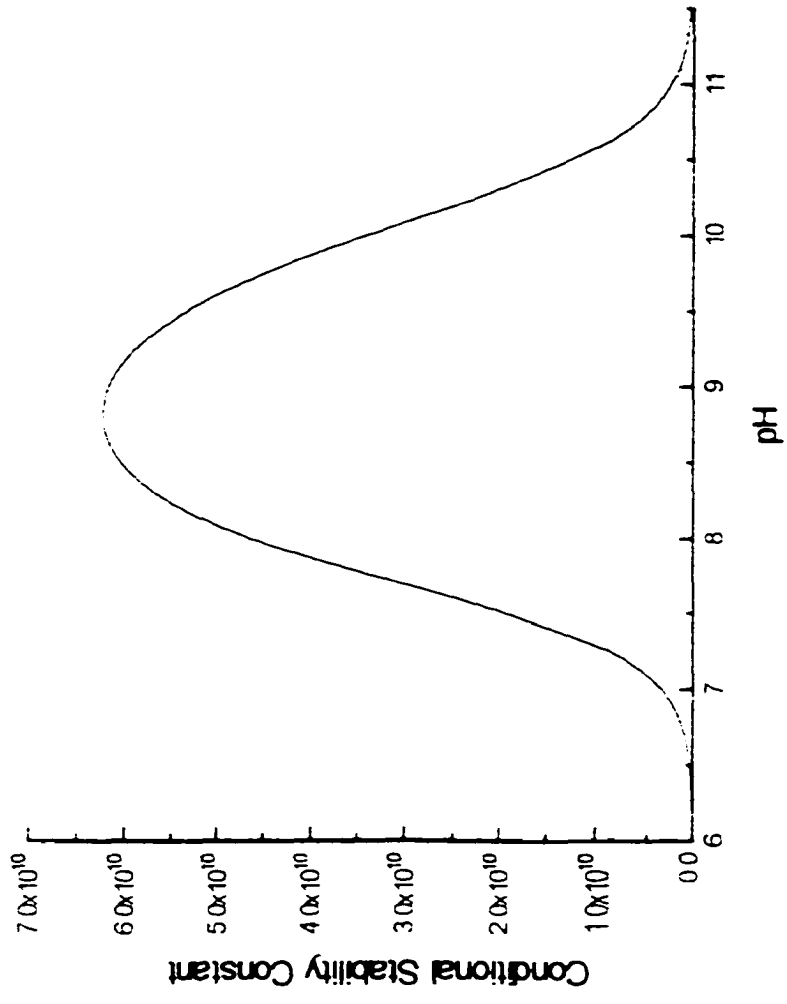

Figure 4.6: Calculated conditional stability constant of $Cu(Pro)_2$ as a function of pH

Reproduced with permission of the copyright owner. Further reproduction prohibited without permission.

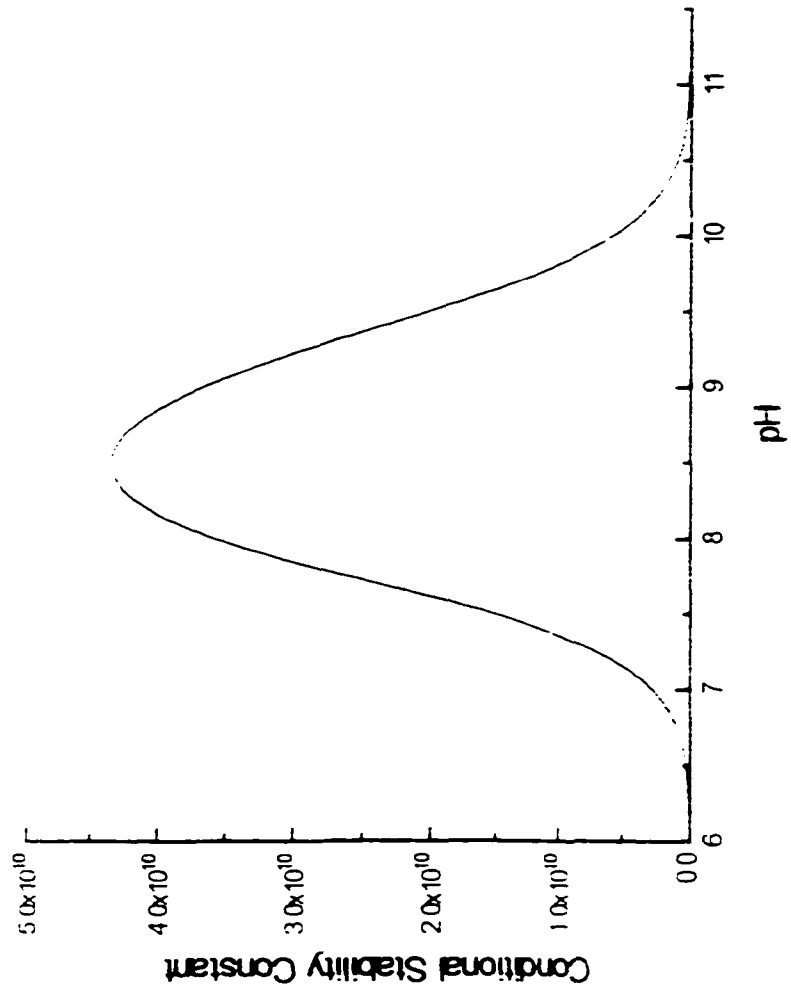

Figure 4.7: Calculated conditional stability constant of $Cu(Ala)_2$ as a function of pH

Reproduced with permission of the copyright owner. Further reproduction prohibited without permission.

Reproduced with permission of the copyright owner. Further reproduction prohibited without permission.

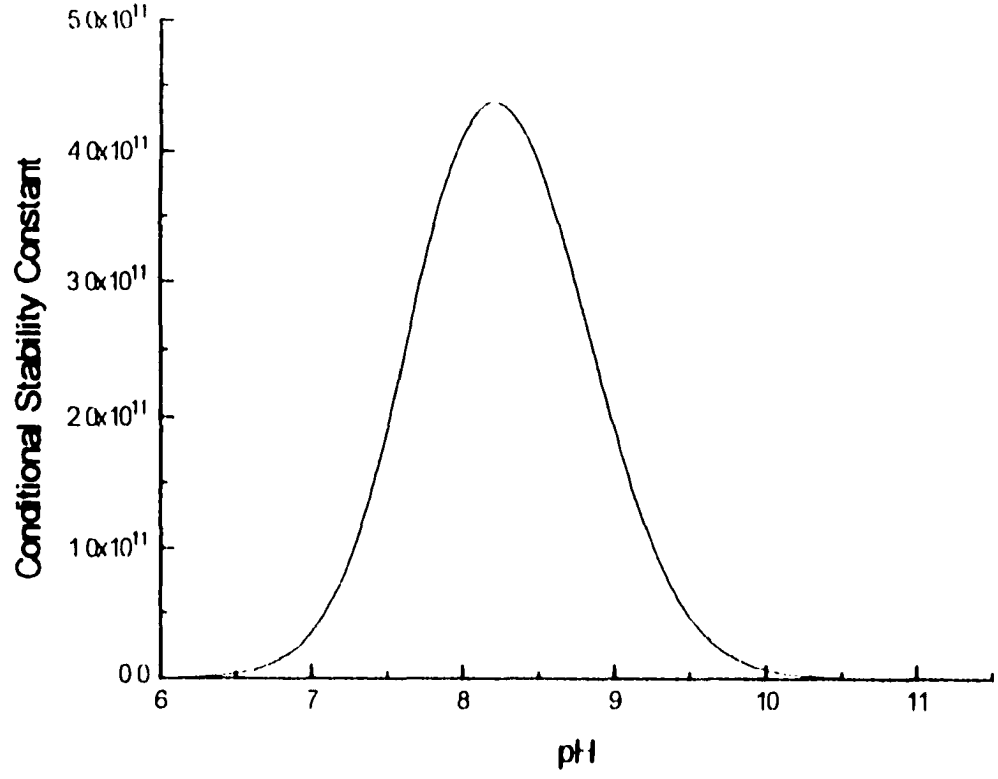

Figure 4.8: Calculated conditional stability constant of $Cu(Tyr)_2$ as a function of pH

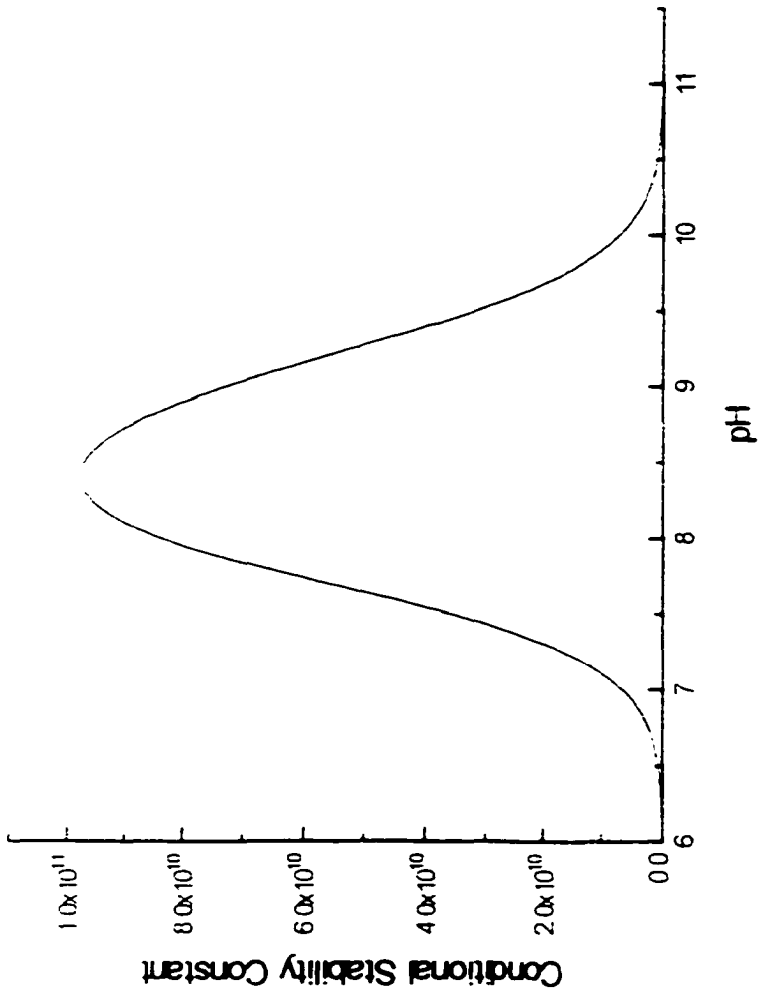

Figure 4.9: Calculated conditional stability constant of $Cu(Val)_2$ as a function of pH

Reproduced with permission of the copyright owner. Further reproduction prohibited without permission.

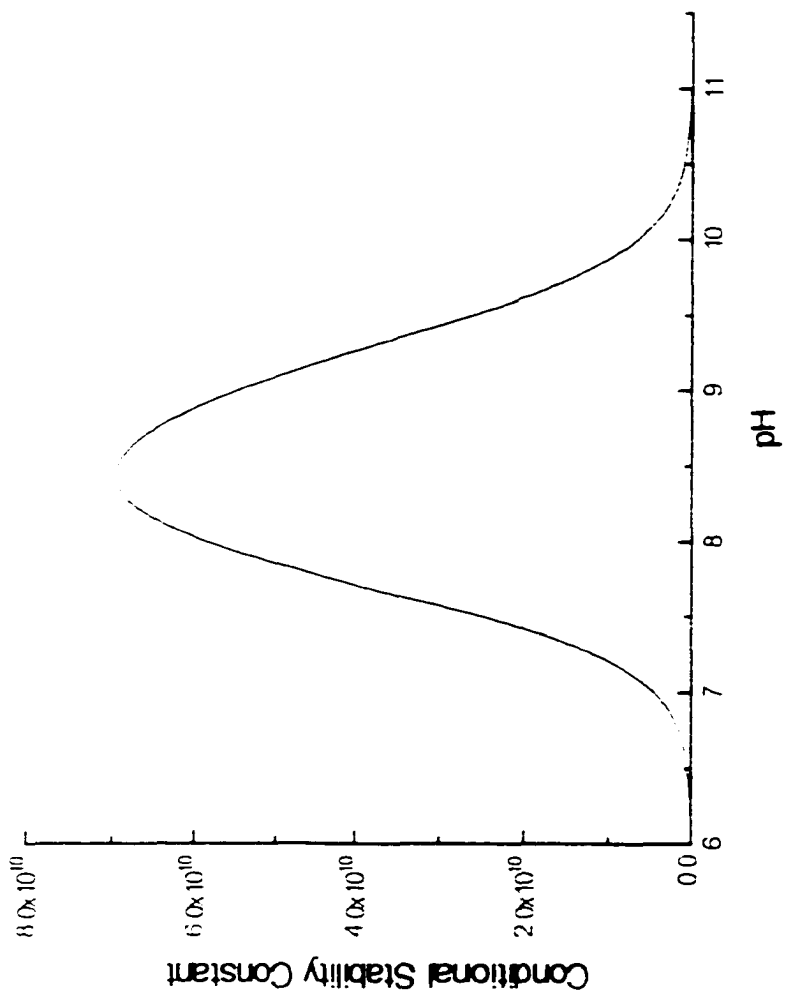

Figure 4.10 Calculated conditional stability constant of $Cu(Leu)_2$ as a function of pH

Reproduced with permission of the copyright owner. Further reproduction prohibited without permission.

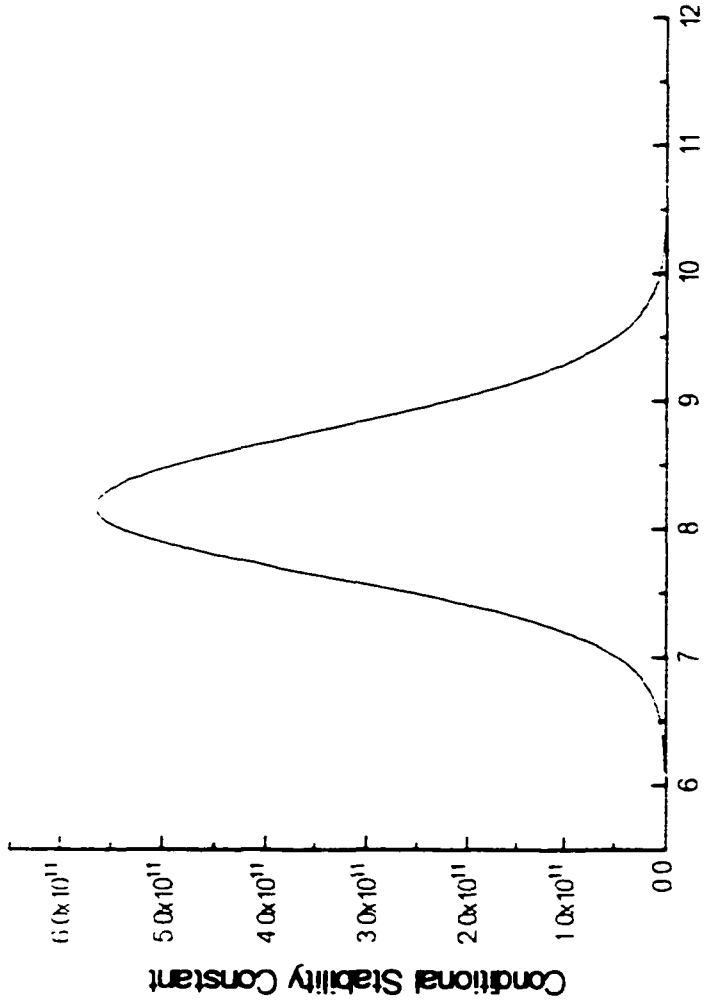

Figure 4.11: Calculated conditional stability constant of $Cu(Thr)_2$ as a function of pH

Reproduced with permission of the copyright owner. Further reproduction prohibited without permission.

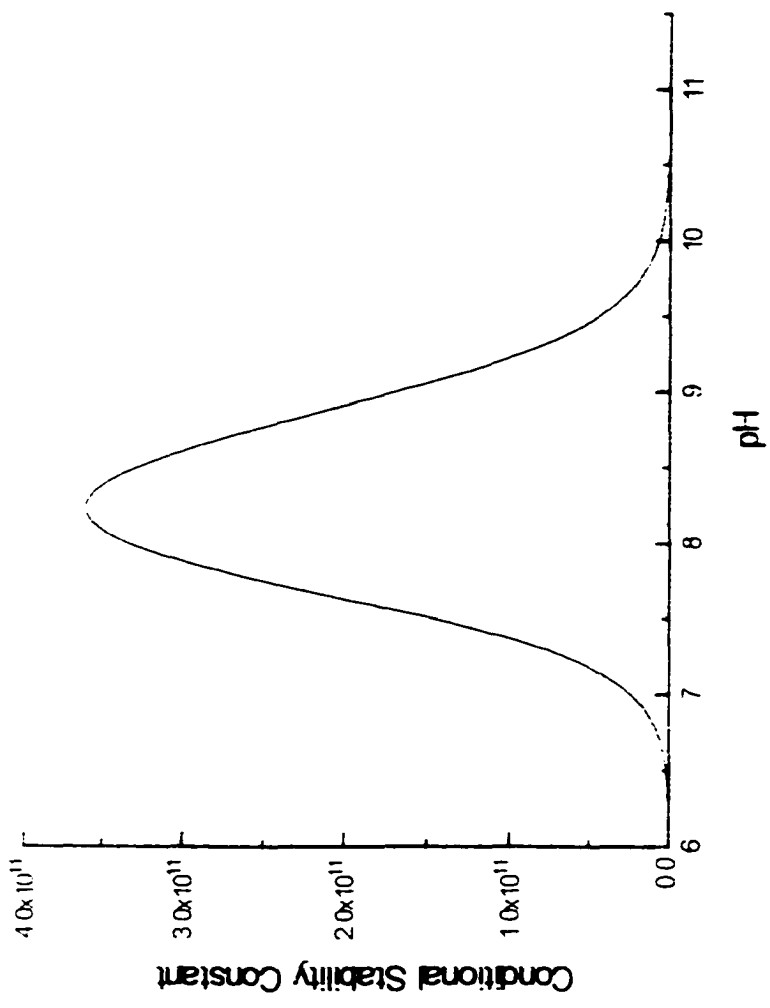

Figure 4.12: Calculated conditional stability constant of $Cu(His)_2$ as a function of pH

Reproduced with permission of the copyright owner. Further reproduction prohibited without permission.

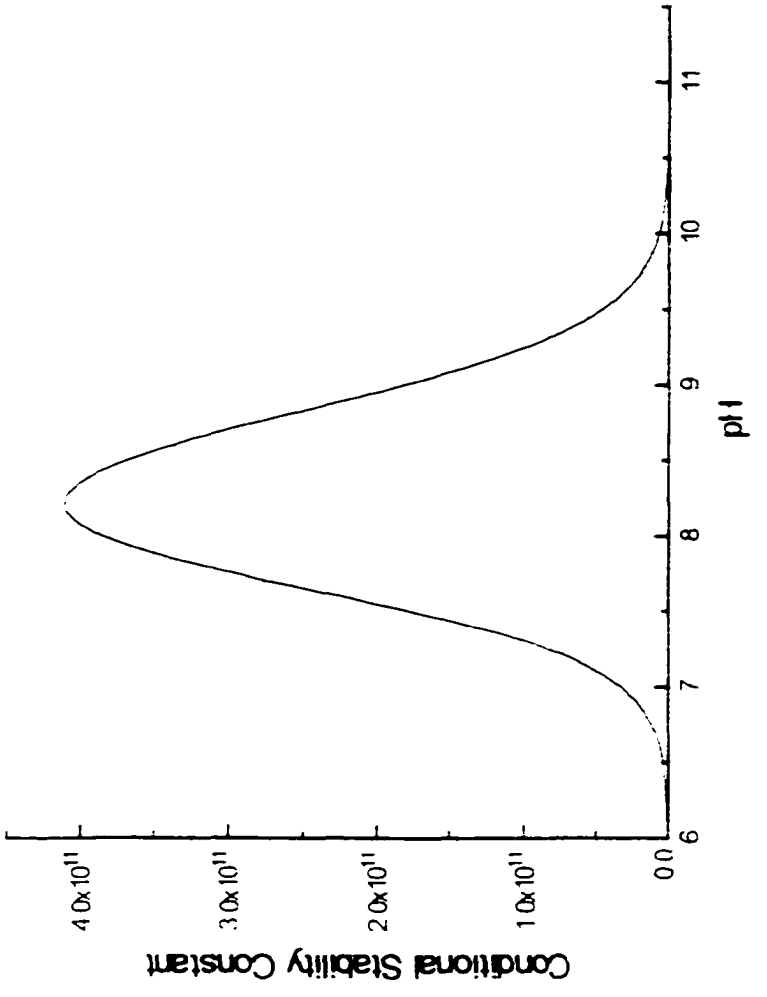

Figure 4.13: Calculated conditional stability constant of $Cu(Met)_2$ as a Function of pH

Reproduced with permission of the copyright owner. Further reproduction prohibited without permission.

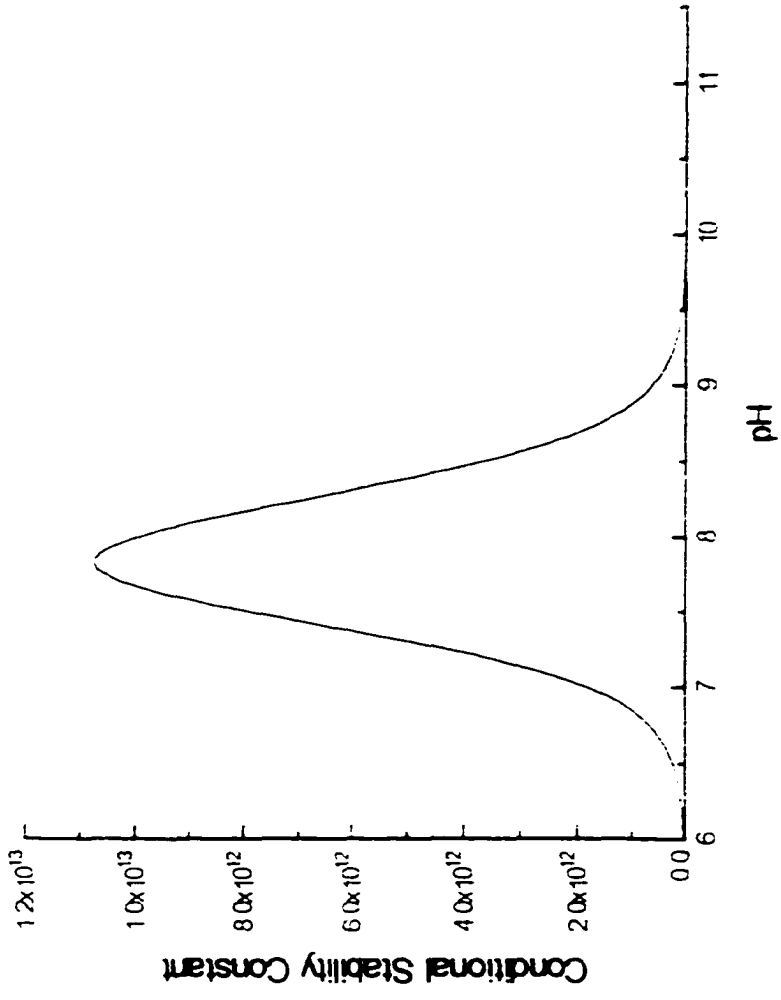

Figure 4.14: Calculated conditional stability constant of $Cu(CysH)_2$ as a function of pH

Reproduced with permission of the copyright owner. Further reproduction prohibited without permission.

the postcolumn buffer solution was adjusted. The peak intensities of eight weakly retained amino acids. Lys. Ala. Gly. Val. Pro. Ile. Leu. and Met are presented in Figure 4.15. Representative chromatograms obtained for five strongly retained amino acids. Phen. Glu. Asp. Cys and Tyr at detection conditions ranging from pH 7.8 to 9.4 are presented in Figure 4.16. It can be seen that for all the amino acids tested. the peak intensities increase steadily as detection pH increases in the range from 7.8 to 9.4. Based on the results of these experiments it was concluded that in this test pH range the second factor plays a dominant role in determining the detection efficiency. Slow $Cu(OH)_2$ deposition developed overnight when the postcolumn solution pH was higher than 9.1. resulting in detection irreproducibility due to the change in solution composition. The optimum pH was set between 8.8 to 9.0 to assure the long term stability of the postcolumn solution .

4.3.3 Effect of Postcolumn Reagent Flow Rate on Detection

The flow rate of the postcolumn reagent was adjusted in the range of 0.5 - 3.5 ml/min for the separation of the three amino acids Met. Cys and Hcys. Figure 4.17 shows the chromatograms obtained at different postcolumn reagent flow rates. As observed in these chromatograms. the chromatographic signal intensities for the amino acids decrease as the postcolumn reagent flow rate increases. due to the dilution of the analytes by the postcolumn reagent. However. for the particular postcolumn pumping system we used. the flow instability increases as the flow rate is below 1.5 ml/min. As shown in the Figure

Reproduced with permission of the copyright owner. Further reproduction prohibited without permission.

Reproduced with permission of the copyright owner. Further reproduction prohibited without permission.

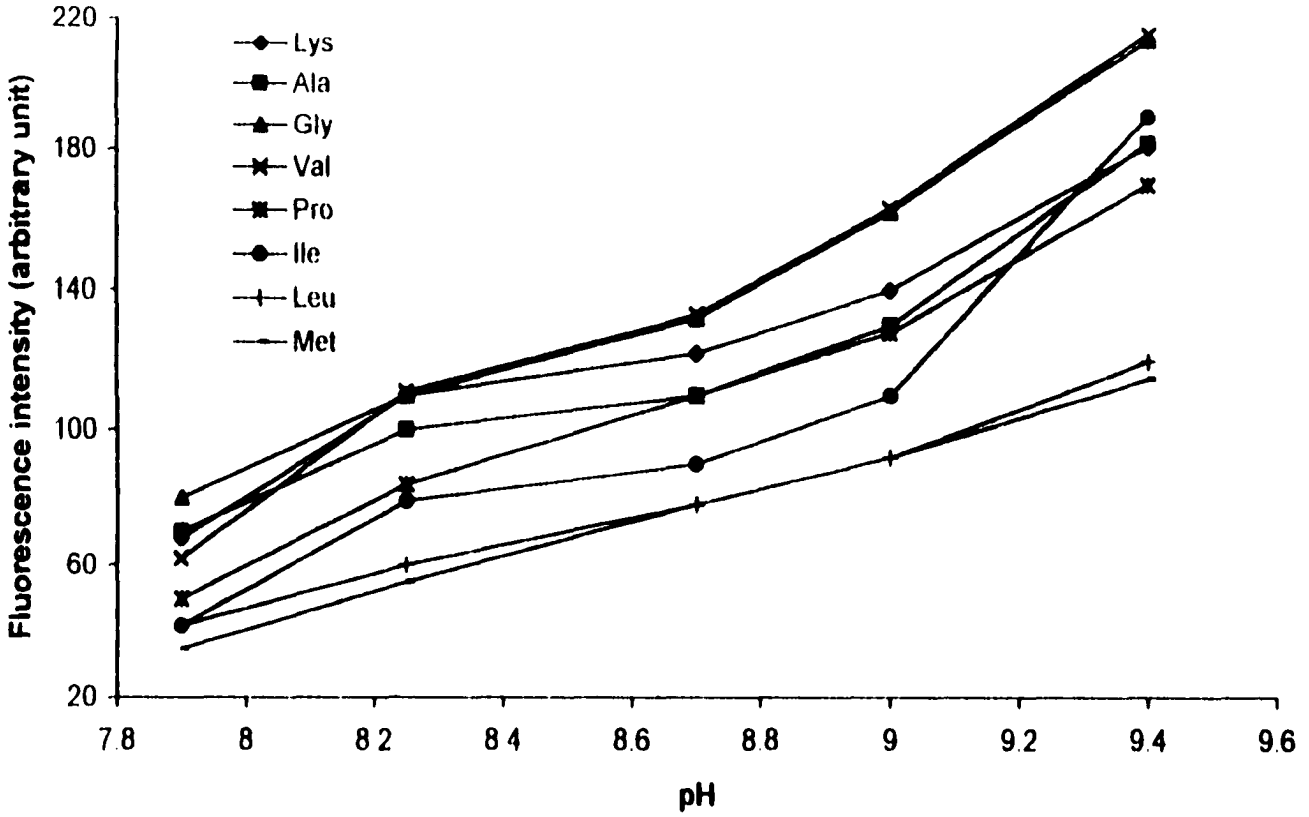

Figure 4.15: Chromatographic peak intensities as a Function of detection pH. The mobile phase was 8 mM NaAc at pH 11.6. The postcolumn reagent was 0.05 mM $Cu(L\text{-}Trp)_2$ in a 3 mM sodium borate buffer. The mobile phase and postcolumn reagent flow rates were 0.3 and 1.5 ml/min respectively. The mass of sample injected was 250 pmol for each amino acid.

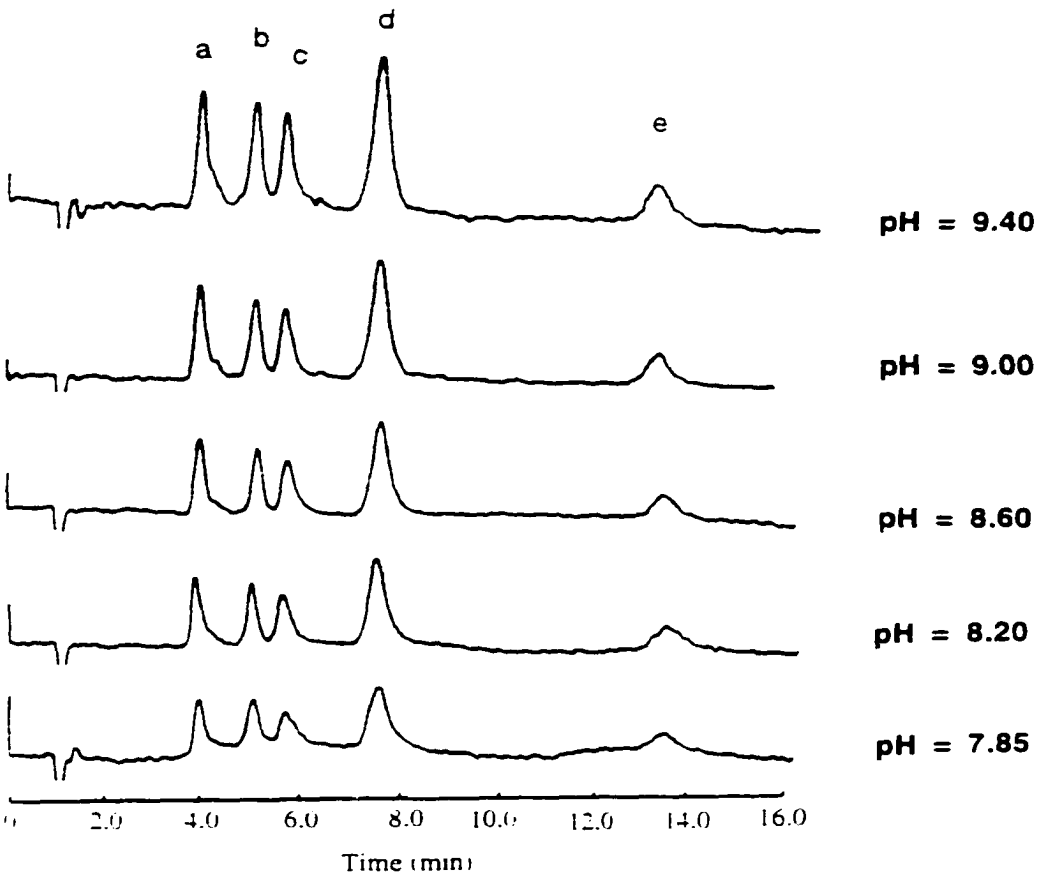

Figure 4.16 Representative chromatograms of 5 amino acids at detection pHs ranging from ~ 8.5 to 9.40. Separation was achieved on a Dionex AMINOPAC-PA10 SAX analytical column at ambient temperature. The mobile phase was 0.25M NaAc at pH 11.6. The postcolumn reagent was 0.05 mM Cu(L-Trp)$_2$ in a 3 mM sodium borate. The mass of sample injected was 250 pmol for each amino acid. (a) Phen. (b) Glu. (c) Asp. (d) Cys. (e) Tyr.

Reproduced with permission of the copyright owner. Further reproduction prohibited without permission.

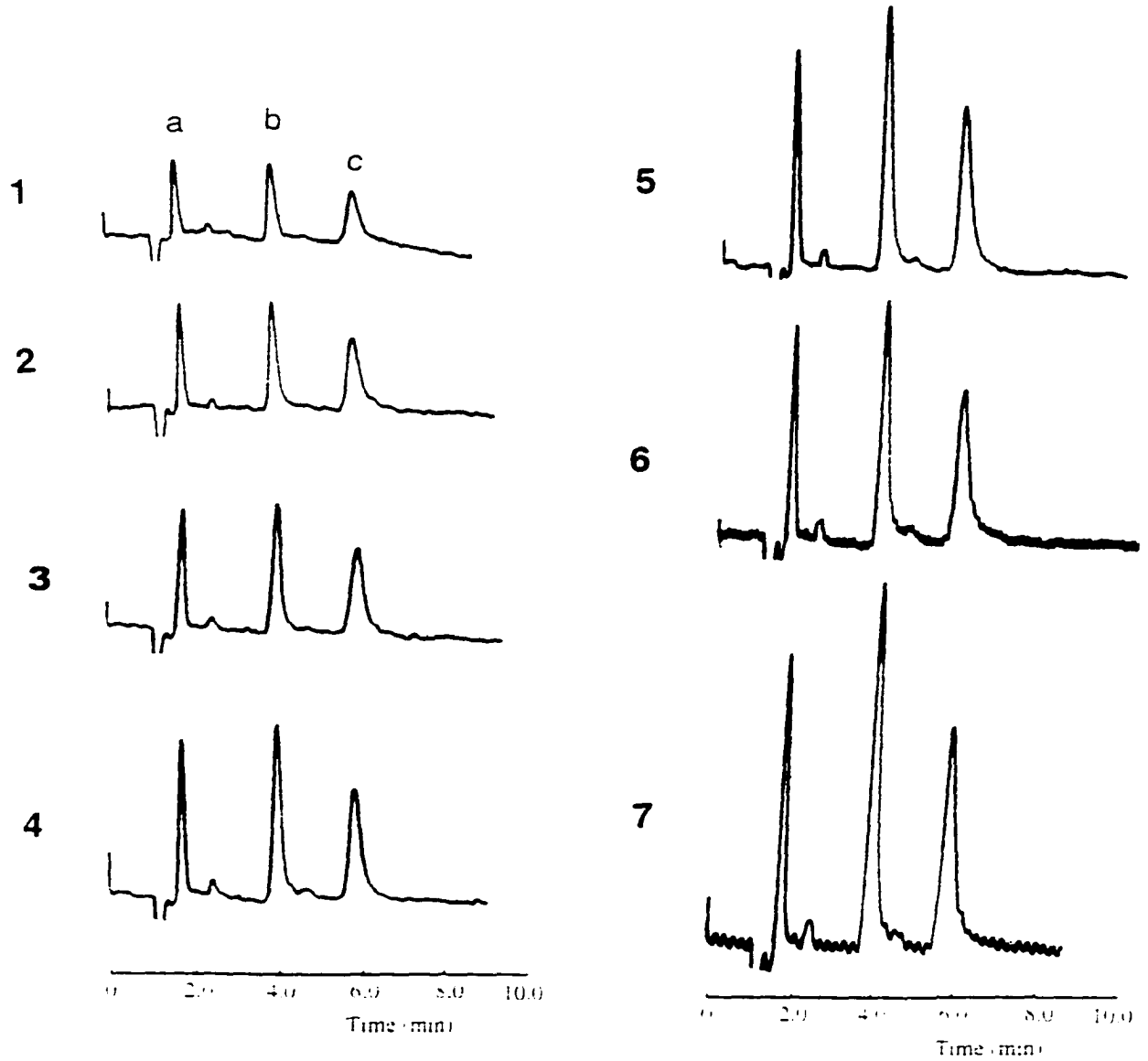

Figure 4.17: Representative chromatograms of amino acids obtained at different postcolumn reagent flow rates. Separation was achieved on a Dionex AMINOPAC-PA10 SAX analytical column at ambient temperature. The mobile phase was 0.4M NaAc at pH 11.5. The postcolumn reagent was 0.05 mM Cu-L-Trp$_2$ buffered at pH 8.70 in a 3 mM sodium borate solution. The mass of sample injected were 250 pmol for each amino acid. (a) Met, (b) Cys, (c) Hcys. Postcolumn reagent flow rate: chromatogram 1: 3.5 ml/min; 2: 2.5 ml/min; 3: 2.0 ml/min; 4: 1.5 ml/min; 5: 1.2 ml/min; 6: 0.8 ml/min; 7: 0.5 ml/min

Reproduced with permission of the copyright owner. Further reproduction prohibited without permission.

4.17, the baseline variability increases as the flow rate decreases. A compromise was made between the chromatographic signal intensities and baseline variability. The flow rate of the postcolumn reagent was set at 1.5 ml/min for this study.

4.3.4 Detection of Amino Acids under Optimized Separation/detection Conditions

Representative chromatograms showing the separation of 8 weakly retained amino acids and 3 sulphur-containing amino acids obtained using the optimized chromatographic separation and detection conditions are presented in Figures 4.18 and 4.19, respectively. The detection limit for Cys is 3.8 pmol injected using a 10 µl injection loop. Detection was reproducible, with relative standard deviations less than 3.0% for all three sulphur containing amino acids injected at two different concentrations (see Table 4.1). Linearity is excellent for the tested amino acids up to low nmol (For methionine, $y = 0.741 * x - 0.639$, $r^2 = 0.9999$, in the range 25 - 1000 pmol for a seven point linearity test). The detection limits for all of the amino acids tested are below 10 pmol with the exception of Tyr, which has a detection limit of 25 pmol under the conditions tested.

The sensitivity of the developed chromatographic detection scheme for the amino acids compares favorably to both the most sensitive direct detection methods reported thus far [34, 106], and UV-VIS detection using precolumn derivatization [38, 107]. This detection scheme also has the advantage of simplicity, good linearity, and good reproducibility. One other potential advantage is its selectivity. Most of the small peptides and biogenic monoamines have much lower affinities for Cu(II) than the

Reproduced with permission of the copyright owner. Further reproduction prohibited without permission.

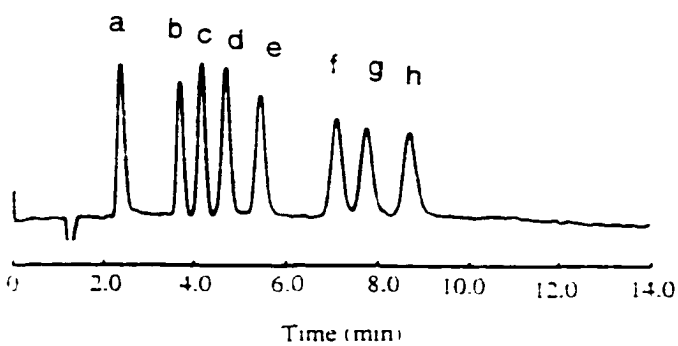

Figure 4.18: Representative chromatogram for the separation of 8 amino acids. Separation was achieved on a Dionex AMINOPAC-PA10 SAX analytical column at ambient temperature. The mobile phase was 8×10^{-2}M NaAc at pH 11.6. The postcolumn reagent was 0.05 mM Cu(L-Trp)$_2$ buffered at pH 8.70 in a 3 mM sodium borate solution. The mass of sample injected was 250 pmol for each amino acid. (a) Lys. (b) Ala. (c) Gly. (d) Val. (e) Pro. (f) Ile. (g) Leu. (h) Met.

Reproduced with permission of the copyright owner. Further reproduction prohibited without permission.

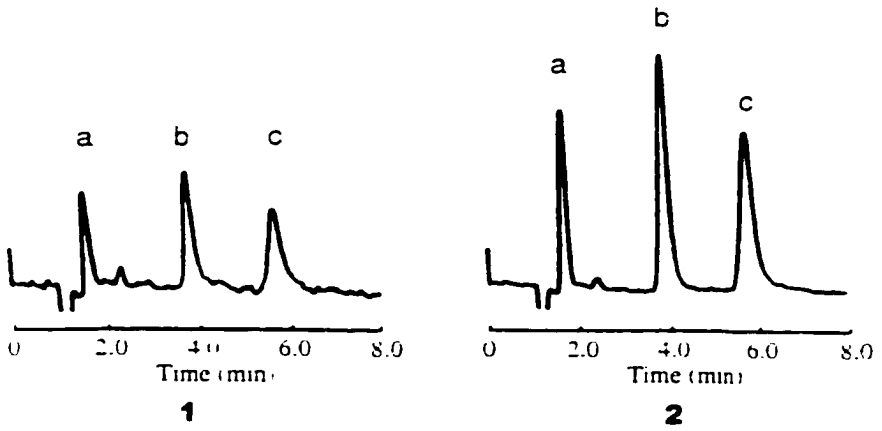

Figure 4.19: Representative chromatograms for the separation of 3 sulphur-containing amino acids. Separation was achieved on a Dionex AMINOPAC-PA10 SAX analytical column at ambient temperature. The mobile phase was 0.4M NaAc at pH 11.6. The postcolumn reagent was 0.05 mM Cu(L-Trp)$_2$ buffered at pH 8.70 in a 3 mM sodium borate solution. The mass of sample injected were: (1) 50 pmol; (2) 250 pmol for each amino acid. (a) Met. (b) Cys. (c) Hcys.

Reproduced with permission of the copyright owner. Further reproduction prohibited without permission.

	Met		Cys		Hcys	
	50 pmol	250 pmol	50 pmol	250 pmol	50 pmol	250 pmol
mean peak height (relative intensity)	116	585	144	778	102	512
RSD(%) (N=4)	2.6	1.9	2.9	0.6	1.7	1.7
Detection limit (pmol) (S/N = 3)	4.7		3.8		5.4	

Table 4.1. Statistical summary for detection of three sulphur -containing amino acids following chromatographic separation, as represented in Figure 2.19.

Reproduced with permission of the copyright owner. Further reproduction prohibited without permission.

individual amino acids [63], resulting in much lower responses, which may prove to be an advantage for studies involving real biological samples.

It should be noted that for reasonably good detection limits to be achieved, the analytes should have an affinity for Cu(II) at least comparable to L-Trp. Weaker affinity for the Cu^{2+} ion by the analytes will result in significantly less L-Trp being displaced from the $Cu(L\text{-}Trp)_2$ complex. Most of the amino acids have similar chelating ability for Cu(II), containing one amino group and one carboxyl group, indicating that all the analyte amino acids have an affinity for Cu(II) ion which is similar to L-Trp, though Cys has two amino groups and two carboxyl groups, resulting in a stronger chelating capacity and the lowest detection limit.

4.4 Conclusions

Indirect fluorescence detection of several amino acids based on utilization of $Cu(L\text{-}Trp)_2$ as a postcolumn reagent was coupled to a HPLC system. A Dionex SAX AMINOPAC-PA10 stationary phase was used for the separation of the amino acids. Retention of the amino acids on this phase is controlled by adjusting the concentration of sodium acetate in the mobile phase. As the most important detection parameter, detection pH was optimized by taking into consideration three factors that are expected to affect the detection. These three factors include effect of the pH on the complexation between Cu(II) ion and L-Trp, the effect of pH on the free L-Trp fluorescence and the effect of pH on the affinities between Cu(II) and amino acids. Based on the chromatographic data,

Reproduced with permission of the copyright owner. Further reproduction prohibited without permission.

it was determined that increasing fluorescence efficiency of L-Trp with increasing pH dominates the pH dependent pattern of the chromatographic signals. Detection limits of most of the amino acids following chromatographic separation are on the order of low pmol injected. Dynamic range is up to the order of nmol. The developed detection method has several advantages compared to conventional HPLC detection approaches for amino acids. It does not require complicated sample preparation and is free from the problems associated with the derivatization process, such as derivative instability.

Reproduced with permission of the copyright owner. Further reproduction prohibited without permission.

Chapter 5

Separation and Detection of Aminoglycoside Antibiotics Following HPLC Separation with Cu(L-Trp)$_2$ as the Postcolumn Reagent

5.1 Introduction

The aminoglycosides are a group of compounds which are used clinically to treat serious infections. Since the discovery and clinical use of streptomycin in the 1940's, numerous aminoglycosides have been developed and introduced as commercially available pharmaceuticals. These aminoglycosides have a very broad antimicrobial spectrum extending from gram-positive cocci to gram-negative bacilli [9]. Recently, the discovery of a neamine dimer, the first antibiotic that inhibits both bacterial ribosomal RNA and bacterial resistant enzymes [108, 109], may initiate a major revival in interest in the aminoglycoside antibiotics. The mechanism of actions for these drugs is that they bind to the surface of the bacteria and are transported through the cell wall. Once within the cell, aminoglycosides inhibit protein synthesis by the microorganisms, resulting in a rapid, concentration - dependent bactericidal action [10, 110].

Monitoring of the aminoglycoside concentration is important in drug pharmacokinetic studies, as well as studies concerning the clinical efficacy and side effects of these drugs [111]. Traditionally, HPLC analysis of the aminoglycosides involves either precolumn or postcolumn derivatization, since they do not possess functional groups which strongly

Reproduced with permission of the copyright owner. Further reproduction prohibited without permission.

absorb or fluoresce [112 - 114], as demonstrated by the representative molecular structures of the four aminoglycosides given in Figure 1.3. Common derivatization agents for the aminoglycosides are 1-fluoro-2,4-dinitrobenzene (FDNB) [115, 116] and related nitrophenylation reagents such as 2,4,6 - trinitrobenzenesulphonic acid [109], and o-phthaldehyde (OPA) derivatives [118]. Limitations of detection approaches involving derivatization often include time-consuming and labor-intensive sample preparation and the instability of the derivatives. Various experimental factors such as the concentration of the derivatization agent, pH, temperature and solvent composition need to be adjusted to optimize the derivatization reaction. Derivatives may degrade within a few hours after the derivatization reaction [111], which increases the complexity and lowers the reproducibility of the analysis. In the case of the aminoglycosides, because they possess several amino groups, multiple derivatives may be produced for a single compound [113]. Much effort has been, and currently is being expended to seek nonderivatization methods for the analysis of the aminoglycoside antibiotics, among which pulsed electrochemical detection [119 - 121] and mass spectrometric detection [122, 123] have been studied extensively. Recently, detection of several aminoglycosides following chromatographic separation based on light scattering has also been reported [124].

In this study, the goal was to apply an indirect fluorescence detection scheme for the analysis of the aminoglycoside antibiotics, using $Cu(L\text{-}Trp)_2$ as a postcolumn reagent. Chromatographic separation and detection conditions were optimized, and the detection performance was evaluated. The effect of an organic modifier in the chromatographic

Reproduced with permission of the copyright owner. Further reproduction prohibited without permission.

mobile phase on detection was evaluated, since reversed-phase chromatography with an organic mobile phase usually provides superior separation efficiency. Another natural fluorescent amino acid, tyrosine (Tyr), was also investigated for use with its Cu(II) complex $Cu(Tyr)_2$ as the postcolumn reagent.

5.2 Materials and Methods

5.2.1 Materials

The aminoglycosides, amikacin sulfate ($C_{22}H_{43}N_5O_{13} \cdot 2H_2SO_4$), kanamycin A sulfate ($C_{18}H_{36}N_4O_{11} \cdot H_2SO_4$), kanamycin B sulfate ($C_{18}H_{37}N_5O_{10} \cdot 2H_2SO_4$), neomycin sulfate ($C_{23}H_{46}N_6O_{13} \cdot 2H_2SO_4$), tobramycin sulfate ($C_{18}H_{37}N_5O_9 \cdot 2H_2SO_4$) and geneticin sulfate ($C_{20}H_{40}N_4O_{10} \cdot 2H_2SO_4$) were purchased from Sigma (St. Louis, MO, USA). The aminoglycosides ribostamycin sulfate ($C_{17}H_{34}N_4O_{10} \cdot 2H_2SO_4$), hygromycin B ($C_{20}H_{37}N_3O_{13}$) and neamine ($C_{12}H_{26}N_4O_6$), together with an aminoglycoside related compound, spectinomycin sulfate ($C_{14}H_{24}N_2O_7 \cdot H_2SO_4$), were purchased from ICN Pharmaceuticals (Costa Mesa, CA, USA). L-Trp was purchased from Aldrich (Milwaukee, WI, USA). Reagent-grade copper sulfate was purchased from Fisher (Pittsburgh, PA, USA). Reagent-grade sodium acetate, sodium borate ($Na_2B_4O_7 \cdot 10H_2O$) and naphthalene were purchased from Baker (Phillipsburg, NJ, USA). The deionized water used in the preparation of standard solutions and eluents was obtained from a Milli-Q water system (Millipore, Bedford, MA, USA). All mobile phases and

Reproduced with permission of the copyright owner. Further reproduction prohibited without permission.

postcolumn reagents were filtered through a 0.45 µm nylon filter (Whatman, Hillsboro, OR, USA) prior to use. Dilute aqueous solutions of reagent-grade sodium hydroxide (Fisher, Pittsburgh, PA, USA) and hydrochloric acid (Baker, Phillipsburg, NJ, USA) were used to adjust the pHs of the mobile phases and postcolumn reagent. Commercial aminoglycoside formulations were obtained locally.

A SIM AMINCO luminescence spectrometer (SIM Instruments Inc., Urbana, IL) was used for the static fluorescence studies. The instrumentations for the chromatographic separation and detection are similar to the instrumentations used in Chapter 3 & 4. A Hamilton PRP-X200 column (250 x 4.6 mm I.D.; Reno, NV, USA), containing a polymer-based strong cation exchanger with a particle size of 10 µm, was used in the cation exchange chromatographic mode for the separation of aminoglycosides. A Supelcosil^{TM} octadecyl (C_{18}) column (150 x 4.6 mm I.D.; Supelco, Bellefonte, PA, USA) was used in the reversed-phase ion pair chromatographic mode for the separation of aminoglycosides. For studies involving Cu(L-Trp)$_2$ as the postcolumn reagent, the excitation wavelength of the fluorescence detector was set at 280 nm and a 350 nm longpass glass filter was utilized for selecting emission; for studies involving Cu(L-Tyr)$_2$ as the postcolumn reagent, the excitation wavelength of the detector was set at 280 nm and a 300 nm longpass glass filter was utilized for selecting emission.

Reproduced with permission of the copyright owner. Further reproduction prohibited without permission.

5.2.2 Measurement Fluorescence of L-Tyrosine (L-Tyr) and $Cu(L\text{-}Tyr)_2$ as a Function of pH

A solution of 0.1 mM L-Tyr was prepared by dissolving the appropriate mass of solid L-Tyr in deionized water. The pH of the solution was adjusted in the pH range of 1.8 - 11.0. Fluorescence of the solutions at different pHs was measured. The excitation and emission wavelengths were set at 280 nm and 300 nm, respectively, based on Ref. [56].

A solution of 0.05 mM $Cu(L\text{-}Tyr)_2$ was prepared by dissolving the appropriate masses of solid L-Tyr and $CuSO_4 \cdot 5H_2O$ in deionized water. The pH of the solution was adjusted in the pH range of 1.8 - 11.0. The fluorescence data of the solutions at different pHs were measured with the excitation and emission wavelengths set at 280 nm and 300 nm, respectively. Figure 5.1 gives the fluorescence intensities of 0.1mM L-Tyr and 0.05 mM $Cu(L\text{-}Tyr)_2$ as a function of pH.

5.2.3 Studies on the Effect of Methanol on L-Trp Fluorescence Quenching

Solutions containing 0.05 mM $Cu(L\text{-}Trp)_2$ were prepared by dissolving the appropriate masses of solid L-Trp and $CuSO_4 \cdot 5H_2O$ in a methanol water mixture with methanol concentrations in the range of 5 - 50% (by volume). The apparent solution pH was set at 8.1. The solutions were buffered with a 4 mM sodium borate solution. The fluorescence data of the solutions with different methanol concentrations were measured. The excitation and emission wavelengths were set at 280 nm and 350 nm, respectively.

Reproduced with permission of the copyright owner. Further reproduction prohibited without permission.

Reproduced with permission of the copyright owner. Further reproduction prohibited without permission.

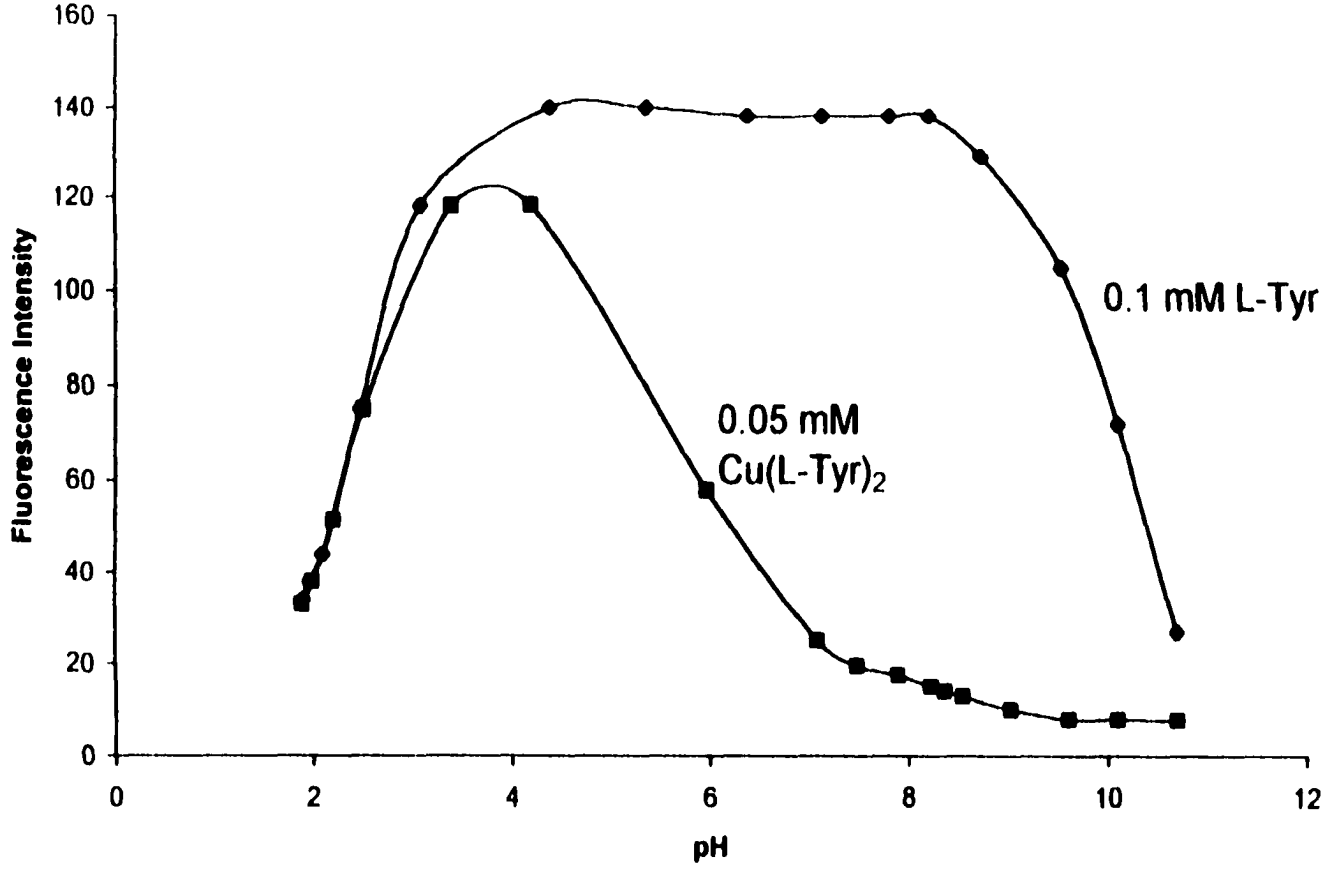

Figure 5.1: Fluorescence of L-Tyr and $Cu(L\text{-}Tyr)_2$ as a Function of pH. Excitation and emission wavelengths are 280 nm and 300 nm, respectively.

Figure 5.2 gives the fluorescence intensities of 0.05 mM Cu(L-Trp)$_2$ solutions having different methanol compositions at an apparent pH 8.1.

A solution of 0.05 mM Cu(L-Trp)$_2$ was prepared by dissolving the appropriate masses of solid L-Trp and $CuSO_4 \cdot 5H_2O$ in 30% methanol (by volume). The apparent pH of the solution was adjusted in the range of 1.8-11.0. The fluorescence data of solutions at different apparent pHs were measured. The excitation and emission wavelengths were set at 280 nm and 350 nm, respectively. Figure 5.3 gives the fluorescence intensities of 0.1mM L-Trp and 0.05 mM Cu(L-Trp)$_2$ in a 30% methanol solution as a function of apparent pH.

5.2.4 Fluorescence "Titration" of Cu(L-Trp)$_2$ with Several Aminoglycosides

A solution of Cu(L-Trp)$_2$ was prepared by dissolving the appropriate masses of solid L-Trp and $CuSO_4 \cdot 5H_2O$ in an aqueous sodium borate solution. Solutions containing different concentrations of the aminoglycosides were added to standard 0.05 mM Cu(L-Trp)$_2$ solutions containing 4 mM sodium borate adjusted at pH 8.1. This approach provided a titration of the Cu(L-Trp)$_2$ with these compounds in aqueous solution. The fluorescence intensities measured versus the concentration of the four aminoglycosides: amikacin, kanamycin A, kanamycin B and neomycin, are plotted in Figures 5.4 through 5.7.

The titration experiments were repeated using solutions containing 30% methanol by volume at an apparent pH of 8.1. The fluorescence intensities obtained are plotted versus

Reproduced with permission of the copyright owner. Further reproduction prohibited without permission.

Reproduced with permission of the copyright owner. Further reproduction prohibited without permission.

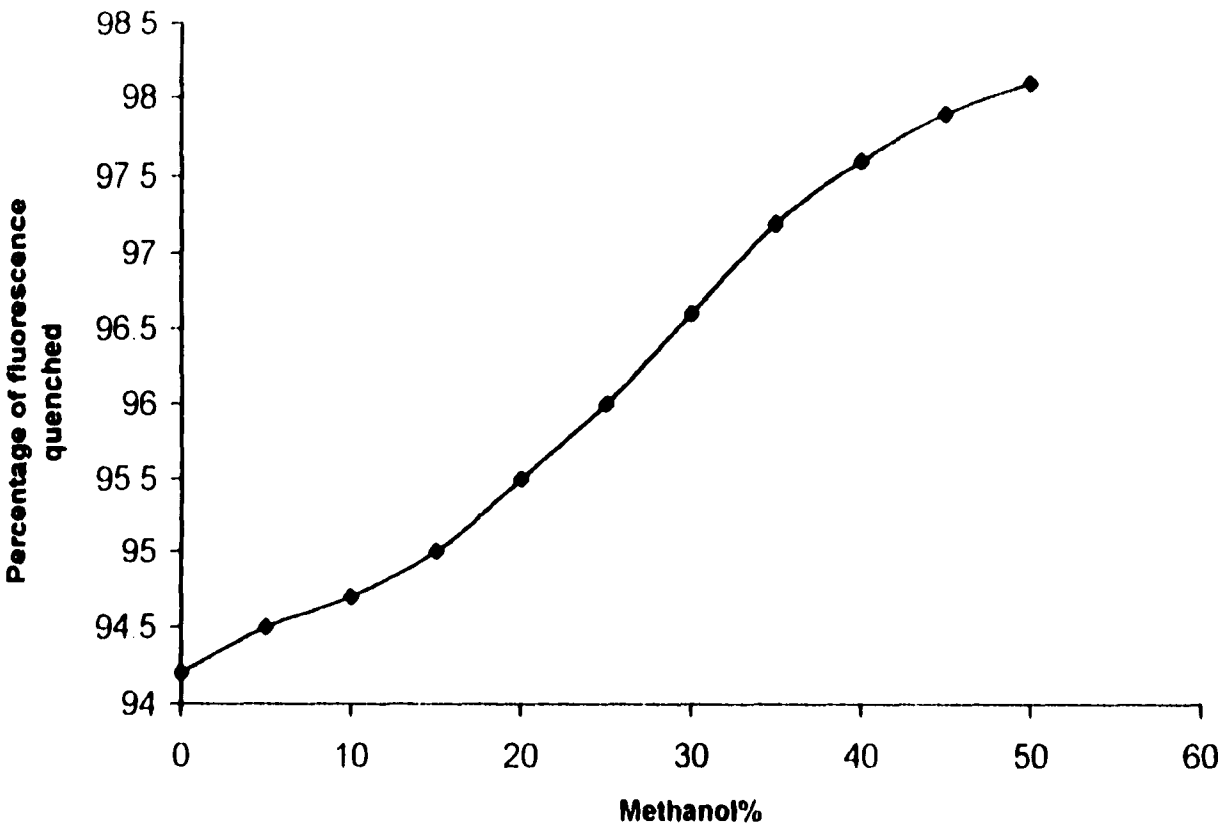

Figure 5.2: Effect of methanol concentration on flourescence quenching of 0.1 mM L-Trp by 0.05 mM Cu^{2+}. Excitation and emission wavelengths are 280 nm and 350 nm, respectively.

Reproduced with permission of the copyright owner. Further reproduction prohibited without permission.

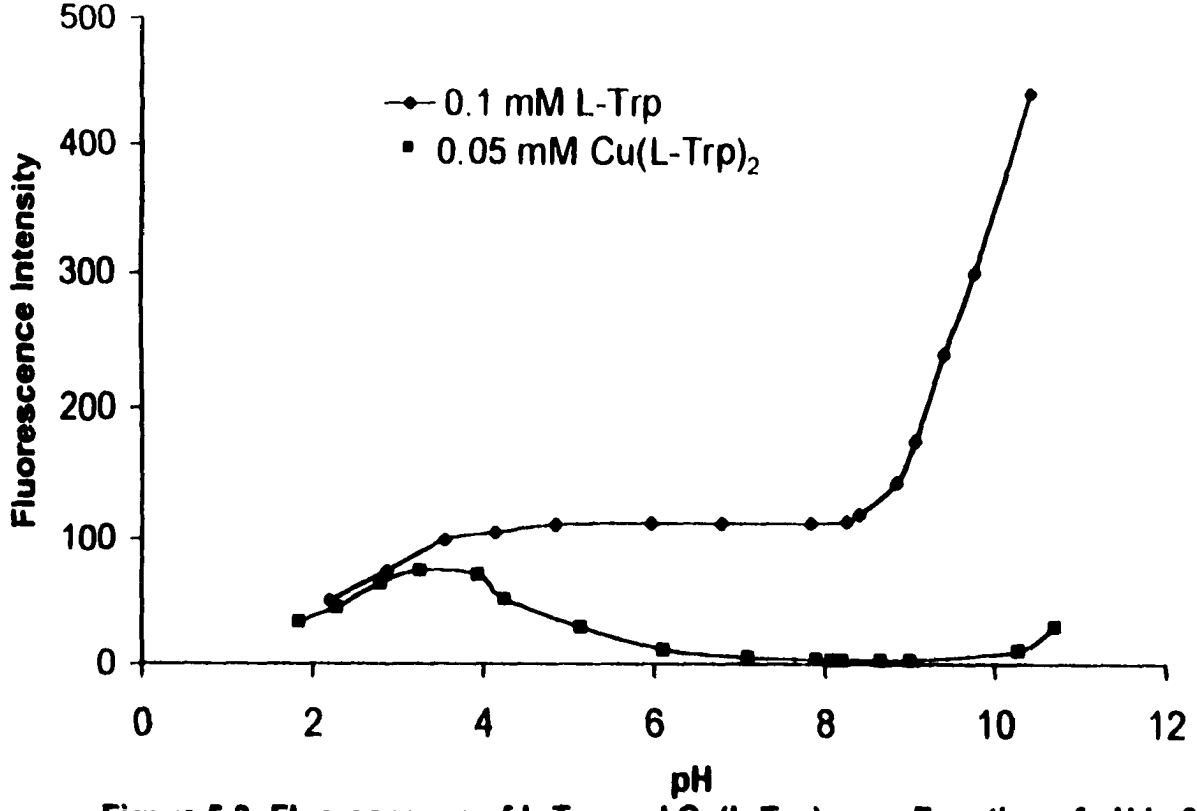

Figure 5.3: Fluorescence of L-Trp and $Cu(L\text{-}Trp)_2$ as a Function of pH in 30% methanol. Excitation and emission wavelengths are 280 nm and 350 nm, respectively.

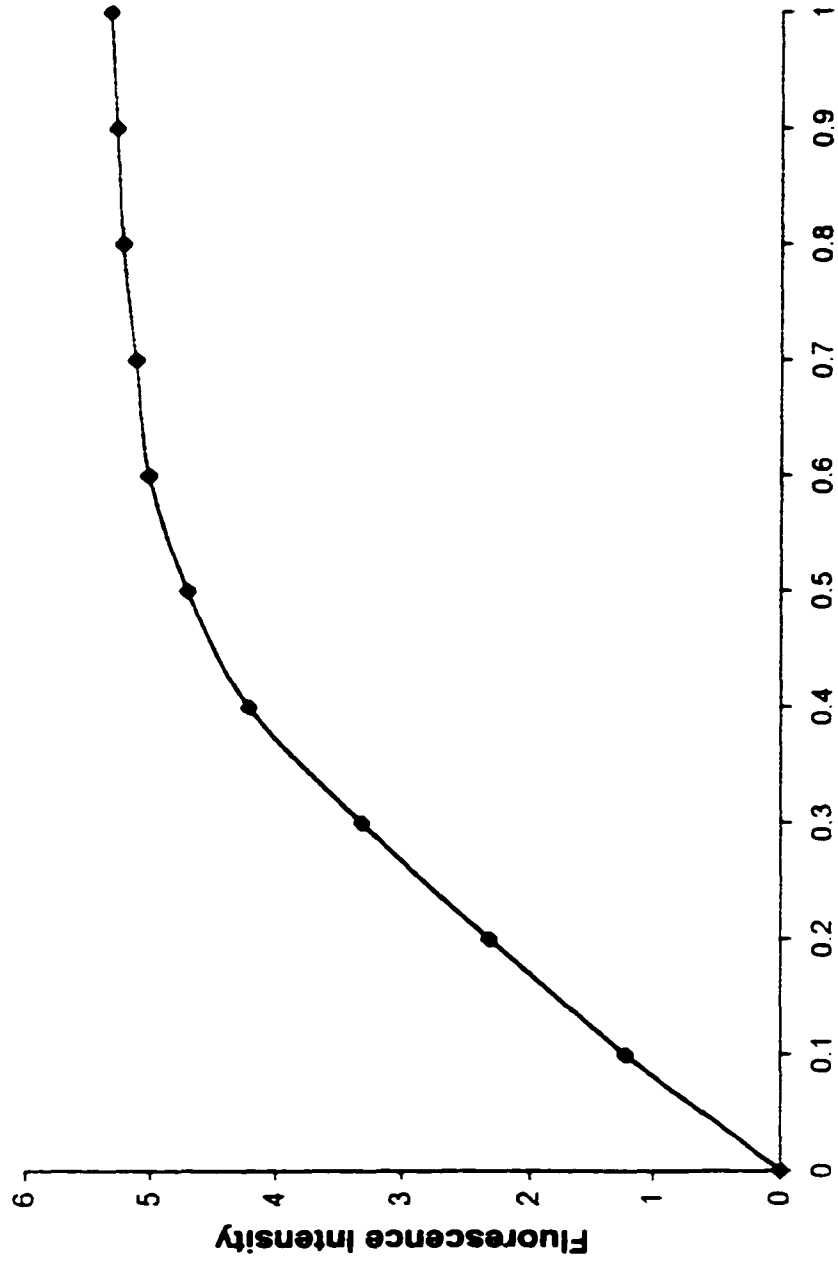

Figure 5.4 Stoichiometric study of the reaction of 0.05 mM $Cu(L\text{-}Trp)_2$ with amikacin. The pH of the solutions was buffered at 8.1 with 4 mM sodium borate

Reproduced with permission of the copyright owner. Further reproduction prohibited without permission.

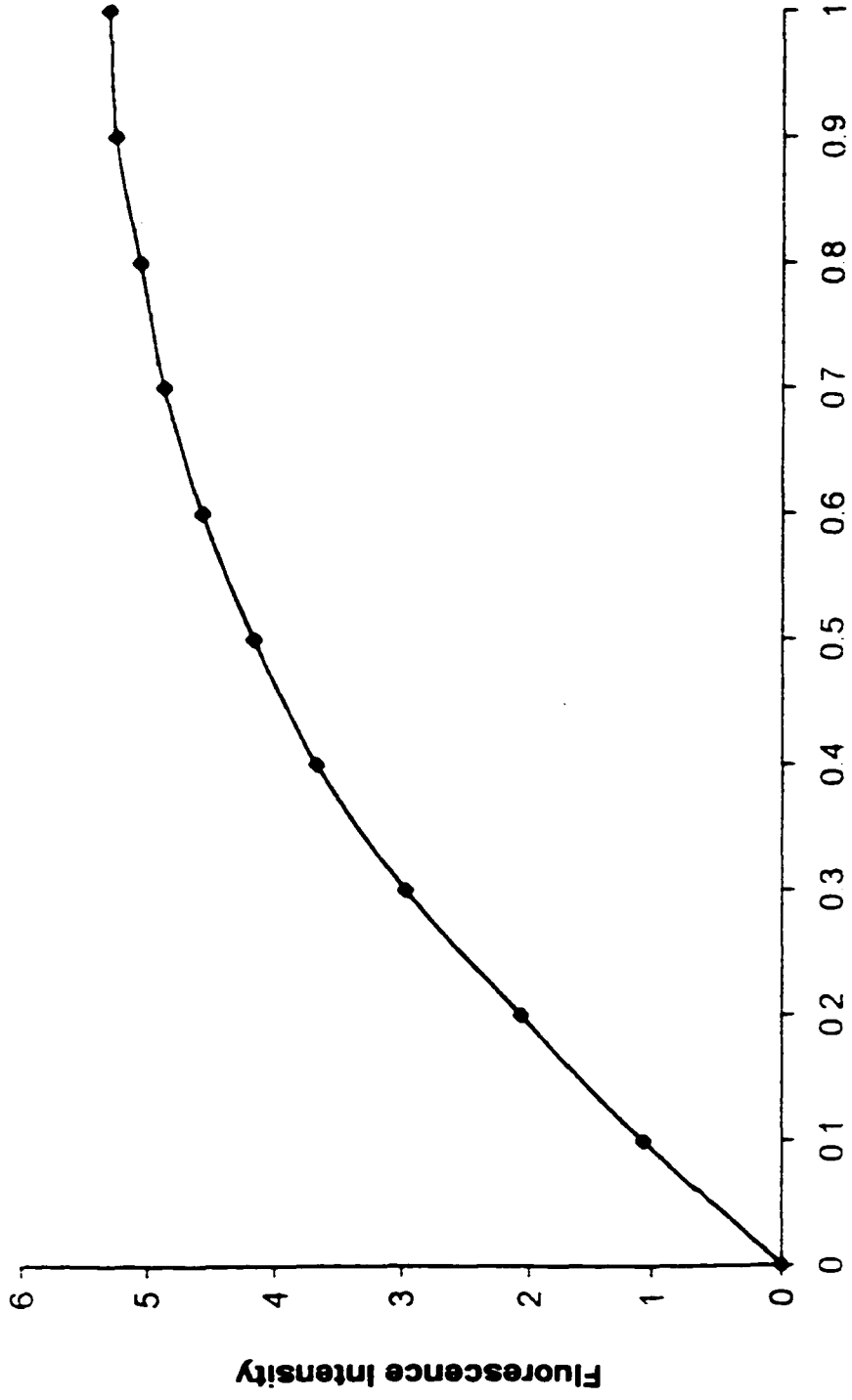

Figure 5.5: Stoichiometric study of the reaction of 0.05 mM $Cu(L\text{-}Trp)_2$ with kanamycin A. The pH of the solutions was buffered at 8.1 with 4 mM sodium borate

Reproduced with permission of the copyright owner. Further reproduction prohibited without permission.

Reproduced with permission of the copyright owner. Further reproduction prohibited without permission.

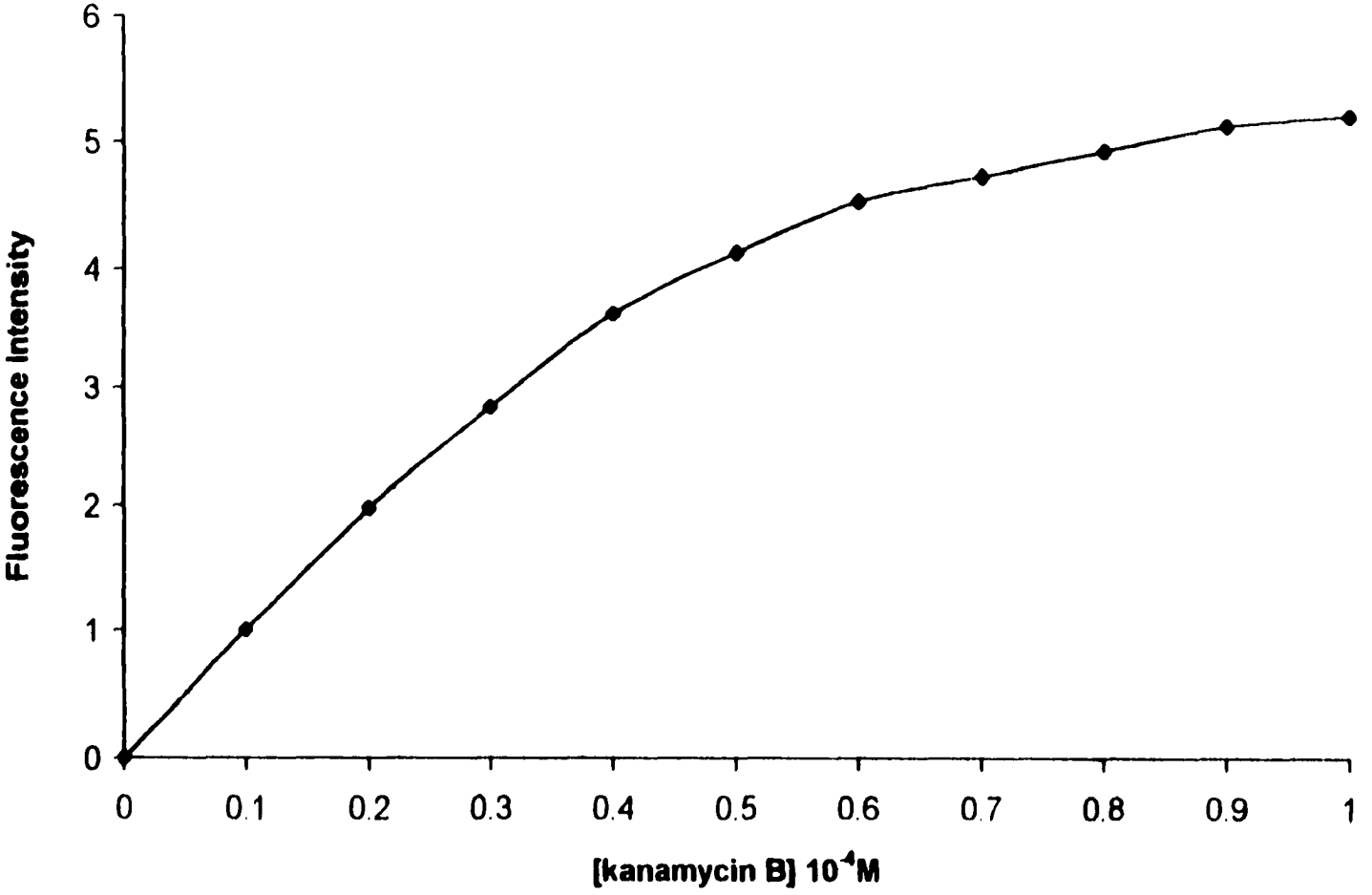

Figure 5.6: Stoichiometric study of the reaction of 0.05 mM $Cu(L\text{-}Trp)_2$ with kanamycin B. The pH of the solutions was buffered at 8.1 with 4 mM sodium borate

Reproduced with permission of the copyright owner. Further reproduction prohibited without permission.

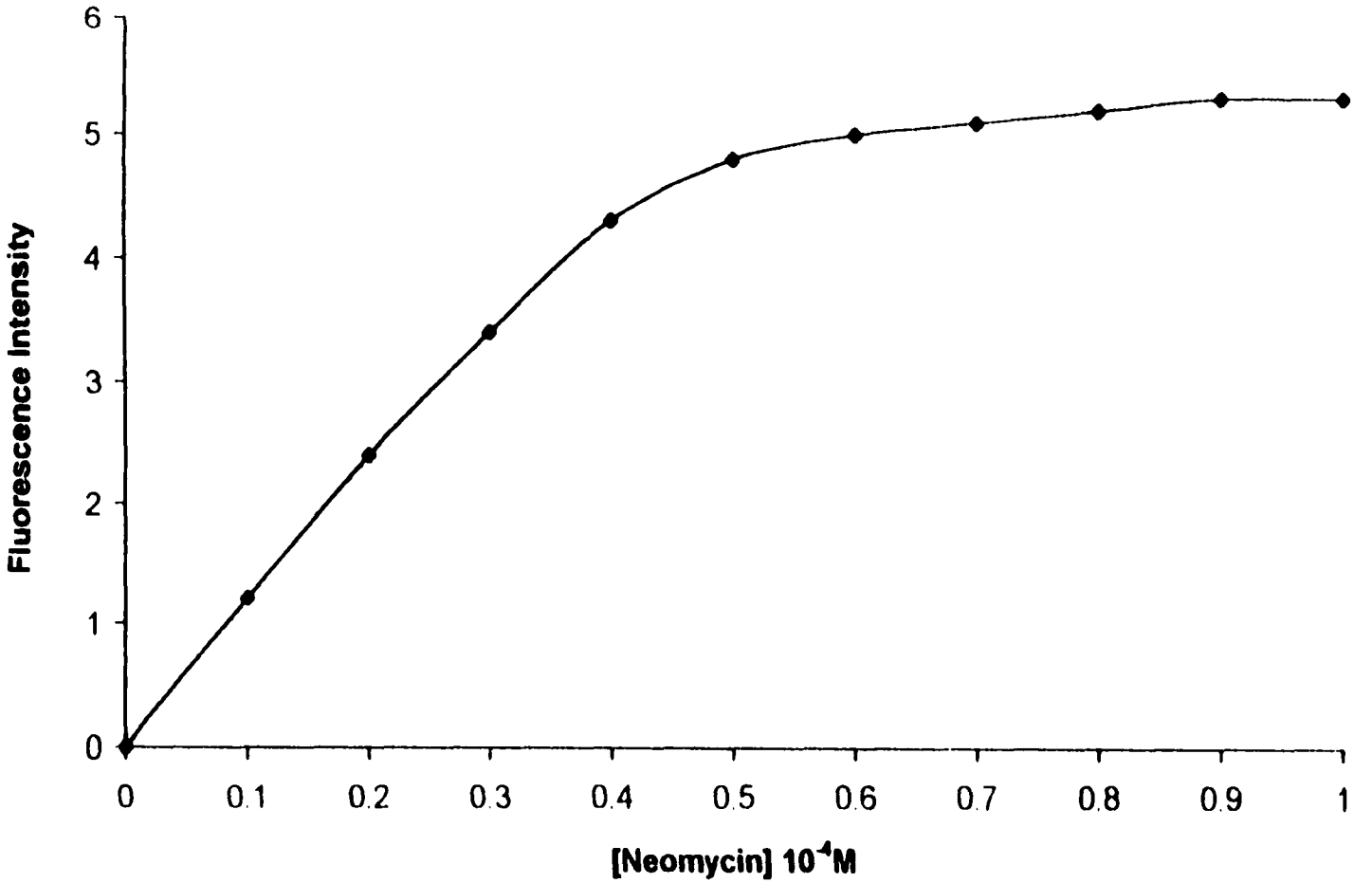

Figure 5.7: Stoichiometric study of the reaction of 0.05 mM $Cu(L\text{-}Trp)_2$ with neomycin. The pH of the solutions was buffered at 8.1 with 4 mM sodium borate

the concentration of aminoglycosides added and are presented in Figures 5.8 through 5.11.

5.2.5 Separation/detection of Aminoglycoside Antibiotics in a Cation Exchange Chromatographic Mode

A Hamilton PRP-X200 cation exchange column was used for the chromatographic separation of the aminoglycosides. Separation of the aminoglycoside antibiotics was achieved by adjusting the concentration of potassium bromide in the mobile phase. The pH of the mobile phase was buffered with 1.5 mM sodium acetate at pH 5.5. The postcolumn reagent, a 0.05 mM Cu(L-Trp)$_2$ aqueous solution buffered with a 4 mM sodium borate ($Na_2B_4O_7$), was added via a mixing tee to the column eluent. The pH of the postcolumn reagent was adjusted in the range of 8.1 - 9.0.

5.2.6 Separation/detection of Aminoglycoside Antibiotics in a Reversed Phase Ion-pair Chromatographic Mode

Another set of experiments were performed using Supelcosil^{TM} C_{18} column for the chromatographic separation of the aminoglycosides. Separation of the aminoglycoside antibiotics was achieved by adjusting the concentrations of pentafluoropropionic acid (PFPA) and methanol in the mobile phase. The postcolumn reagent, was a 0.05 mM Cu(L-Trp)$_2$ in a 30% methanol solution buffered with a 40 mM sodium borate. The apparent pH of the postcolumn reagent was adjusted in the range of 8.1 - 9.4.

Reproduced with permission of the copyright owner. Further reproduction prohibited without permission.

Reproduced with permission of the copyright owner. Further reproduction prohibited without permission.

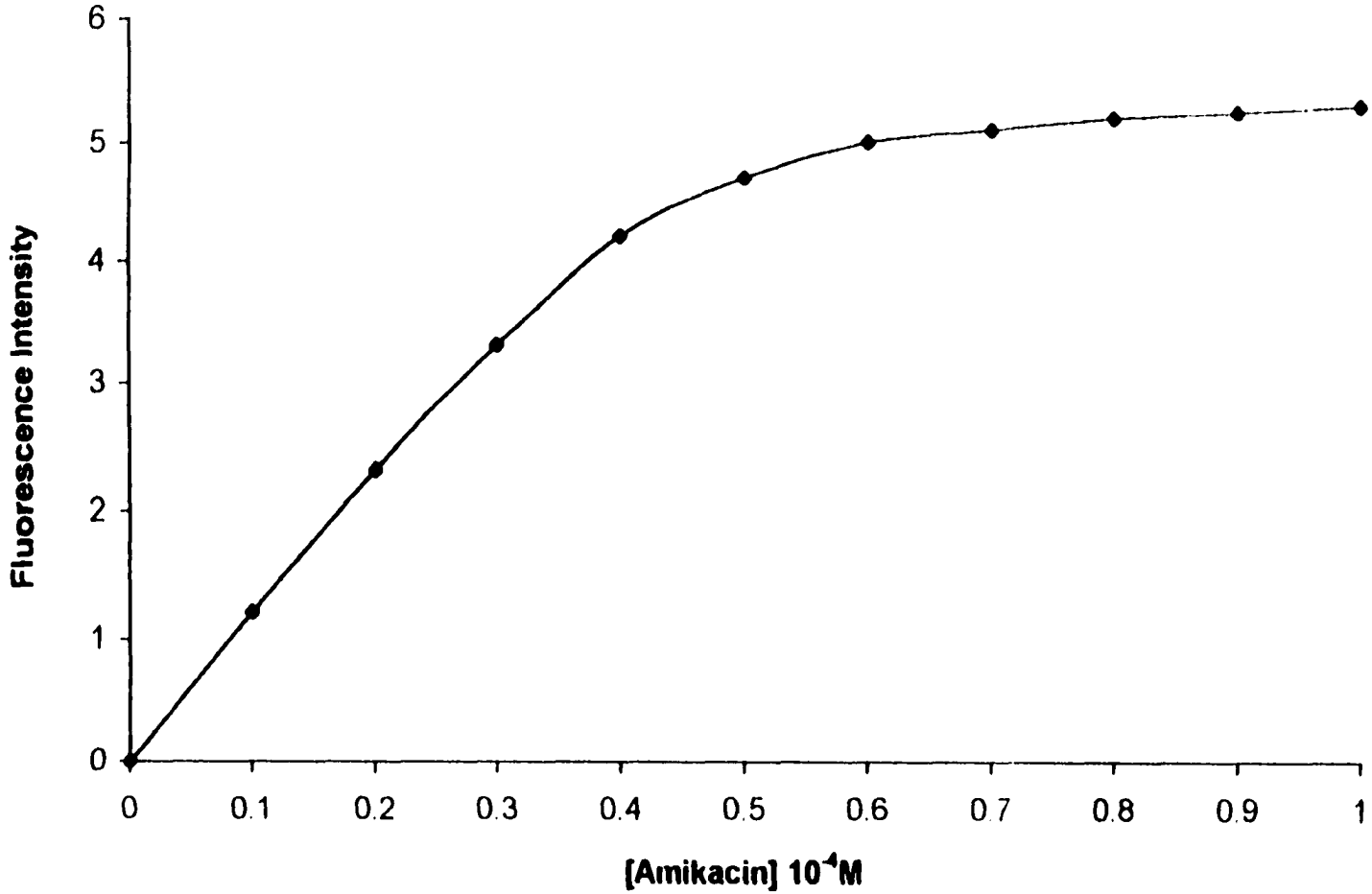

Figure 5.8: Stoichiometric study of the reaction of 0.05 mM $Cu(L\text{-}Trp)_2$ with amikacin. The solutions contained 4 mM sodium borate ($Na_2B_4O_7$) and 30% methanol (by volume). The apparent pH was 8.1.

Reproduced with permission of the copyright owner. Further reproduction prohibited without permission.

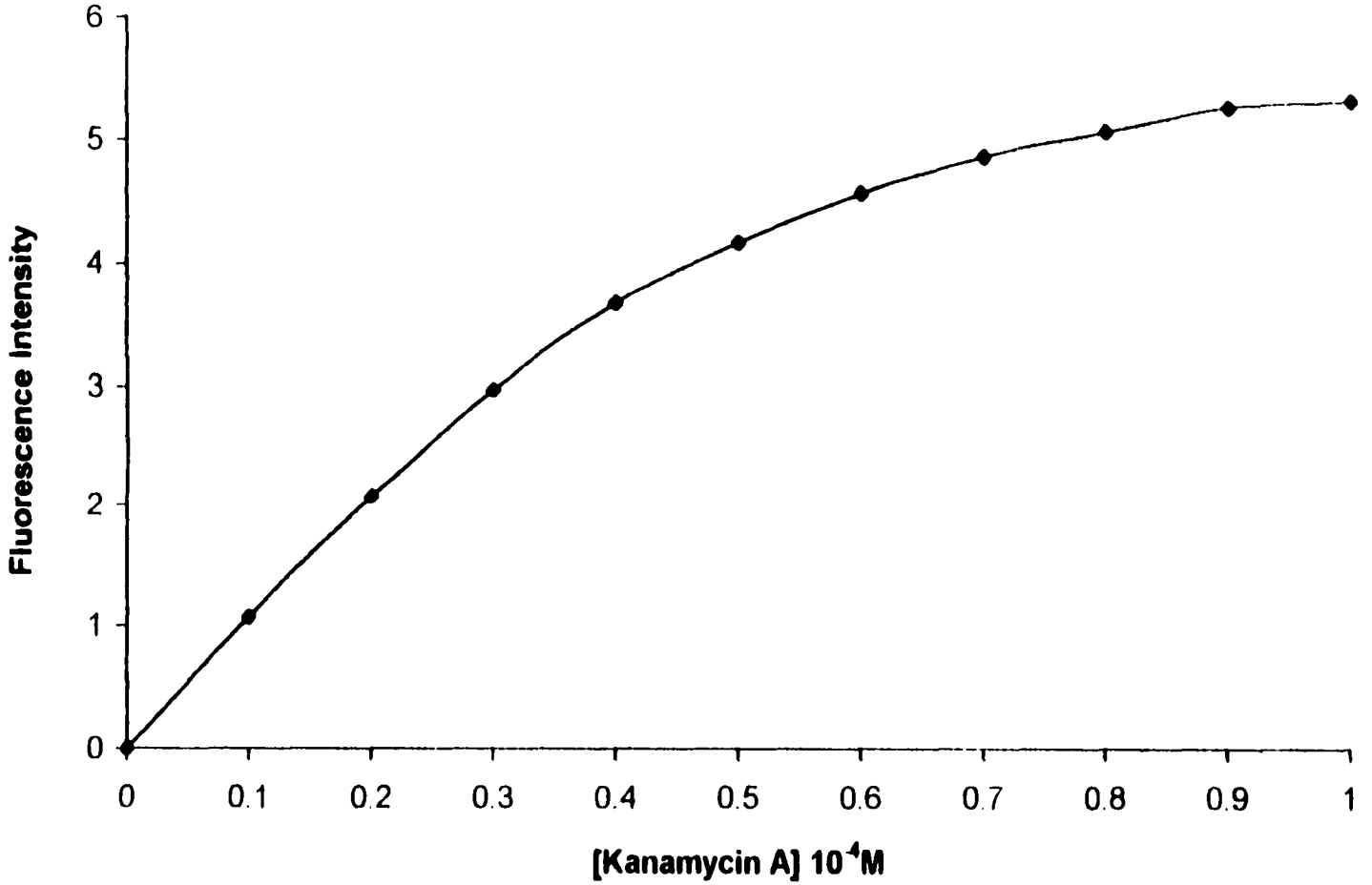

Figure 5.9: Stoichiometric study of the reaction of 0.05 mM $Cu(L\text{-}Trp)_2$ with kanamycin A. The solutions contained 4 mM sodium borate ($Na_2B_4O_7$) and 30% methanol (by volume). The apparent pH was 8.1.

Reproduced with permission of the copyright owner. Further reproduction prohibited without permission.

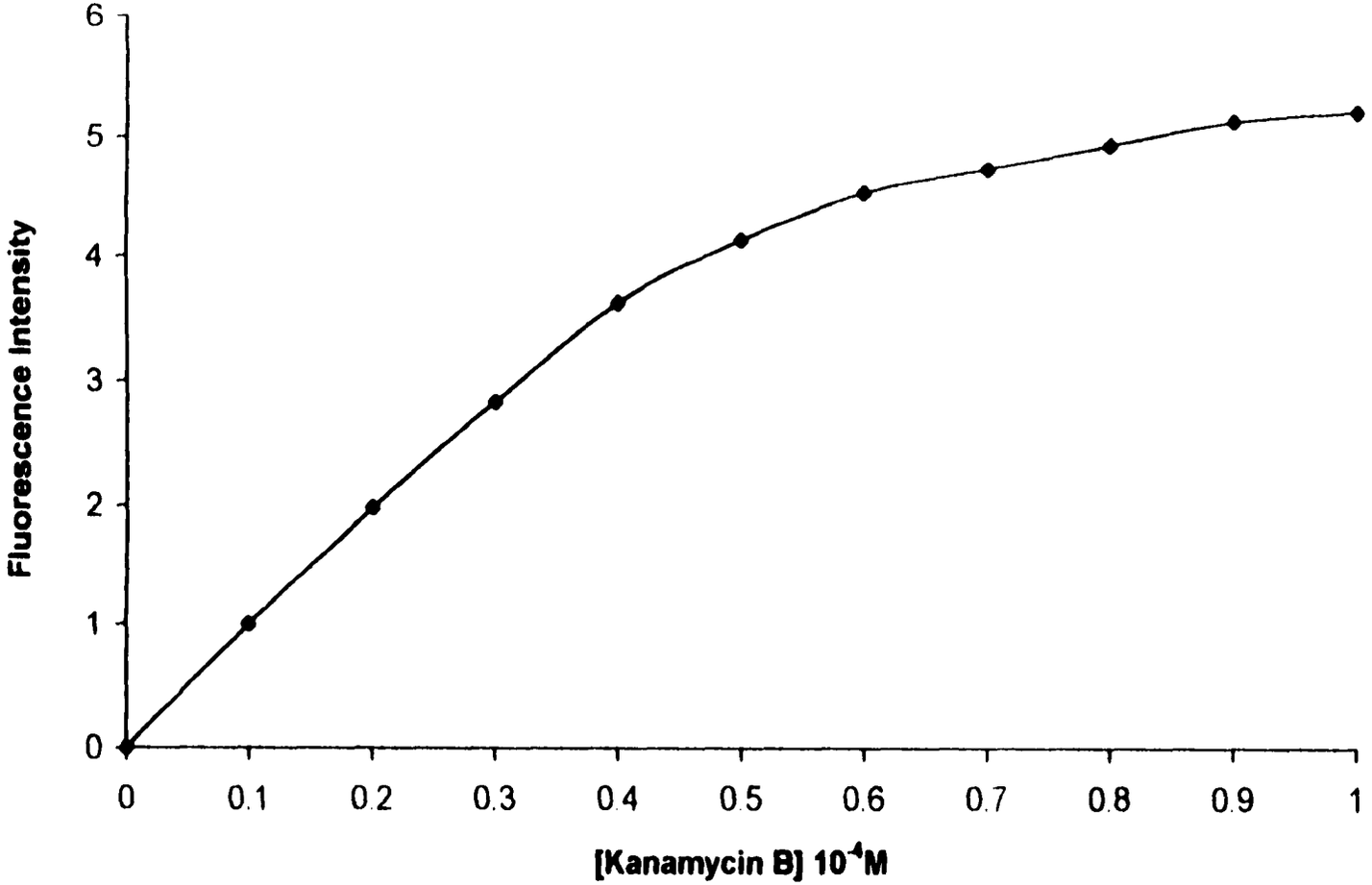

Figure 5.10: Stoichiometric study of the reaction of 0.05 mM $Cu(L\text{-}Trp)_2$ with kanamycin B. The solutions contained 4 mM sodium borate ($Na_2B_4O_7$) and 30% methanol (by volume). The apparent pH was 8.1.

Reproduced with permission of the copyright owner. Further reproduction prohibited without permission.

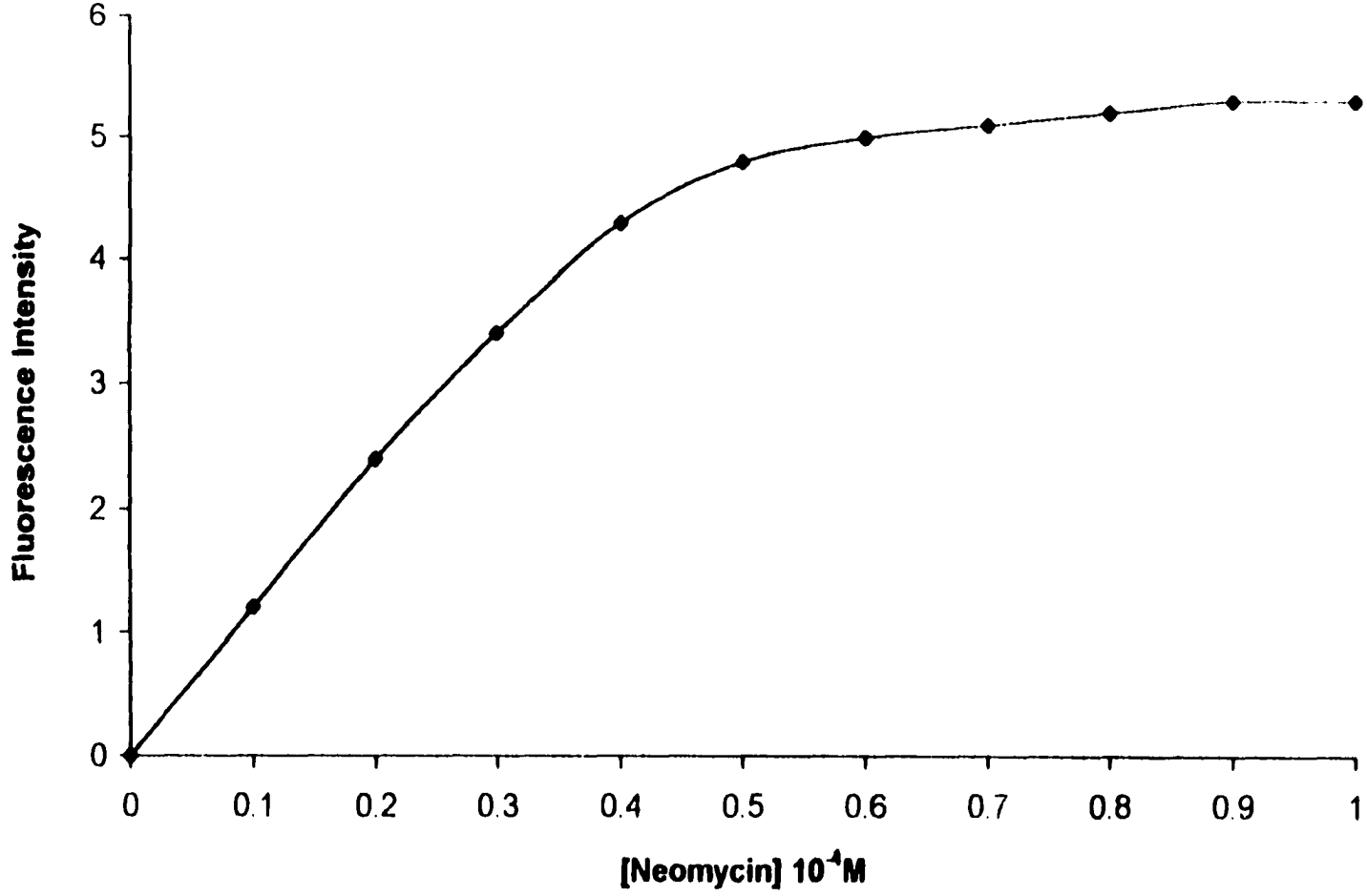

Figure 5.11: Stoichiometric study of the reaction of 0.05 mM $Cu(L\text{-}Trp)_2$ with neomycin. The solutions contained 4 mM sodium borate ($Na_2B_4O_7$) and 30% methanol (by volume). The apparent pH was 8.1.

5.2.7 Effect of Addition of Postcolumn Reagent on Chromatographic Column Efficiency

A Supelcosil™ C_{18} column was used for this study. A solution of 100 ppm naphthalene was prepared by dissolving the appropriate amount of naphthalene in methanol. The mobile phase was a 60% (by volume) methanol solution. The mobile phase flow rate was set at 1.0 ml/min. The excitation wavelength of the fluorescence detector was set at 280 nm and a longpass glass filter with a cutoff wavelength at 290 nm was used to select the emission. The 100 ppm naphthalene standard samples were injected. Postcolumn reagent with the same composition of mobile phase was added to the column eluent via the mixing tee, with the flow rate at 0, 1.0, 2.0 and 3.0 ml/min, respectively. The chromatograms obtained at different postcolumn flow rates are presented in Figure 5.12. The number of the theoretic plates (N), a measure of the experimental efficiency, were calculated at different flow rates based on:

$$N = 5.54 \times (t_r / W_{1/2})^2 \qquad \text{(Eq. 5.1)}$$

in which t_r and $W_{1/2}$ represent the chromatographic retention time and peak half width, respectively.

Reproduced with permission of the copyright owner. Further reproduction prohibited without permission.

Reproduced with permission of the copyright owner. Further reproduction prohibited without permission.

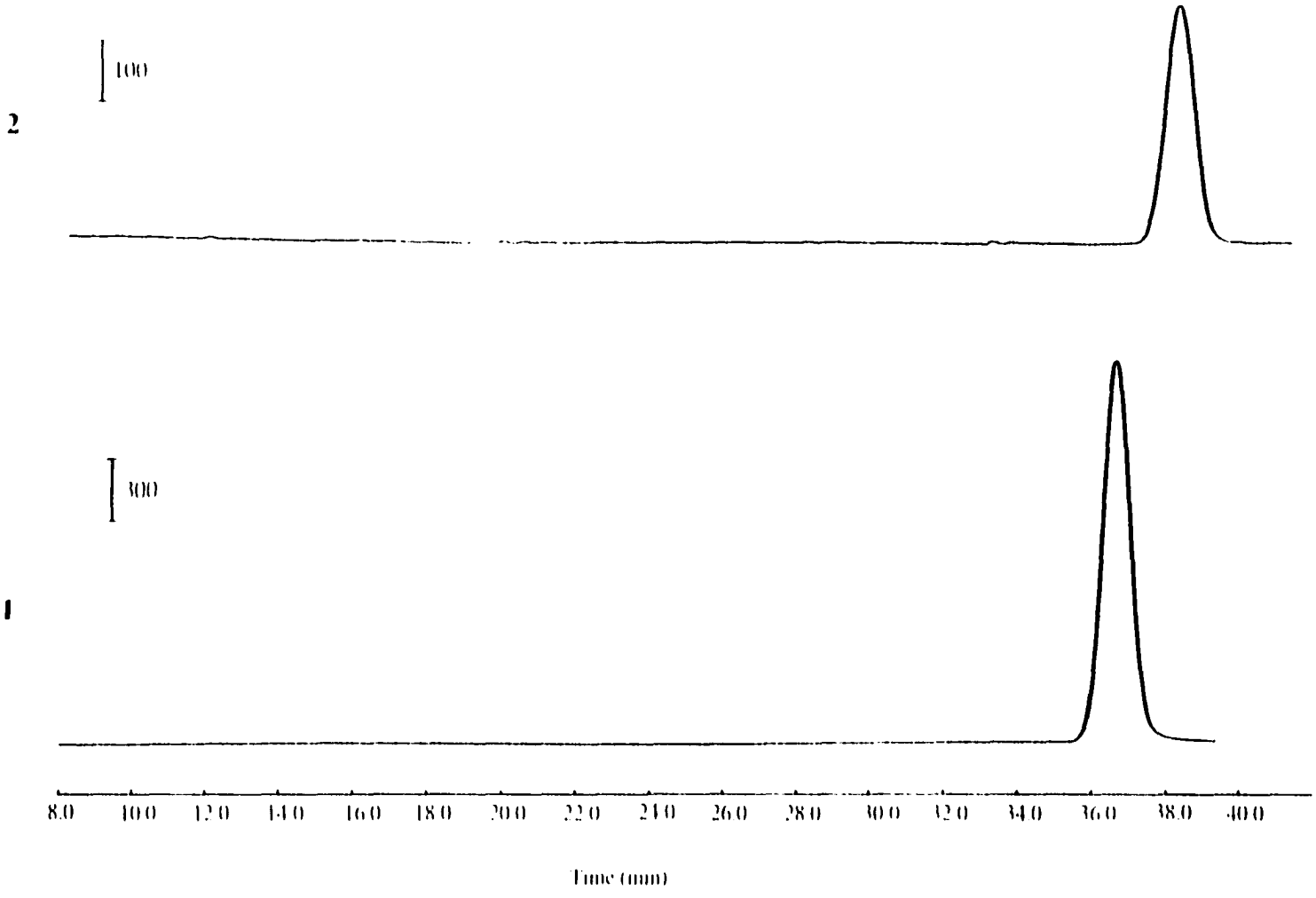

Figure 5.12: Chromatograms of naphthalene obtained at different postcolumn reagent flow rates. Mobile phase is 60% methanol at a flow rate of 1.0 ml/min. Postcolumn reagent has the same composition with the mobile phase. Excitation and emission wavelengths are 280 nm and 290 nm, respectively. Postcolumn reagent flow rate: chromatogram 1: 0 ml/min; chromatogram 2: 3.0 ml/min. The retention time shift is attributed to the evaporation of methanol in the mobile phase

5.3 Results and Discussions

5.3.1 Stoichiometric Study of the Detection Reaction

Based on the titration data shown in Figure 5.4 to Figure 5.7, the fluorescence intensities of the solutions increase as the amount of aminoglycosides added increase. All the plots show that the recovered fluorescence signal reaches a plateau when a stoichiometric amount of the compound is added to the detection reagent. A stoichiometric ratio of 1 : 1 for [A] : [Cu(L-Trp)$_2$] (A represents aminoglycosides here) is determined from the titration data, which corresponds to the reaction:

$$Cu(L\text{-}Trp)_2 + A = Cu(A) + 2\ L\text{-}Trp^* \qquad \text{(Eq. 5.2)}$$

in which L-Trp* represents fluorescently active L-Trp. This reaction is in good agreement with the results of electrochemical and other spectroscopic studies, in which aminoglycosides form 1 : 1 complexes with Cu(II) [125 - 127]. Thus, every aminoglycoside molecule displaces two fluorescent L-Trp molecules from the complex Cu(L-Trp)$_2$.

Similar stoichiometric studies were conducted for the 30% methanol solutions. The data presented in Figures 5.8 through 5.11, indicate that the presence of an organic solvent doesn't affect the 1 : 1 stoichiometric ratio for the reactions between aminoglycosides and the Cu(L-Trp)$_2$ complex.

Reproduced with permission of the copyright owner. Further reproduction prohibited without permission.

5.3.2 Detection of Aminoglycoside Antibiotics Separated in a Cation Exchange Chromatographic Mode

5.3.2.1 Separation Condition Optimization

A schematic diagram of the instrumental setup was presented in Figure 3.3. Due to the strong hydrophilicity of the aminoglycosides, these compounds are difficult to retain under reversed-phase conditions. Current separation methods for these compounds include reversed phase ion-pair chromatography [122, 128], and either cation exchange or anion exchange chromatography [119 - 121, 129]. A strong cation exchange stationary phase was utilized here. The retention of most of the aminoglycosides on the Hamilton SCX column is based on the cationic nature of these compounds within an appropriate pH range for the protonation of the amino groups. Most aminoglycosides have a first acidic association constant in the range of 8.8 to 10.0 [125 - 127]. For the cation exchange stationary phase used in this study, to assure appropriate and adequate ionization of the aminoglycosides, the pH of the mobile phase was adjusted to 5.5 with acetate buffer. KBr was used to adjust the strength of the mobile phase. A plot of the capacity factors of four of the aminoglycosides tested versus the KBr concentration of the mobile phase is given in Figure 5.13. A mixture containing amikacin, kanamycin A, kanamycin B and neomycin can be baseline separated using a mobile phase containing 0.7M KBr. This mobile phase condition is also capable of providing baseline separation for a mixture containing hygromycin B, ribostamycin, tobramycin and spectinomycin, or a mixture of geneticin and neamine. With the exception of spectinomycin, the elution order is consistent with the number of amino groups, the aminoglycosides possessing more amino groups being

Reproduced with permission of the copyright owner. Further reproduction prohibited without permission.

Reproduced with permission of the copyright owner. Further reproduction prohibited without permission.

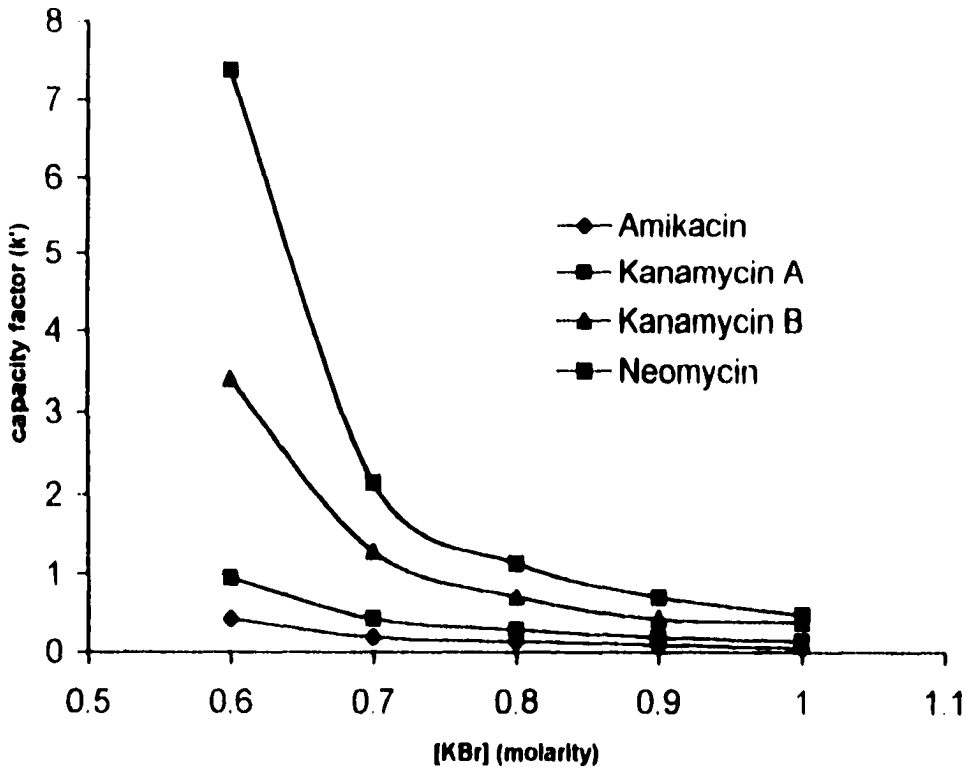

Figure 5.13: Capacity factors (k') for selected aminoglycosides plotted versus the concentration of KBr in the mobile phase

retained longer. Spectinomycin, however, has a constant capacity factor of 2.4, which is independent of the KBr concentration of the mobile phase in the range from 0.6 - 1.0 M, suggesting a retention mechanism other than ion exchange.

5.3.2.2 Optimization of the Detection Conditions

Possessing multiple amino groups, the aminoglycosides are effective chelators of Cu(II) ions [125 - 127]. Upon mixing with a Cu(L-Trp)$_2$ solution, the aminoglycosides displace the L-Trp from the complex and the fluorescence of L-Trp is thereby recovered. Thus an increase in L-Trp fluorescence is indicative of the presence of the aminoglycosides.

Detection pH, which is one of the most important parameters for this approach to HPLC detection, was optimized by adjusting the pH of the postcolumn reagent, which is 0.05 mM Cu(L-Trp)$_2$ in a 4 mM sodium borate buffer. As shown in Figure 5.14, the chromatographic signal intensities of the aminoglycosides generally increase in the pH range of 8.1 - 9.0, except for neomycin, for which the fluorescence signal intensity decreases slightly above pH 8.7. A comprehensive interpretation of how the following three pH dependent factors affect detection, was given earlier [130, 131]: (1). Fluorescence of free L-Trp steadily increases above pH 8.0, since the deprotonated free L-Trp has a higher fluorescence efficiency than zwitterionic L-Trp. (2). A second important factor is that L-Trp binds to Cu^{2+} ion most efficiently at a pH of 8.1 with the greatest fluorescence quenching observed at this point. Dissociation of Cu(L-Trp)$_2$

Reproduced with permission of the copyright owner. Further reproduction prohibited without permission.

Reproduced with permission of the copyright owner. Further reproduction prohibited without permission.

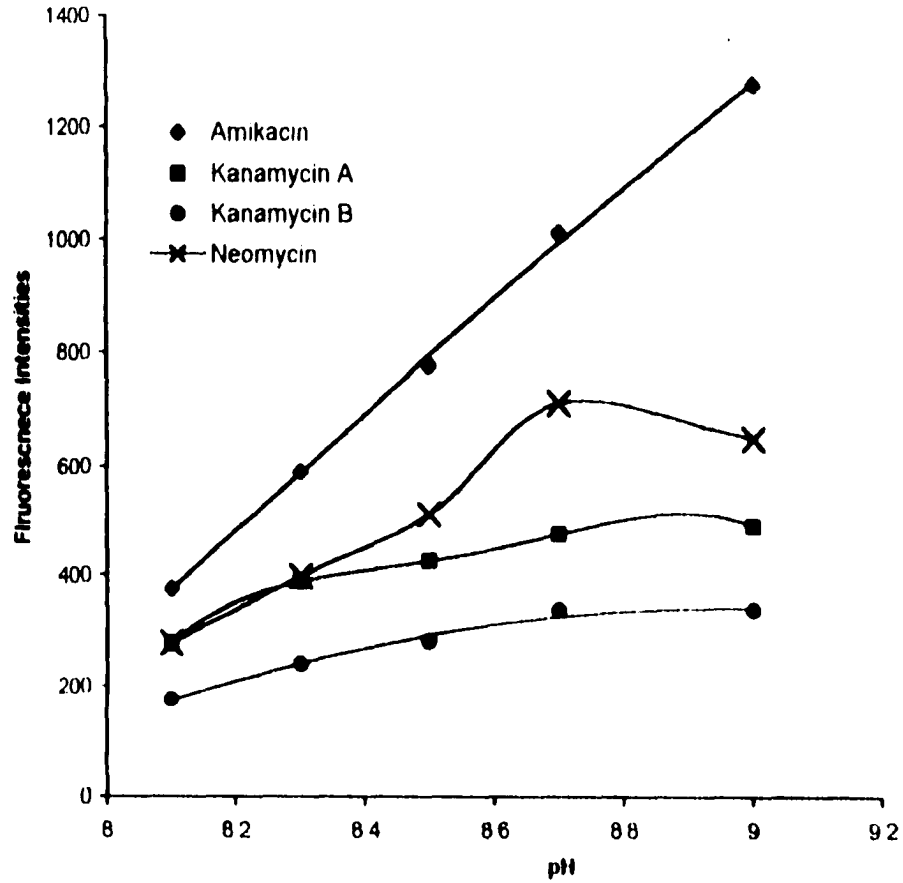

Figure 5.14: Chromatographic peak intensities measured for the aminoglycosides versus detection pH. The amounts of samples injected were amikacin : 293 ng; kanamycin A: 242 ng; kanamycin B: 242 ng; neomycin: 307.5 ng

increases both above and below pH 8.1: (3). The affinities of the analytes for Cu^{2+}, which in this study are the aminoglycosides, are pH dependent, since the binding between the analytes and Cu^{2+} ion is affected by both the degree of analyte protonation and Cu^{2+} complexation with hydroxide ions. For the three factors given here, the first one tends to lead to a chromatographic signal decrease when the detection pH is away from 8.1, while the other two factors tend to result in an increase in the signal intensities as the pH increases. The change of pH affects the three factors for the different aminoglycosides to a different extent, due to the difference in their acidic association constants and number of amino groups. As shown in Figure 5.14, the second and third factors are generally the dominant factors affecting the chromatographic peak intensities as the pH increases, except for neomycin, for which the first factor dominates when the detection pH is higher than 8.7. Due to the slow precipitation of $Cu(OH)_2$ in the postcolumn reagent above pH 9.0, the detection pH was set at 8.8 to assure long term stability of the reagent. The flow rates of the postcolumn reagent were evaluated in the range of 1.0 to 2.2 ml/min, for the separation of a mixture of amikacin, kanamycin A, kanamycin B and neomycin. A compromise was made between the decrease in signal due to dilution at higher postcolumn reagent flow rates and increase in baseline fluctuation at lower flow rates, as shown in Figure 5.15. The flow rate of the postcolumn reagent was set at 1.8 ml/min as a compromise.

Standard solutions of the aminoglycoside were prepared in distilled water and the dynamic ranges were obtained for the chosen compounds under the optimized separation

Reproduced with permission of the copyright owner. Further reproduction prohibited without permission.

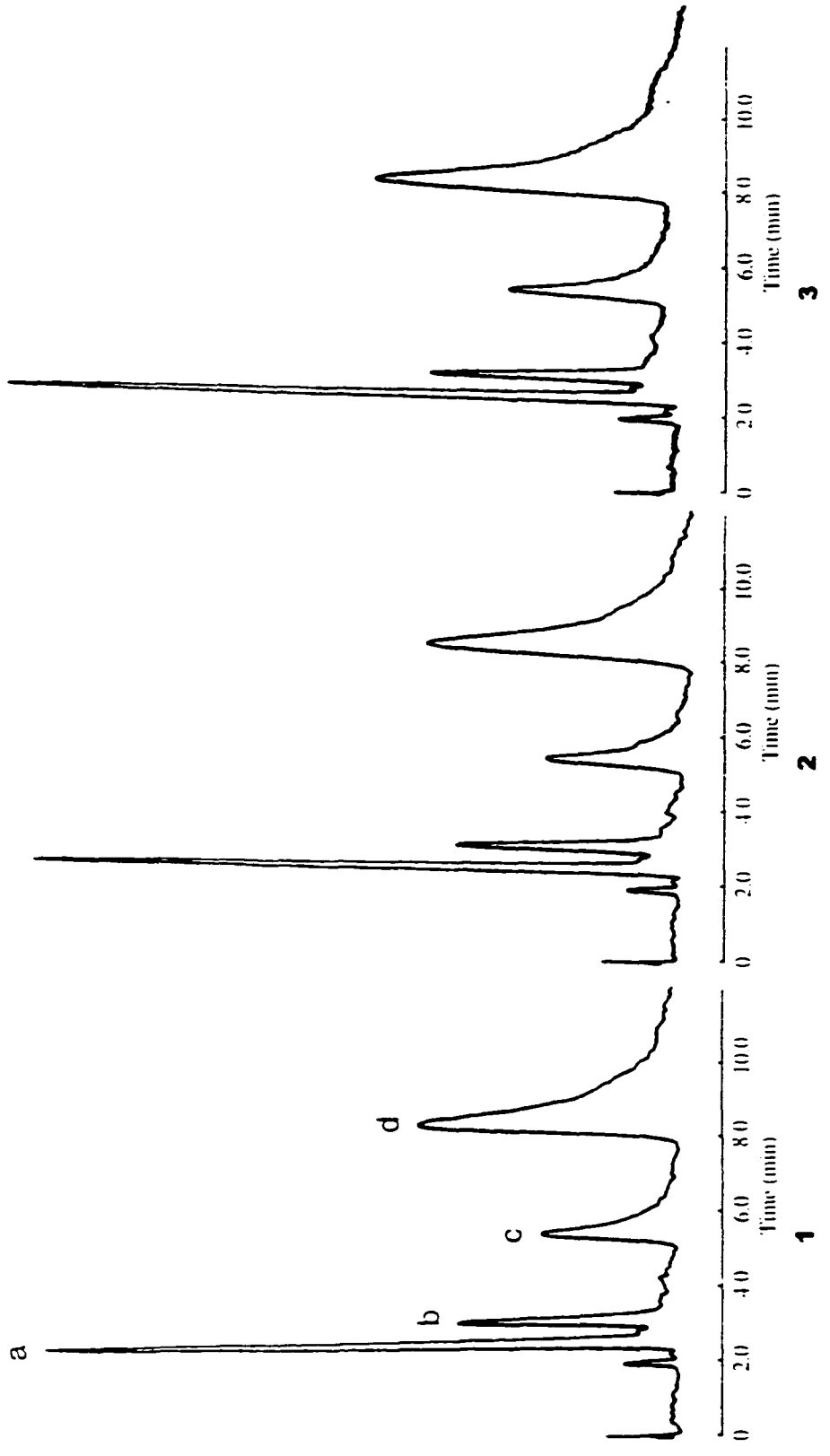

Figure 5.15: Representative chromatograms of aminoglycosides obtained at different postcolumn reagent flow rates. Measurements were made using the same detection range. Separation was achieved with the use of a Hamilton PRP X200 SCX column. Mobile phase: 0.7M KBr, 15 mM sodium acetate buffer at pH 5.5, 1.2 ml/min. Postcolumn reagent: 0.05 mM $CuCl_2$.Tiron, 4 mM sodium borate ($Na_2B_4O_7$) buffer at pH 8.8. Peak a: amikacin; b: kanamycin A; c: kanamycin B; d: neomycin. The masses of samples injected were (1) a: 293 ng; b: 242 ng; c: 242 ng; d: 307.5 ng; Postcolumn reagent flow rate: chromatogram 1: 1.8 ml/min; 2: 1.4 ml/min; 3: 1.0 ml/min

Reproduced with permission of the copyright owner. Further reproduction prohibited without permission.

and detection conditions. Representative chromatograms showing the separation of the 4 aminoglycosides, amikacin, kanamycin A, kanamycin B and neomycin at two different concentrations are given in Figure 5.16. Table 5.1 lists the statistical performance results. The detection limits for the four aminoglycosides range from 4.2 ng for amikacin to 14.5 ng for kanamycin B injected on column with a 10 µl injection volume, which are comparable to detection limits obtained for the well-developed pulsed electrochemical detection for the aminoglycosides, ranging from 4 to 15 ng [119 - 122]. Representative chromatograms for the separation of six other aminoglycosides, hygromycin B, ribostamycin, spectinomycin, tobramycin, geneticin and neamine are shown in Figure 5.17.

Commercial aminoglycoside samples in either intravenous injectable or ophthalmic formulations were obtained and analyzed based on the developed separation and detection method. Samples were diluted with distilled water but no further sample treatment was required. The representative chromatograms of the samples are shown in Figure 5.18. For an intravenous amikacin sample, the determined concentration is 252 ± 5.5 mg/ml, compared to an expected concentration of 250 mg/ml; for an ophthalmic neomycin sample, the determined concentration is 3.58 ± 0.13 mg/ml, compared to an expected concentration of 3.5 mg/ml.

Reproduced with permission of the copyright owner. Further reproduction prohibited without permission.

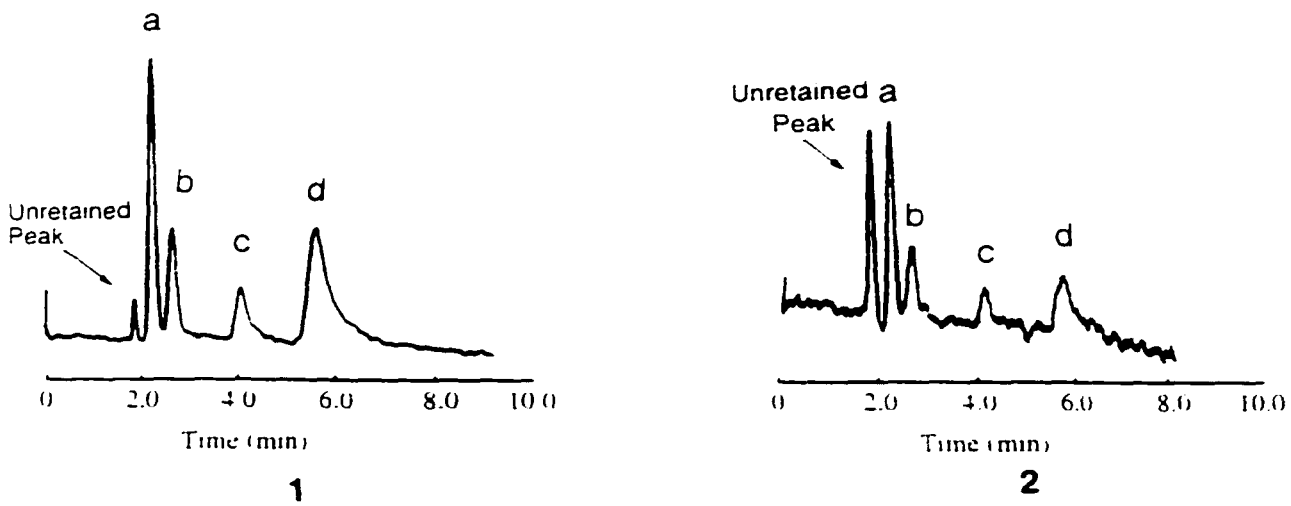

Figure 5.16: Representative chromatograms of the aminoglycoside standards. Separation was achieved with the use of a Hamilton PRP-X200 SCX column. Mobile phase: 0.7M KBr, 1.5 mM sodium acetate buffer at pH 5.5, 1.2 ml/min; Postcolumn reagent: 0.05 mM Cu(L-Trp)$_2$, 4 mM sodium borate ($Na_2B_4O_7$)buffer at pH 8.8, 1.8 ml/min. Peak a: amikacin; b: kanamycin A; c: kanamycin B; d: neomycin. The masses of samples injected were (1) a: 293 ng; b: 242 ng; c: 242 ng; d: 307.5 ng; (2) a: 29.3 ng; b: 24.2 ng; c: 24.2 ng; d: 30.7 ng.

Reproduced with permission of the copyright owner. Further reproduction prohibited without permission.

Aminoglycoside	Range (ng)	Regression equation[a]	r[b]	DL[c] (ng)	DL[c] (ppm)	RSD[d] (%)
Amikacin	29 - 586	H = 55.5 + 3.7 x C	0.9986	4.2	0.42	2.2
Kanamycin A	24 - 483	H = 6.4 + 2.0 x C	0.9997	9.3	0.93	2.9
Kanamycin B	24 - 483	H = 5.6 + 1.0 x C	0.9994	14.5	1.45	3.5
Neomycin	31 - 615	H = 4.0 + 1.6 x C	0.9998	11.8	1.18	3.6

[a] H, peak height, C, analyte mass injected (in ng). [b] Correlation coefficient. [c] Detection limit. [d] Relative standard deviation (N = 5, for 293 ng amikacin, 242 ng kanamycin A, 242 ng kanamycin B and 307.5 ng neomycin injected respectively).

Table 5.1: Characteristic parameters of the calibration graphs and analytical figures of merit for the determination of four aminoglycosides

Reproduced with permission of the copyright owner. Further reproduction prohibited without permission.

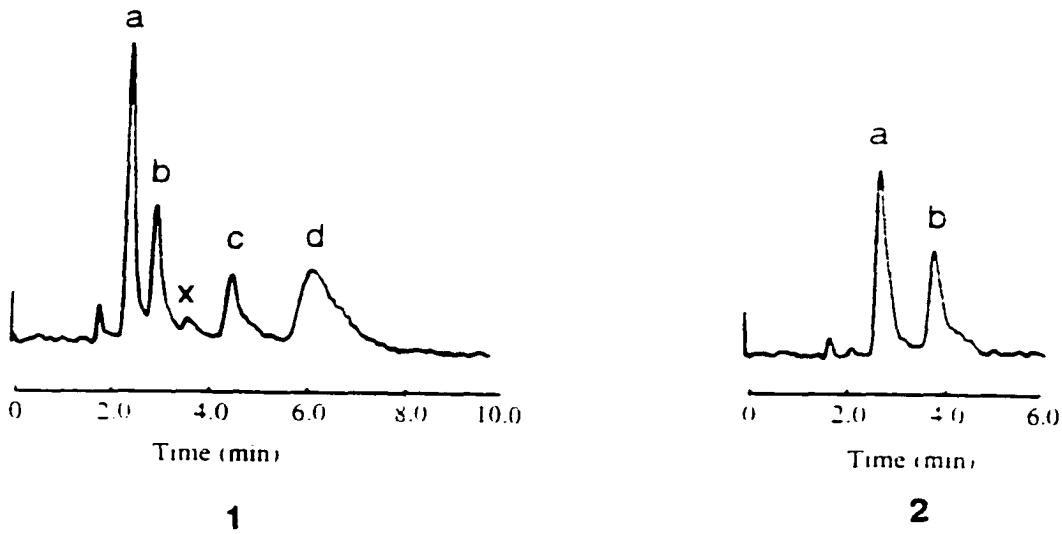

Figure 5.17: Representative chromatograms of the aminoglycoside standards. Separation was achieved with the use of a Hamilton PRP-X200 SCX column. Mobile phase: 0.7M KBr, 1.5 mM sodium acetate buffer at pH 5.5, 1.2 ml/min: Postcolumn reagent: 0.05 mM $Cu(L\text{-}Trp)_2$, 4 mM sodium borate buffer at pH 8.8, 1.8 ml/min. Chromatogram 1: Peak a: hygromycin B (527 ng); b: ribostamycin (454.5 ng); c: tobramycin (467.5 ng); d: spectinomycin (332.3 ng). Chromatogram 2: Peak a: geneticin (496.7 ng); b: neamine (322.4 ng). Peak x is an unknown impurity present in the spectinomycin standard.

Reproduced with permission of the copyright owner. Further reproduction prohibited without permission.

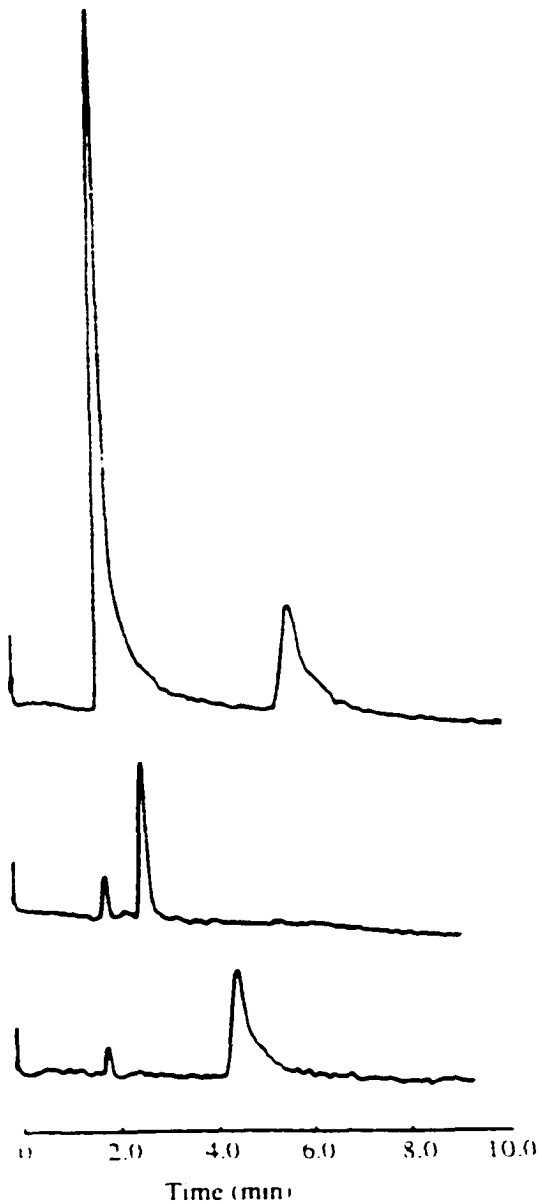

Figure 5.18: Representative chromatograms of aminoglycosides in commercial formulations. Analyses were performed with the use of a Hamilton PRP-X200 SCX column. Mobile phase: 0.7M KBr, 1.5 mM sodium acetate buffer at pH 5.5, 1.2ml/min: Postcolumn reagent: 0.05 mM Cu(L-Trp)$_2$, 4 mM sodium borate buffer at pH 8.8, 1.8ml/min. Chromatogram 1: a diluted ophthalmic neomycin sample (1:100 dilution): chromatogram 2: a diluted intravenous kanamycin A sample (1:10.000 dilution): chromatogram 3: a diluted ophthalmic tobromycin sample (3:100).

Reproduced with permission of the copyright owner. Further reproduction prohibited without permission.

5.3.3 Separation and Detection of Aminoglycoside Antibiotics in a Reversed Phase Ion Pair Chromatographic Mode

5.3.3.1 Optimization of Separation Conditions for Aminoglycosides

Aminoglycosides are difficult to retain in a reversed phase chromatographic mode because of their strong hydrophilicity. In reversed phase ion-pair chromatography, the retention of the aminoglycosides is based on the cationic nature of these compounds. PFPA was chosen as the ion pairing agent in the mobile phase based on the results of previous studies [122, 132]. The elution order of the aminoglycosides correlates with the number of amino groups in these compounds, with spectinomycin, which possesses only two amino groups, having the lowest retention, while neomycin, with six amino groups, having the strongest retention. The effects of PFPA concentration and methanol composition of the mobile phase on the retention of the aminoglycoside antibiotics were studied. Figure 5.19 (a) shows the change in the capacity factor of the aminoglycosides as a function of the methanol composition in the mobile phase at a constant PFPA concentration of 30 mM. Figure 5.19 (b) shows the change in the capacity factor of the same five aminoglycosides as a function of the concentration of the ion pairing agent, PFPA, at a constant methanol concentration of 50% (by volume). The retention of the aminoglycosides increases as the concentration of PFPA increases. Retention times decrease with increasing methanol concentration. These data suggest the retention of the aminoglycosides is controlled by the concentration of the pairing ions adsorbed on the stationary phase. Both decreasing the PFPA concentration and increasing the methanol

Reproduced with permission of the copyright owner. Further reproduction prohibited without permission.

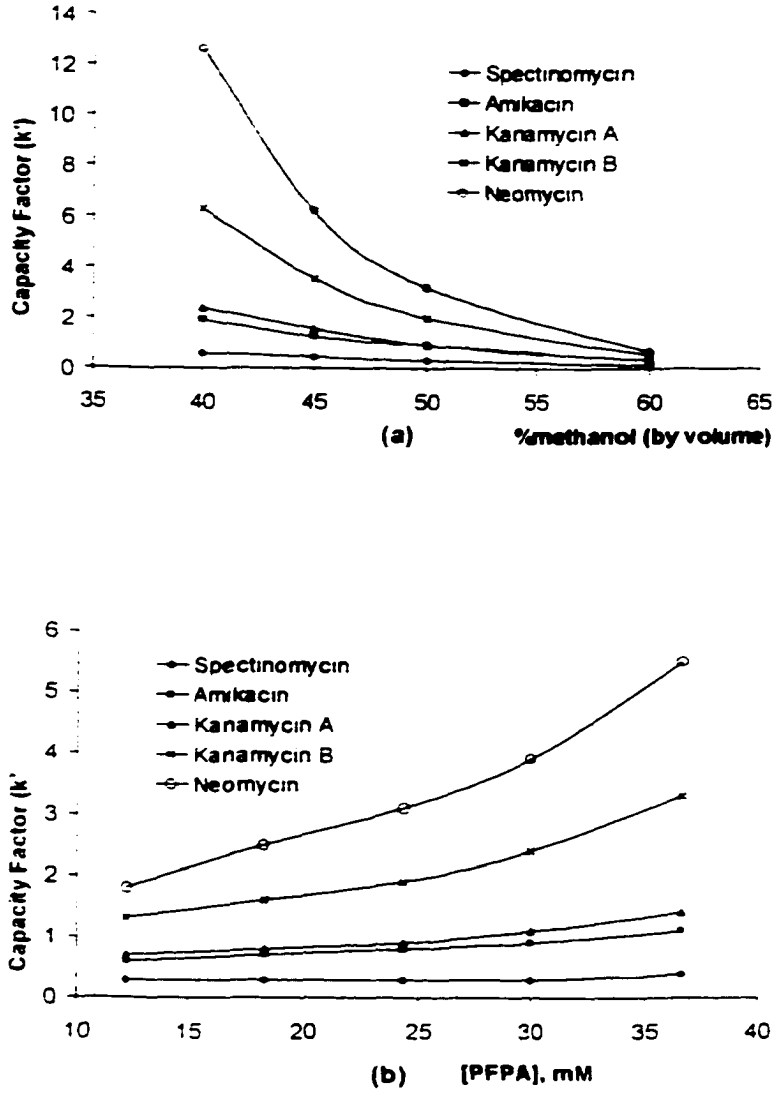

Figure 5.19: (a) Capacity factors of five aminoglycosides on a Supelcosil^{TM} C_{18} column as a function of methanol percentage in the mobile phase. The concentration of pentafluoropropionic acid (PFPA) is 30 mM. (b) Capacity factors of five aminoglycosides in a Supelcosil^{TM} C_{18} column as a function of PFPA concentration. The methanol concentration is 50% by volume.

Reproduced with permission of the copyright owner. Further reproduction prohibited without permission.

composition in the mobile phase result in decreasing the concentration of the ion-pairing agent in the stationary phase, leading to a weaker retention of the aminoglycosides. Based on these results, it was decided to use a PFPA concentration of 30 mM and a methanol concentration of 50% (by volume) for isocratical elution of the aminoglycosides tested: spectinomycin, amikacin, kanamycin A, kanamycin B and neomycin. The apparent pH of the mobile phase was set at 2.1, since lower pH may lead to increase the degradation of the silica-based stationary phase.

5.3.3.2 Optimization of Chromatographic Detection Conditions

The fluorescence profiles of 0.1 mM Trp and 0.05 mM Cu(L-Trp)$_2$ in an aqueous mixture containing 30% methanol as a function of apparent pH are given in Figure 5.3. Compared to an aqueous solution, in which 94 - 95% of L-Trp fluorescence is quenched at the optimum pH, as shown in Figure 2.4, more than 96% of the L-Trp fluorescence is quenched with the addition of 30% of methanol into the solution within an appropriate pH range. With the introduction of methanol, the pH range for effective fluorescence quenching is also significantly broadened, which allows a wider working pH range for detection.

The detection reagent, 0.05 mM Cu(L-Trp)$_2$ in 30% methanol, was added postcolumn to the eluent via a mixing tee. The pH of the postcolumn reagent was buffered with 40 mM sodium borate ($Na_2B_4O_7$) solution. It was found with the addition of 30% of methanol to the Cu(L-Trp)$_2$ solution, the postcolumn reagent is stable over several days

Reproduced with permission of the copyright owner. Further reproduction prohibited without permission.

at pH 9.4, compared to a maximum pH for long term reagent stability of 9.0 for an aqueous solution without added organic modifier. The chromatographic peak intensities for five of the aminoglycosides are shown in Figure 5.20 as a function of detection pH. The signals increase in the pH range from 8.1 to 9.4. As indicated in Figure 5.20, the chromatographic peak intensities for these five aminoglycosides increase in this pH range. A detailed explanation on how detection pH affects the chromatographic peak intensities was given in Chapters 3 and 4. The increasing fluorescence efficiency of L-Trp with increasing pH dominates the chromatographic signals in the pH range of 8.1 to 9.4. Considering the increasing baseline variability at lower postcolumn flow rates, as shown in Figure 5.21, the postcolumn flow rate was set at 1.8 ml/min for the optimum detection condition.

A representative chromatogram is given in Figure 5.22 for a mixture of the five aminoglycosides injected with masses on the order of ng injected under the optimized separation and detection conditions. A representative chromatogram is also presented in Figure 5.23 for a mixture of three additional aminoglycosides. The detection limits for the five aminoglycosides range from 1.7 ng injected for spectinomycin to 12.8 ng injected for kanamycin B. Table 5.2 lists the statistical performance of the detection.

Based on the separation method developed for the aminoglycosides, detection using Cu(L-Tyr)$_2$ as the postcolumn reagent was also studied. The representative chromatograms for the aminoglycosides obtained at different detection pHs with Cu(L-Tyr)$_2$ as the postcolumn reagent are given in Figure 5.24. Figure 5.25 indicates that the

Reproduced with permission of the copyright owner. Further reproduction prohibited without permission.

Reproduced with permission of the copyright owner. Further reproduction prohibited without permission.

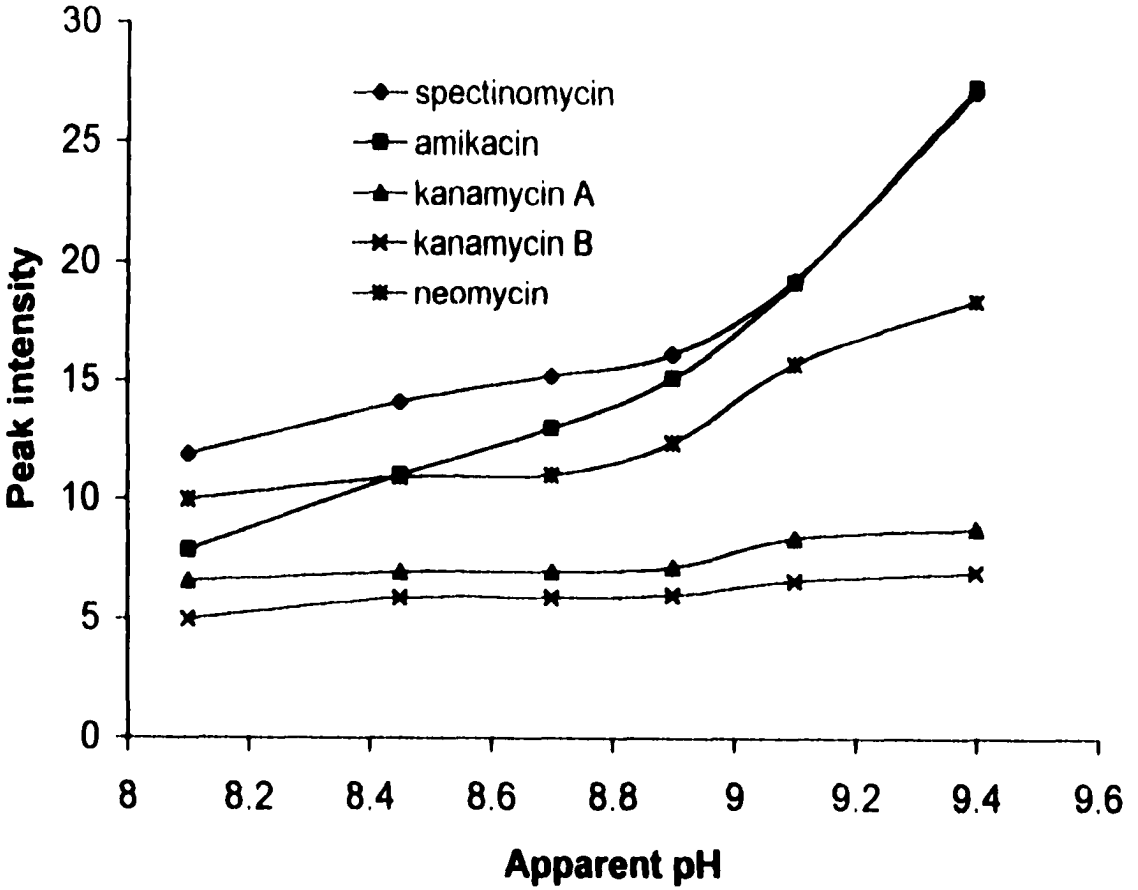

Figure 5.20. Chromatographic peak intensities as a function of detection pH. The amounts of samples injected were spectinomycin: 41.6 ng; amikacin: 73.2 ng; kanamycin A: 120.7 ng; kanamycin B: 120.7 ng; neomycin:153.7 ng.

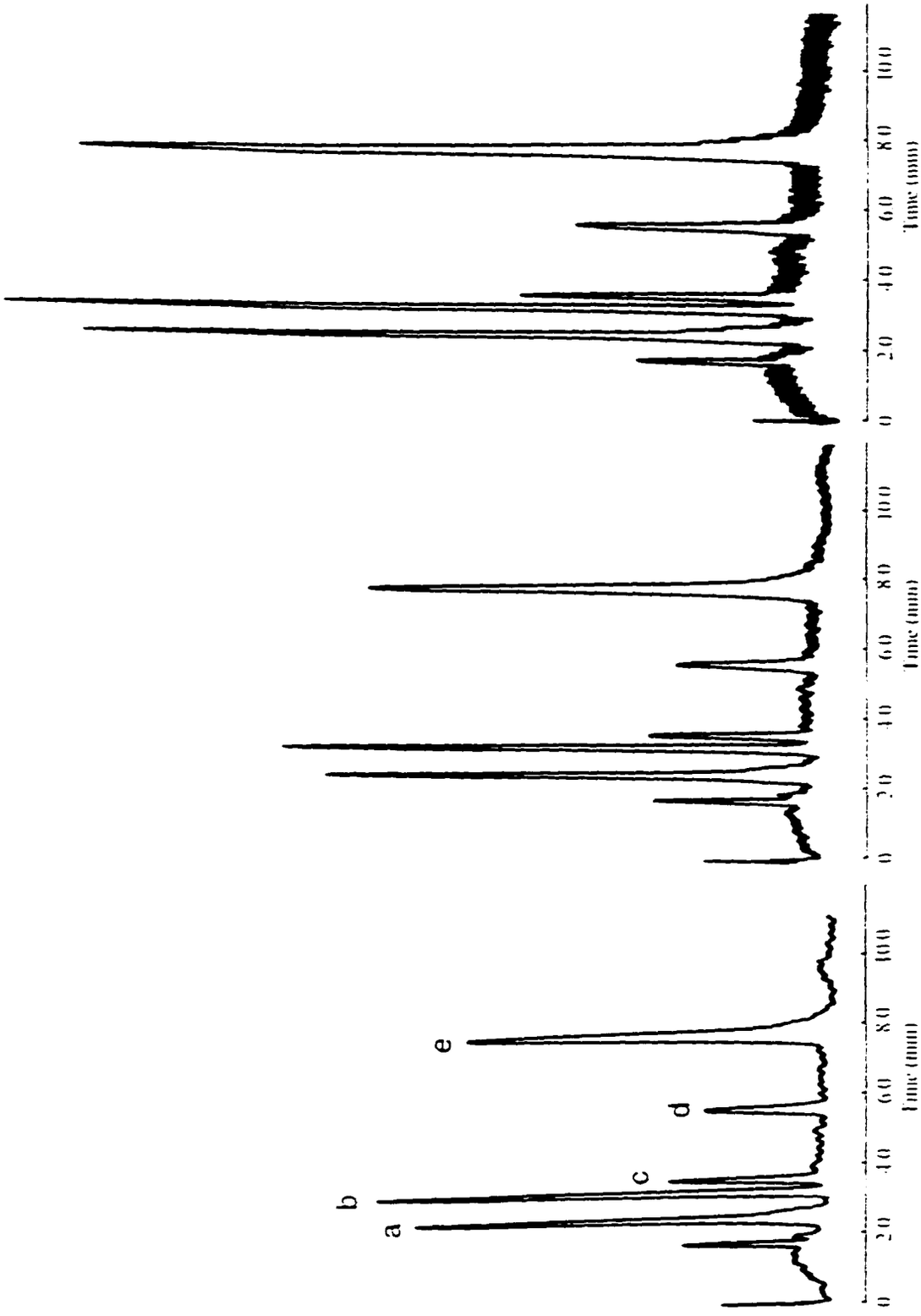

Figure 5.21: Representative chromatograms of the aminoglycosides obtained at different postcolumn reagent flow rates. Measurements were made using the same detector scale. Separation was achieved with the use of a Supelcosil™ C18 column. Mobile phase: 50% methanol, 80 mM PIPA, pH 2.1, 1ml/min; Postcolumn reagent: 0.05 mM Cu(I). Trace in 30% methanol, 40 mM sodium borate at pH 9.4. Peak a: spectinomycin, 83.1 ng; peak b: amikacin, 146.4 ng; peak c: kanamycin A, 241.4 ng; peak d: kanamycin B, 241.4 ng; peak e: neomycin, 307.4 ng; Postcolumn reagent flow rate: chromatogram 1: 2.0 ml/min; 2: 1.5 ml/min; 3: 1.0 ml/min.

Reproduced with permission of the copyright owner. Further reproduction prohibited without permission.

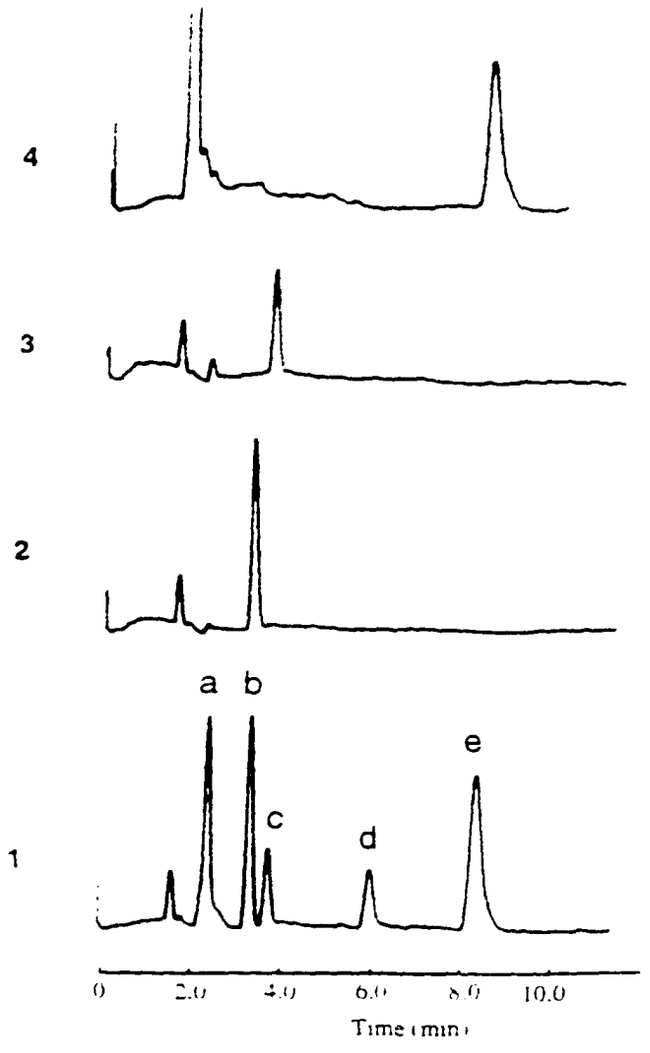

Figure 5.22: Representative chromatogram of the aminoglycosides. Separation was achieved with the use of a Supelcosil™ C_{18} column. Mobile phase: 50% methanol, 30mM PFPA, apparent pH 2.1, 1ml/min; Postcolumn reagent: 0.05 mM Cu(L-Trp)$_2$ in 30% methanol, 40 mM sodium borate at an apparent pH 9.4, 1.8 ml/min. Chromatogram 1. Peak a: spectinomycin, 83.1 ng; peak b: amikacin, 146.4 ng; peak c: kanamycin A, 241.4 ng; peak d: kanamycin B, 241.4 ng; peak e: neomycin, 307.4 ng; Chromatogram 2: a diluted intravenous amikacin sample (1:20,000 dilution); chromatogram 3: a diluted intravenous kanamycin A sample (1:10,000 dilution); chromatogram 4: a diluted ophthalmic neomycin sample (1:100 dilution).

Reproduced with permission of the copyright owner. Further reproduction prohibited without permission.

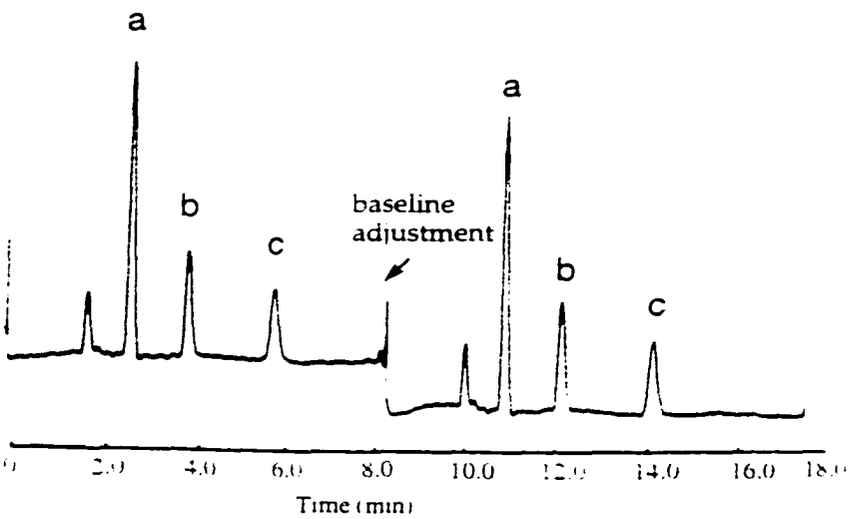

Figure 5.23: Repetitive injections of a mixture containing three aminoglycoside standards. Separation was achieved with the use of a Supelcosil™ C_{18} column. Mobile phase: 50% methanol, 30mM PFPA, pH 2.1, 1ml/min; Postcolumn reagent: 0.05 mM Cu(L-Trp)$_2$ in 30% methanol, 40 mM sodium borate at an apparent pH 9.4, 1.8 ml/min. Peak a: hygromycin B (527 ng); b: ribostamycin (454.5 ng); c: tobramycin (467.5 ng).

Reproduced with permission of the copyright owner. Further reproduction prohibited without permission.

Aminoglycoside	Range (ng)	Regression equation[a]	DL[b] (ng)	DL[b] (ppm	RSD[c] (%)
Spectinomycin	8.3 - 166.2	H = -0.42 + 0.58 x C	1.7	0.17	3.2
Amikacin	14.5 - 586	H = -0.55 + 0.33 x C	2.2	0.22	2.5
Kanamycin A	24 - 483	H = -0.05 + 0.059 x C	12.0	1.2	2.7
Kanamycin B	24 - 483	H = 0.01 + 0.05 x C	12 x	1.3	2.9
Neomycin	31 - 615	H = 0.4 + 0.1 x C	9.5	0.95	3.4

[a] H, peak height; C, analyte mass injected (in ng). [b] Detection limit. [c] Relative standard deviation (N = 5, for 83.1 ng spectinomycin, 146.4 ng amikacin, 242 ng kanamycin A, 242 ng kanamycin B and 307.5 ng neomycin injected respectively).

Table 5.2: Characteristic parameters of the calibration graphs and analytical figures of merit for the determination of aminoglycosides

Reproduced with permission of the copyright owner. Further reproduction prohibited without permission.

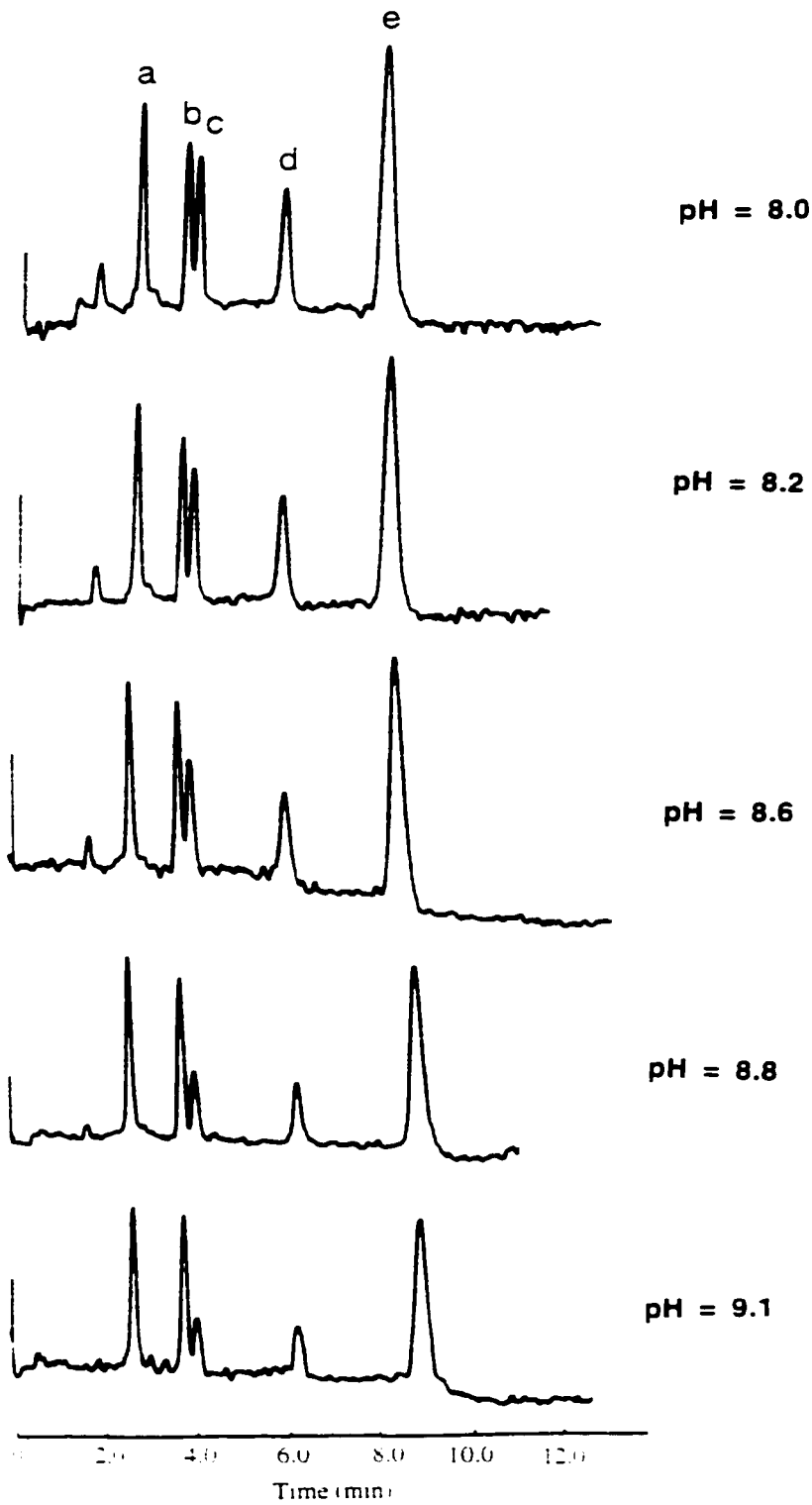

Figure 5.24: Representative chromatograms of the aminoglycosides obtained with Cu(L-Tyr)$_2$ as the postcolumn reagent at different detection pH. Separation was achieved with the use of a Supelcosil^{TM} C_{18} column. Mobile phase: 50% methanol, 30 mM PFPA, apparent pH 2.1, 1ml/min; Postcolumn reagent: 0.05 mM Cu(L-Tyr)$_2$ in 30% methanol, 40 mM sodium borate 1.8 ml/min. Peak a: spectinomycin, 332.4 ng; peak b: amikacin, 585.6 ng; peak c: kanamycin A, 482.8 ng; peak d: kanamycin B, 482.8 ng; peak e: neomycin, 614.8 ng.

Reproduced with permission of the copyright owner. Further reproduction prohibited without permission.

Reproduced with permission of the copyright owner. Further reproduction prohibited without permission.

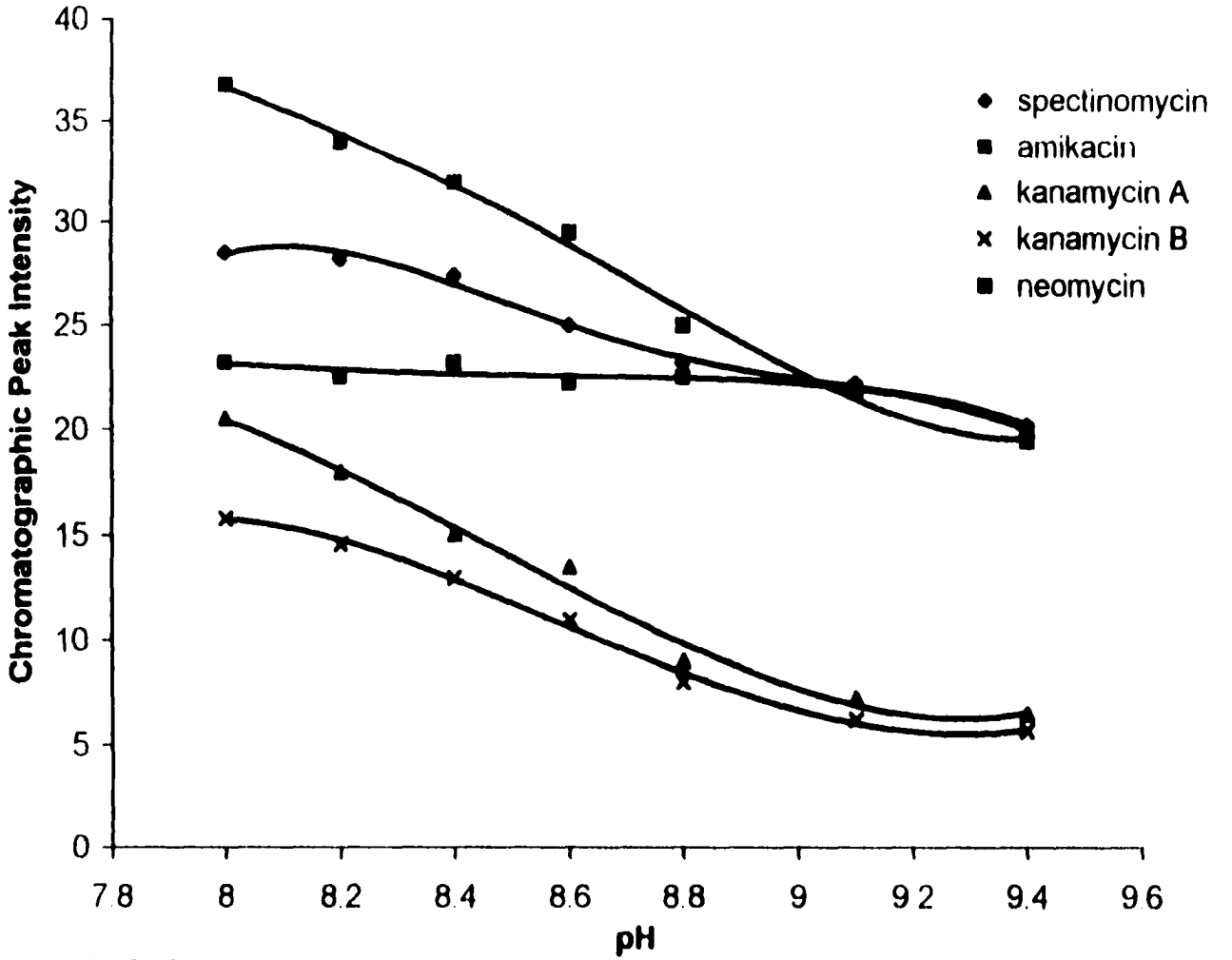

Figure 5.25: Chromatographic peak intensities as a function of detection pH. The amounts of samples injected were spectinomycin: 83.2 ng; amikacin: 146.4 ng; kanamycin A: 241.4 ng; kanamycin B: 241.4 ng; neomycin: 307.4 ng.

peak intensities of the five aminoglycosides decrease as the pH increases in the range from 8.1 - 9.4. This pH dependent pattern is attributed to the decreasing fluorescence of L-Tyr as the pH increases, which is indicated in Figure 5.1. $Cu(L\text{-}Trp)_2$ generally provides chromatographic peak intensities approximately 5 times the peak intensities when using $Cu(L\text{-}Tyr)_2$ as the postcolumn reagent. It was concluded that $Cu(L\text{-}Trp)_2$ provides superior detection performance compared to $Cu(L\text{-}Tyr)_2$ as the postcolumn reagent for aminoglycosides under optimized detection conditions.

Representative chromatograms of the aminoglycosides obtained with gradient elution are presented in Figure 5.26. Those chromatograms were obtained by programming the methanol composition of the mobile phase. It is believed the detection scheme is compatible with gradient elution as long as the postcolumn reagent has a strong enough buffering capacity to make the detection pH stable during the elution.

Commercially available samples of aminoglycosides in several formulations were obtained and analyzed using the developed separation and detection method. No sample pretreatment was required except for dilution with distilled water. Sample chromatograms are presented in Figure 5.21. For an intravenous kanamycin A sample, the determined original concentration is 325 ± 10 mg/ml, compared to a claimed 333 mg/ml; for an ophthalmic neomycin sample, the determined original concentration is 3.56 ± 0.09 mg/ml, compared to a claimed 3.5 mg/ml.

Reproduced with permission of the copyright owner. Further reproduction prohibited without permission.

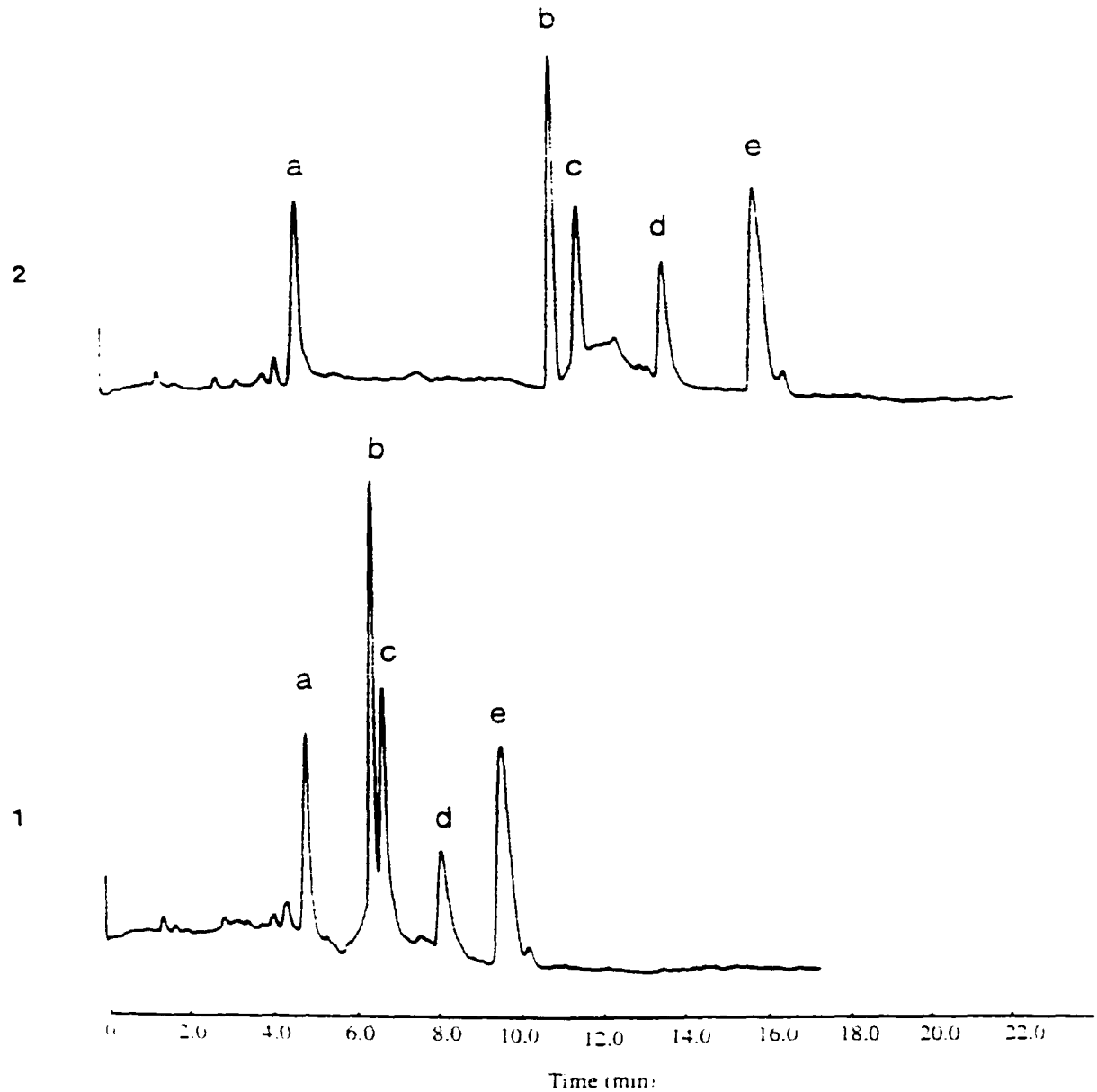

Figure 5.26: Test chromatograms of the aminoglycosides with gradient elution. Separation was achieved with the use of a Supelcosil™ C_{18} column. Postcolumn reagent: 0.05 mM Cu(L-Trp)$_2$ in 30% methanol, 40 mM sodium borate at pH 9.4, 1.8 ml/min. Chromatogram 1: Mobile phase: 30% to 65% methanol in 4 minutes, 30 mM PFPA, pH 2.1, 1ml/min: Chromatogram 2: Mobile phase: 30% to 50% methanol in 4 minutes, 30mM PFPA, pH 2.1, 1ml min. Peak a: spectinomycin, 116.2 ng; peak b: amikacin, 292.8 ng; peak c: kanamycin A, 482.8 ng; peak d: kanamycin B, 482.8 ng; peak e: neomycin, 614.8 ng.

Reproduced with permission of the copyright owner. Further reproduction prohibited without permission.

5.3.4 Comparison of the Developed Detection Method for Aminoglycosides with other Detection Methods

The detection method developed is free from the problems encountered when using derivatization approaches, such as labor-intensive sample preparation and derivative instability. Also, compared to traditional postcolumn derivatization methods which may require several ml of mixing volume, extracolumn bandbroadening was significantly reduced, due to the minimum mixing volume used in this study. The calculated number of theoretic plates for separation without the addition of postcolumn reagent was 9909, compared to 9950 for the separation with the addition of a postcolumn reagent with a flow rate of 3.0 ml/min, as shown in Figure 5.12. These efficiencies are considered to be the same within the measurement variability, due to the minimum mixing volume introduced. Furthermore, the detection limits obtained for aminoglycosides with the detection methods developed in this study are comparable to detection limits obtained from precolumn derivatization methods using either fluorescence [113] or UV-VIS detection [133, 134], which generally have detection limits around 10 ng injected on column or higher.

The detection limits in this study are also comparable to the detection limits obtained for the well-developed pulsed electrochemical detection for the aminoglycosides, which range from 4 to 15 ng. Normally detection limits as low as several picograms can be achieved in the selected ion monitoring (SIM) mode in HPLC-MS detection in reversed phase liquid chromatography [17]. However, for optimized detection of the

Reproduced with permission of the copyright owner. Further reproduction prohibited without permission.

aminoglycosides in a SIM mode in HPLC-MS, reportedly the detection limits are in a range of 1 - 50 ng [135], possibly due to the effects of the presence of nonvolatile ion pairing agents used in the ion pair chromatography.

5.4 Conclusions

Indirect fluorescence detection based on a fluorescence displacement reaction was applied for the detection of the aminoglycoside antibiotics following chromatographic separation. This non-derivatization detection scheme is free from many of the common problems encountered when using conventional derivatization methods.

This indirect detection method was demonstrated for two chromatographic separation modes, cation exchange chromatography and reversed-phase ion pair chromatography, for detection of aminoglycosides. Detection limits for both chromatographic modes are on the order of low ng injected. Reversed-phase ion pair chromatography proved to provide superior separation efficiency for the aminoglycosides compared to cation exchange chromatography. The indirect fluorescence detection scheme was demonstrated to be compatible with a mobile phase containing a high level of organic solvent modifier in the reversed phase ion pair chromatographic mode. Introduction of the organic modifier to the mobile phase improved the fluorescence quenching of L-Trp by Cu(II) and broadened the detection pH range.

Detection of the aminoglycosides with Cu(L-Tyr)$_2$ as the postcolumn reagent was also studied. Cu(L-Tyr)$_2$ provided inferior detection performance compared to Cu(L-

Reproduced with permission of the copyright owner. Further reproduction prohibited without permission.

Trp)2, due to L-Tyr's decreasing fluorescence efficiency as the pH increases.

Detection limits obtained with the developed detection methods correspond to a sub ppm to low ppm concentration level with a 10 µl injection volume. The methods have been successfully applied to formulated pharmaceutical products. Considering human serum aminoglycoside levels during administrations are in the range of 0.5 - 30 ppm [10]. this method may be applicable to monitoring serum concentrations of the aminoglycosides.

Reproduced with permission of the copyright owner. Further reproduction prohibited without permission.

CHAPTER 6

Summary and Future Studies

An indirect fluorescence detection method has been developed for the detection of natural amino acids, biogenic polyamines and aminoglycoside antibiotics following chromatographic separation. This method is based on a ligand displacement reaction between the analytes, which have superior binding ability for transition metal ions such as Cu^{2+}, with a Cu(II) – L-Trp complex $Cu(L\text{-}Trp)_2$. The fluorescence of L-Trp is quenched when complexed but its fluorescence recovers when displaced from the complex. The increase in fluorescence is taken as a measure of the presence of the analyte. Systematic studies, both experimental and theoretical, were carried out to investigate the effects of experimental parameters on the detection system, such as the stoichiometric ratio for the displacement reactions, the detection pH, and the impact of an organic modifier in the mobile phase. The advantages of this method over traditional detection methods include the following:

1. Compared to methods requiring precolumn derivatization: 1). The time-consuming and labor-intensive sample preparation process is avoided. 2). The method is also free from the problems associated with the derivatization, such as derivative degradation and the formation of multiple derivative species.

Reproduced with permission of the copyright owner. Further reproduction prohibited without permission.

2. Compared to methods requiring postcolumn derivatization: 1). The instrumentation is simplified by removing the specially designed postcolumn reaction chamber. 2). The elimination of the postcolumn reactor also significantly improves the separation efficiency by reducing postcolumn bandbroadening associated with reaction chamber.

3. Compared to methods using electrochemical detection, which is the most developed nonderivatization detection method: 1). This method is simple and robust. 2). Electrode poisoning continues to be a problem encountered when using electrochemical detection.

Considering the importance of the amino acids, biogenic amines and aminoglycosides in biological and clinical studies, further investigations are necessary to develop simple, sensitive and robust detection methods for these compounds following chromatographic separation. Development of this indirect fluorescence detection method is still in its preliminary stage. Efforts could be expended on a number of aspects to further improve the detection performance based on this detection scheme.

As the first fluorescent agent tested for this detection approach, L-Trp offers reasonably good detection limits for the amino group-containing species tested, generally in the low pmol injected range. However, sensitivity is still limited by the fluorescence efficiency of the L-Trp molecule. Flow injection experiments were conducted by injecting the L-Trp into a flow system without the HPLC column, indicating for the particular fluorescence detector used in this study, the detection limit for L-Trp is approximately 1-2 pmol. The use of other fluorescent agents

Reproduced with permission of the copyright owner. Further reproduction prohibited without permission.

should be explored in the future, with the general criteria for the candidate fluorescent agents being:

1. It should possess a high fluorescence quantum efficiency. The presence of analytes is inferred by the fluorescence of the candidate fluorescent agent. A stronger fluorescence efficiency of the fluorescent agent simply results in a stronger chromatographic signal for the analyte.

2. Upon binding to the transition metal ions, the fluorescence of the fluorescence agent should be effectively quenched. The fluorescence quenching should be controlled by the complexation between the metal ions and the fluorescence agent, since the detection scheme is based on a ligand displacement mechanism. The fluorescence quenching provides a "dark" background for the chromatographic baseline, thus significantly reducing the baseline noise level.

3. The affinity which the fluorescent agent has for the transition metal ion should be either weaker or comparable to the affinity which the analyte has for the transition metal ion. If binding interaction between the metal ions and the fluorescent agent is too strong, the competition for binding to the transition metal ions will favor the fluorescent agent, resulting in less of the fluorescence agent being displaced, thereby resulting in a weaker fluorescence signal.

It may be fruitful to introduce structurally modified Trp analogs as the candidate fluorescent agents, since it can be reasonably assumed that those analogs have similar affinities for transition metal ions as the unmodified Trp molecule does. This makes them qualify for the third criteria

Reproduced with permission of the copyright owner. Further reproduction prohibited without permission.

listed above, because Trp has proved to be effectively displaced by amino acids, biogenic amines and aminoglycosides from its Cu(II) complex. Although the second factor above concerning the relationship between binding and fluorescence quenching still needs to be tested for these analogs, the systematic work described earlier in this study has paved the way for such investigations. For example, 5-hydroxy-Trp [136, 137] has a fluorescence efficiency approximately 2 times of that of Trp, while N-acetyl -Trp has a fluorescence efficiency which is 1.25 times of that of Trp [64]. Both of these compounds can be tested as candidates to replace Trp as the fluorescence agent in future studies.

A limitation when using Trp analogs as the candidate fluorescence agents however, is that fluorescence quantum efficiency of these compounds can not be significantly increased compared to Trp. Although fluorescence quenching by transition metal ions has been studied extensively, care needs to be taken to choose other fluorescence agents concerning the third criteria listed above. Efforts need to be expended to seek fluorescent agents that can be effectively displaced from their metal complexes by the analytes.

Studies can also be performed to incorporate the postcolumn reagent into the HPLC mobile phase or a CZE running buffer. This will not only simplify the instrumentation required for the detection method by removing the postcolumn pump, but also avoid dilution of the analyte upon mixing with the postcolumn reagent. However, care should be taken to assure the detection conditions are compatible with the separation conditions for the analytes. For instance, the transition metal complex may interfere with the separation by interacting with the chromatographic stationary phase. In this sense, addition of the detection reagent into a CZE

Reproduced with permission of the copyright owner. Further reproduction prohibited without permission.

running buffer may be more feasible, since the separation in a CZE system is determined by the externally applied high-voltage potential, instead of the stationary phase, although the effect of the binding with the metal ions needs to be considered.

Reproduced with permission of the copyright owner. Further reproduction prohibited without permission.

References

[1] W. J. Lough and I. W. Wainer. High Performance Liquid Chromatography. Blackie Academic & Professional. 1996

[2] G. C. Barrett and D. T. Elmore. Amino acids and peptides. Cambridge. New York. Cambridge University Press. 1998

[3] L. M. Smith. Anal. Chem.. 60 (1988) 381A

[4] H. E. Flores. A. W. Galston. Plant Phys.. 69 (1982) 901

[5] R. H. Dainty. R. A. Edwards. C. M. Hibbard and S. V. Rrnantanis. J. Appl. Bacteriol.. 61 (1986) 117

[6] A. E. Pegg. J. Biochem.. 234 (1986) 2493

[7] C. M. Caldarera. B. Barbiroli. G. Moruzzu. Biochm.. 97 (1965) 84

[8] W. J. P. Neish. L. Key. Int. J. Cancer 2 (1967) 69

[9] S. A. Waksman. E. Bugie and a. Schatz. Proc. Staff. Meet. Mayo. Clin.. 19 (1944) 537

[10] W. E. Siegenthaler. A. Bonett and R. Luthy. Am. J. Med.. 80 (6B) (1986) 2

[11] V. R. Meyer. Practical High Performance Liquid Chromatography. John Wiley & Sons. 1999

[12] H. M. L. J. Doosten and C. Olieman. J. Chromatogr.. 356 (1986) 311

[13] Y. Hiraga and T. Kinoshita. J. Chromatogr.. 342 (1985) 269

[14] D. G. Musson. S. M. Maglietto and W. F. Bayne. J. Chromatogr.. 338 (1985) 357

[15] M. Roth. Anal. Chem.. 43 (1971) 880

[16] H. Miyano. T. Toyo'oka and K. Iami. Anal. Chim. Acta.. 170 (1985) 81

[17] D. Parriott. A practical guide to HPLC detection. San Diego. Academic Press. Inc. 1992

Reproduced with permission of the copyright owner. Further reproduction prohibited without permission.

[18] H. Engelhardt and U. D. Neue., Chromatographia. 15 (1982) 403

[19] C. M. Selavka. K. S. Jiao and I. S. Krull. Anal. Chem., 59 (1987) 2221

[20] B. Lillig and H. Engelhardt. Reaction Detection in Liquid Chromatography. Marcel Dekker. 1986. New York

[21] L. R. Snyder. J. Chromatogr., 125 (1976) 287

[22] M. V. Pickering. LC-GC. 6 (1988) 994

[23] L. He. K.A. Cox. N. D. Danielson. Anal. Lett., 23 (2) (1990) 195

[24] S. N. Brune. D. R. Bbbitt. Anal. Chem., 64 (1992) 166

[25] W. A. Jackson. D. R. Bobbitt. Anal. Chim. Acta., 285 (1994) 309

[26] S. R. Skotty. W. Y. Lee. T.A. Nieman. Anal. Chem., 68(1996) 1530

[27] J. B. Noffsinger. N. D. Danileson. J. Chromatogr., 387 (1987) 520

[28] M. A. Targove. N. D. Danileson. J. Chromatogr. Sci., 28(1990) 505

[29] M. Denkert. L. Hackzell. G. Schill. E. Sjogren. J. Chromatogr., 218 (1981) 31

[30] M. Esiami. P. Hashemi. M. N. Sarboiouki. J. Chromatogr. Sci., 31 (1993) 480

[31] W. G. Kuhr. E. S. Yeung. Anal. Chem., 60 (1999) 213

[32] D. A. Dobberpuhl. J. C. Howkstra. D. C. Johnson. Anal. Chim. Acta., 322 (1996) 55

[33] J. C. Hoekstra. D. C. Johnson. Anal. Chem., 70 (1998) 83

[34] L. E. Welch. W. R. LaCoursse. D. A. Mead. D. C. Johnson. Anal. Chem., 61 (1989) 555

[35] P. J. Koerner. T. A. Nieman. Mikrochim. Acta., 2 (1987) 79

[36] A. MacDonald. T. A. Nieman. Anal. Chem., 57 (1985) 936

Reproduced with permission of the copyright owner. Further reproduction prohibited without permission.

[37] P. W. Alexander. M. Camelita. Anal. Chem.. 53 (1981) 1590

[38] W. T. Kok. U. A. T. Brinkman. R. W. Frei. J. Chromatogr.. 256 (1983) 17

[39] B. M. Polaneuer. S. V. Ivanov. J. Chromatogr. A. 722 (1996) 311

[40] E. Lindner. K. Toth and E. Pungor.. Anal. Chem. 48 (1976) 1071

[41] B. L. Kepner and D. M. Hercules. Anal. Chem.. 35 (1963) 1238

[42] A. J. Hetley and B. Jaselkis. Anal. Chem.. 46 (1974) 2036

[43] D. F. H. Wallach and T. L. Steck. Anal. Chem.. 35 (1963) 1035

[44] Z. Kocsis. Anal. Chem.. 124 (1942) 42

[45] M. Katyal.. Talanta. 15 (1968) 95

[46] L. A. Saari and W. R. Seitz. Anal. Chem.. 56 (1984) 813

[47] L.A. Saari and W. R. Seitz. 55 (1983) 667

[48] M. A. Kuhn. B. Hoylan. S. Carter. C. Zhang. R. P. Haugland. Proc. Soc. Photo-Optical Instru. Eng.. 2388. 238

[49] J. L. Nowicki. K. S. Johnson. K. H. Coale. V. A. Elrod and S. H. Lieberman. Anal. Chem.. 66 (1994) 2732

[50] J. D. Ingle and S. R. Crouch. Spectrochemical Analysis. 1988. Prentice Hall. NJ].

[51] S. V. Konev. Fluorescence and Phosphorescence of Proteins and Nucleic Acids. Plenum Press. New York. 1967

[52] J. M. Beechem and L. Brand. Ann. Rev. Biochem.. 54 (1985) 43

[53] R. F. Steiner. E. P. Kirby. J. Phys. Chem.. 73 (12) (1969) 4130

[54] M. Tabak. G. Sartor and P. Cavatorta. J. Luminesc.. 43 (1989) 355

Reproduced with permission of the copyright owner. Further reproduction prohibited without permission.

[55] M. Tabak. G. Sartor. P. Neyroz. A. Spisni and P. Cavatorta. J. Luminesc.. 46 (1990) 291

[56] R. Chen. Anal. Lett.. 19(9&10) (1986) 963

[57] J. R. Lakowicz. Principles of fluorescence spectroscopy. Kluwer Academic Plenum Publishers. New York. 1999

[58] M. J. Kronman and L. G. Holmes. Photochem. Photobiol. 14(1971) 113

[59] G. Gilardi. G. Mei. N. Rosato. G. W. Ganters and A. Finazzi-Agro. Biochem.. 33 (1994)1425

[60] M. R. Eftink and C. A. Ghiron. Anal. Biochem.. 114 (1981) 199

[61] R. F. Chen. Arch. Biochem & Biophys.. 142 (1971) 552

[62] A. Sharma. S. G. Schulman. Introduction tofluorescence spectroscopy. John Wiley and Sons. Inc.. 1999

[63] A. E. Martell and R. M. Smith. Critical Stability Constants(Volume 1: Amino Acids) (1974) Plenum Press. New York

[64] A. White. Biochem. J.. 71 (1959) 217

[65] M. C. Chang. J. W. Petrich. D. B. McDonald and G. R. Fleming. J. Am. Chem. Soc.. 105 (1983) 3819

[66] J. W. Petrich. M. C. Chang. D. B. McDonald and G. R. Fleming. J. Am. Chem. Soc.. 105 (1983) 3824

[67] E. Gudgin. R. Lopez-Delgado and W. R. Ware. Can. J. Chem. 59 (1981) 1037

[68] D. M. Jameson. G. Weber. J. Phys. Chem.. 85 (1981) 953

[69]A. E. Martell and R. M. Smith. Critical Stability Constants(Volume 4: Inorganic ligands) (1976) Plenum Press. New York

[70] M. T. S. D. Vasconcelos. M. A. G. O. Azenha and O. M. Lage. Anal. Biochem.. 241 (1996) 248

Reproduced with permission of the copyright owner. Further reproduction prohibited without permission.

[71] R. Maijala. E. Nurmi and A. Fischer. Meat Sci.. 39(1) (1995) 9

[72] R. D. Solcum. H. E. Flores. A. W. Galston and L. H. Weinstein. Plant Phys.. 89 (1989) 512

[73] J. E. Stratton. R. W. Hutkins and S. L. Taylor. J. Food Protect.. 54(6) (1991) 460

[74] C. W. Tabor and H.Tabor. Annu. Rev. Biochem.. 53 (1984) 747

[75] J. Janne. H. Poso and A. Raina. Biochim. Biophys. Acta.. 473 (1978) 241

[76] I. Flink and D. E. Pettijohn. Nature 253 (1975) 62

[77] L. C. Gosule and J. A. Schellman . ibid.. 333 (1976) 259

[78] C. W. Porter. Science. 219 (1983) 1083

[79] M. Siimes and J. Jaune. Acta. Chem. Scand.. 21 (1967) 815

[80] U. Bachrach. Function of Naturally Occuring Polyamines. 1973. Academic Press. New York.

[81] S. L. Rice. R. R. Eitenmiller and P. E. Koehler. J. Milk Food Technol.. 39 (1976) 353

[82] S. T. Edwards and W. E. Sandine. J. Dairy Sci.. 64 (1981) 2431

[83] C. W. Tabor and H. Tabor. Ann. Rev. Biochem.. 45 (1976) 285

[84] H. Yamanaka. Food Rev. Int.. 6 (1990) 591

[85] S. Moret. R. Bortolomeazzi and G. Lercker. J. Chromatogr.. 591 (1992) 175

[86] S. Moret and L. S. Conte. J. Chromatogr. A. 729 (1996) 363

[87] S. Suzuki. K. Kobayashi. J. Noda. T. Suzuki and K. Takama. J. Chromatogr.. 508 (1990) 225

[88] H. Ohta. Y. Takeda. K. Yoza and Y. Nogata. J. Chromatogr.. 628 (1993) 199

[89] H. M. L. Joosten and C. Olieman. J. Chromatogr.. 356 (1986) 311

Reproduced with permission of the copyright owner. Further reproduction prohibited without permission.

[90] J. N. LePage and E. M. Rocha. Anal. Chem.. 55 (1983) 1360

[91] B. Fransson. M. L. S. Almeida. L. Grehn and U. Ragnarsson. J. Chromatogr.. 508 (1990) 229

[92] Y. Ma. R. Zhang and C. L. Cooper. J. Chromatogr.. 608 (1992) 93

[93] R. Draisci. L. Giannetti. P. Boria. L. Lucentini. L. Palleschi and S. Cavalli. J. Chromatogr. A. 798 (1998) 109

[94] A. E. Martell and R. M. Smith. Critical Stability Constants (Volume 2: Amines) (1974) Plenum Press. New York

[95] I. Labadi. E. Jenei. R. Lahti and H. Lonnberg. Acta. Chem. Scand.. 45 (1991) 1055

[96] M. Gold and J. K. J Powell. J. Chem. Soc. Dalton.. (1976) 230

[97] D. M. Templeton and B. Sarkar. Can. J. Chem.. 63 (1985) 3122

[98] R. M. Linares. J. H. Ayala. A. M. Afonso and V. G. Diaz. J. Chromatogr. A.. 808 (1998) 87

[99] M. D. Koppang. M. Witek. J. Blau and G. M. Swain. Anal. Chem.. 71 (1999) 1188

[100] S. A. M. Marzouk. C. X. Xu. B. R. Cosofret. R. P. Buck. S. S. M. Hassan. M. R. Newman. R. H. Sprinkle. Anal. Chim. Acta.. 363 (1998) 57

[101] G. C. Barrett. Amino acids. peptides and proteins (Royal Society of Chemistry) 29 (1998) 1

[102] Y. Tapuhi. D. Schmidt. W. Linder and B. Karger. Anal. Biochem. 115 (1981) 123

[103] C. Dejong. G. J. Hughes. E. Van Wieringer and K. J. Wilson. J. Chromatogr. 241 (1982) 345

[104] N. Sieler and B. Knodgen. J. Chromatogr. 341 (1985) 11

[105] D. J. Strydom. J. Chromatogr. A. 662 (1994) 227

[106] I. G. Casella. M. Gatta and E. Desimoni. J. Chromatogr. A. 814 (1998) 63

Reproduced with permission of the copyright owner. Further reproduction prohibited without permission.

[107] F. J. Marquez. A. R. Quesada. F. Sanchez - Jimenez and I. Nunez De Castro. J. Chromatogr.. 380 (1986) 275

[108] J. Haddad. S. Vakulenko and S. Mobashery. J. Am. Chem. Soc.. 121 (1999) 11922

[109] S. J. Sucheck. A. L. Wong. K. M. Koeller. D. D. Boehr. K. Draker. P. Sears. G. D. Wright and C. H. Wong. J. Am. Chem. Soc.. 122 (2000) 5230

[110] L. E. Bryan and H. M. Van Den Elzen. Antimicrob. Agen. Chem.. 12 (1977) 163

[111] A. Marzo and L. D. Bo. J. Chromatogr. A. 812 (1998) 17

[112] M. Preu and M. Petz. J. Chromatogr. A.. 840 (1999) 81

[113] R. Tawa. H. Macsunaga and T. Fujimoto. J. Chromatogr. A. 812 (1998) 141

[114] E. A. Papp. C. A. Kaupp and R. H. Barbhaiya. J. Chromatogr.. 574 (1992) 93

[115] L. Elrod Jr.. L.B. White. C.F. Wong. J. Chromatogr.. 208 (1981) 357

[116] L. T. Wong. A. R. Beaubien. A. P. Pakuts. J. Chromatogr.. 231 (1982) 145

[117] P. Gambardella. R. Punziano. M. Gionti. G. Guadalupi. G. Mancini and A. Mangia. J. Chromatogr.. 348 (1985) 229

[118] T. A. Graser. H. G. Godel. S. Albers. P. Foldi. P. Furst. Anal. Biochem.. 151 (1985) 142

[119] E. Adams. G. Van Vaerenbergh. E. Rotes and J. Hoogmartens. J. Chromatogr. A. 819 (1998) 93

[120] E. Adams. D. Puelings. M. Rafiee. E. Rotes and J. Hoogmartens. J. Chromatogr. A. 812 (1998) 151

[121] E. Adams. J. Dalle. E. De Bie. I. De Smedt and E. Roets. J. Hoogmartens. J. Chromatogr. A. 766 (1997) 133

[122] L. G. Mclaughlin and J. D. Henion. J. Chromatogr.. 591 (1992) 195

[123] T. A. Getek. M. L. Vestal and T. G. Alexander. J. Chromatogr.. 554 (1991) 191

Reproduced with permission of the copyright owner. Further reproduction prohibited without permission.

[124] L. E. Mannis and M. J. Wilcox. Pittsburgh Conference 2061p. March. 2000. New Orleans. LA

[125] M. Jezowaska-Bojczuk. A. Karaczyn and W. Bal. J. Inorg. Biochem.. 71 (1998) 129

[126] M. Jezowska-Bojczuk. W. Bal and H. Kozlowski. Inorg. Chim. Acta.. 275-276 (1998) 541

[127] M. Jezowska-Bojczuk and W. Bal. J. Chem. Soc.. Dalton Trans.. (1998) 153

[128] G. Inchauspe and D. Samain. J. Chromatogr.. 303 (1984) 277

[129] J. A. Statler. J. Chromatogr.. 527 (1990) 244

[130] M. Yang. S. Tomellini. J. Chromatogr. A. 841 (1999) 9

[131] M. Yang. S. Tomellini. Anal. Chim. Acta.. 409 (2000) 53

[132] G. Inchauspe. P. Delrieu. P. Dupin. M. Laurent and D. Samain. J. Chromatogr.. 404 (1987) 53

[133] S. G. Spanton. D. G. Stroz. P. J. Cugier and L. A. Luka. Anal. Chem.. 56 (1984) 1786

[134] L. T. Wong. A. R. Beaubien and A. P. Pakuts. J. Chrom.. 231 (1982) 145

[135] M. Sakairi and H. Kambara. Anal. Chem.. 60 (1988) 774

[136] C. Y. Wong and M. R. Eftink. Protein Sic.. 6 (1997) 689

[137] T. M. Laue. D.F. Senear. S. Eaton and J. B.A. Ross. Biochem.. 32 (1993) 2469

Reproduced with permission of the copyright owner. Further reproduction prohibited without permission.

APPENDIX

Reproduced with permission of the copyright owner. Further reproduction prohibited without permission.

APPENDIX A

LIST OF DATA FILE

Figure	Filename
Figure 2.1	fig2.1&2
Figure 2.2	fig2.1&2
Figure 2.3	fig2.345
Figure 2.4	fig2.345
Figure 2.5	fig2.345
Figure 2.6	fig2.6
Figure 2.7	fig2.7
Figure 2.8	fig2.8
Figure 2.10	fig2.10
Figure 3.1	fig3.1
Figure 3.2	fig3.2
Figure 3.4	fig3.4
Figure 3.5	fig3.5
Figure 3.6	fig3.6.1spd fig3.6.2spm fig3.6
Figure 4.1	fig4.1-14
Figure 4.2	fig4.1-14

Reproduced with permission of the copyright owner. Further reproduction prohibited without permission.

Reproduced with permission of the copyright owner. Further reproduction prohibited without permission.

Reproduced with permission of the copyright owner. Further reproduction prohibited without permission.